3.2 Flooding in Rivers and Streams

This section addresses the potential for flooding at WSES due to the PMF on streams and rivers. The PMF is the *"hypothetical flood (peak discharge, volume, and hydrograph shape) that is considered to be the most severe reasonably possible, based on comprehensive hydrometeorological application of the probable maximum precipitation (PMP) and other hydrologic factors favorable for maximum flood runoff such as sequential storms and snowmelt"* (NRC, 2011).

This section summarizes the PMF on Streams and Rivers evaluation performed in AREVA Calculation No. 32-9226996-000 (AREVA, 2015).

3.2.1 Method

1. The HHA approach described in NUREG/CR-7046 (NRC, 2011) was used for the evaluation of the PMF on rivers and streams and resultant water surface elevation at WSES. With respect to PMF on the Mississippi and Atchafalaya Rivers, the HHA used the following steps:
2. Estimate the PMF flow rate on the Mississippi River and Atchafalaya River at WSES based on the USACE Project Design Flood (PDF) information.
3. Develop Hydrologic Engineering Center River Analysis System (HEC-RAS) steady flow hydraulic computer model cross sections.
4. Calibrate and verify the HEC-RAS model.
5. Perform PMF hydraulic simulations.
6. Perform a sensitivity test of the model.

3.2.2 Results

WSES is located within a complex hydrologic setting consisting of the Mississippi and Atchafalaya Rivers and their inter-connected, low-lying floodplain. The floodplain includes the meandering Mississippi and Atchafalaya Rivers, as well as levees and hydraulic control structures. The system of levees and hydraulic control structures interconnect the Mississippi River and its floodplain with the Atchafalaya River and its floodplain for the purposes of maintaining channel stability, navigation, and flood control (MRC, 2007b).

The Mississippi River generally flows from north to south, through New Orleans and discharges into the Gulf of Mexico. The Atchafalaya River also flows from north to south, through the Lower Atchafalaya Basin Floodway and then discharges to the Gulf of Mexico.

The major flood control hydraulic structures within the Mississippi River and Atchafalaya River floodplain are the Old River Control structure (i.e., ORCS, located at River Mile 315 on the Mississippi River to divert flow form the Mississippi River to the Atchafalaya River; USACE, 2009), the Bonnet Carre Spillway and Floodway (located at River Mile 128 on the Mississippi River to divert flow from the Mississippi River to Lake Pontchartrain; MRC, 2007a), the Morganza Floodway (located at River Mile 285 on the Mississippi River to divert flow to the Lower Atchafalaya Basin Floodway), and the West Atchafalaya Floodway. See Figure 3-23 for the locations of these rivers/floodways.

The USACE structures along the Mississippi River and Atchafalaya River were designed based on the Mississippi River and Tributaries PDF which created a basis for the project flood flow line for the flood protection program within the lower Mississippi Valley (MRC, 2008). Figure 3-24 shows the PDF flows at various latitudes along the Mississippi River.

3.2.2.1 Probable Maximum Flood – Mississippi River and Atchafalaya River

3.2.2.1.1 Estimate the PMF flow on the Mississippi River and Atchafalaya River

The USACE PDF was judged to be a reasonable basis for estimating the PMF for the Mississippi River Basin because it is considered to be of the same order of magnitude as the PMF (MRC, 2008; WSES, 2013, Section 2.4.3.4). The PDF is approximately equivalent to the Standard Project Flood (SPF) which is generally 40 to 60 percent of the PMF (Chow et al, 1964). The PDF was conservatively assumed to be 40 percent of the PMF, therefore:

PMF Peak Flow = PDF x (1 / 0.4) = PDF x 2.5

The PDF flow rates were obtained from the USACE (MRC, 2008) at the latitude directly upstream of the ORCS because they are the most downstream flows that do not account for the flow diversions through the flood control structures. The PDF division of flow between the Mississippi River and local rivers tributary to the Atchafalaya River was used. The PDF for the Mississippi River is 2,720,000 cubic ft per second (cfs) and the collective PDF for the "local" rivers tributary to the Atchafalaya River is 350,000 cfs (MRC, 2008). Figure 3-24 shows the PDF flows upstream of the ORCS.

The PMF peak flow for the Mississippi River upstream of the ORCS was calculated as 6,800,000 cfs. And the PMF peak flow for the Atchafalaya River was calculated as 875,000 cfs. The total PMF peak flow for the Mississippi-Atchafalaya River system is therefore 7,675,000 cfs.

Peak stream flow data from the Mississippi River stream gage upstream of ORCS at Natchez, Mississippi was checked to ensure that the PMF has not been exceeded. The stream gage data indicates that the highest recorded flow was 2,300,000 cfs on May 14, 2011 (USACE, 2013a). The PMF on the Mississippi River is therefore approximately 3 times higher than the flood of record at Natchez.

3.2.2.1.2 Develop HEC-RAS Hydraulic Computer Model

The PMF peak flow rate calculated using the USACE PDF serves as input to a steady-flow HEC-RAS computer model which was developed from elevation and bathymetric data for the Mississippi River (bathymetry data for the Atchafalaya River was not included) (LOSCO, 2004; USGS, 1999; USACE, 2013b). The right descending levee along the Mississippi River was used to split the Mississippi River and its floodplain into two separate but interconnected river reaches in HEC-RAS (Figure 3-25). One river reach includes the Mississippi River and its left descending bank. The other reach includes the Mississippi River's right descending bank (which includes the Atchafalaya River and the Atchafalaya River's floodplain). The reaches are connected via overtopping of the right descending levee.

The upstream and downstream limits for the WSES HEC-RAS model were selected to be approximately River Mile 320 and River Mile 0 on the Mississippi River, respectively (Figure 3-25). The upstream limit is approximately 5 miles upstream of the ORCS. The downstream limit is at the Head of Passes, which is where the Mississippi River branches into three distinct channels at the river's mouth in the Gulf of Mexico. The ORCS, the Morganza Floodway, the West Atchafalaya Floodway, and the Bonnet Carre Spillway were not included in the HEC-RAS model. The top elevations of the levees range from 74.5 ft, NAVD88 (2004.65) at the upstream end of the model to 16 ft, NAVD88 (2004.65) at the downstream end of the model.

Using HEC-RAS flow optimization tool, flow entering the model at River Mile 320 is gradually split between the Mississippi River and Atchafalaya River as it travels downstream. The split is based on flows overtopping the right descending levee (Figure 3-26). As noted above, controlled diversions from the Mississippi River were not considered. Once the flow is split such that the right descending levees are no longer overtopped, it continues to flow downstream and provides a water surface profile from which the PMF water surface elevation at WSES is computed. Levee overtopping flows were calculated using a conservative weir coefficient of 2.6. Typical weir

coefficients for broad-crested weirs are 2.6 to 3.1 (HEC, 2010). Top of levee elevations are published by the USACE (MRC, 2007b; USACE, 2006; WSES, 2012) and were validated using LiDAR data (NSMG, 2004). The top elevations of the levees range from 74.5 ft, NAVD88 (2004.65) at the upstream end of the model, 28.45 ft to 28.6 ft NAVD88 (2004.65) (30 ft MSL) near WSES, to 16 ft, NAVD88 (2004.65) at the downstream end of the model.

Due to the generally flat, wide, and shared flood plain of the Mississippi and Atchafalaya Rivers, a limited number of cross-sections and elevation data points for the floodplain were selected at representative locations where elevation changes or floodplain geometry changes were noted. Fifteen representative cross sections were calculated from the bathymetric data and Digital Elevation Model (DEM) data and are shown in Figure 3-25. The representative cross section at WSES is located at River Mile 130. Additional cross-sections were interpolated within HEC-RAS to supplement the fifteen cross sections manually input into the model. The capacity of the Atchafalaya River channel to convey the PMF flow is expected to be minimal and was conservatively not accounted for in the cross-section data in the model.

HEC-RAS calculates a normal depth for each profile based on the user-specified energy slope when "normal depth" is specified as the boundary condition (HEC, 2010). The energy slope was approximated using the average slope of known water surface profiles. The water surface profiles for the 2008 flood and the 100-year flood on the Mississippi River, as presented in the USACE publication on the Project Flood publication (MRC, 2007b), were used in determining the average energy slope. The publication includes river profiles between River Miles 320 and 100. The average energy slope was estimated to be 0.00004. This energy slope was used for the upstream and downstream boundary condition for the calibration and verification simulations. A sensitivity analysis of the energy slope used in the calculation is described in Section 3.2.2.1.5.

3.2.2.1.3 Calibrate and Verify HEC-RAS Model

Model calibration is the process of selecting and refining HEC-RAS input parameters to produce a simulated profile for a given flood that shows good agreement with an accepted water surface profile for that given event. The model was calibrated based on flow and stage data for the Mississippi River flood of 2011 at Reserve, LA (about 9 miles upstream of WSES) and was verified using the PDF by adjusting the Manning's n values for the cross section geometry data. The 2011 flood resulted in 1.436 million cfs at the USGS Baton Rouge gage on the Mississippi River (USGS, 2014) and the PDF flow at WSES is 1,500,000 cfs (Figure 3-24; MRC, 2008).

The results of the HEC-RAS model calibration show that the model conservatively over-predicts the water surface elevation relative to the observed peak flood elevation for the 2011 flood by about 0.9 ft at Reserve. The results of the WSES HEC-RAS model verification show that the simulated PDF verification flood generated a peak water surface elevation at WSES within 0.5 ft of the USACE-computed elevation at WSES. The calibration and verification show the HEC-RAS model is appropriately conservative.

3.2.2.1.4 Perform PMF Hydraulic Simulations

The peak PMF stage in the Mississippi River at WSES was calculated to be 28.5 ft, NAVD88 (2004.65) (29.9 ft MSL).

The PMF flow that is not confined within the levees of the Mississippi River is conveyed through the Atchafalaya Floodplain. The peak PMF stage in the Atchafalaya Floodplain at WSES was calculated to be 18.6 ft NAVD88 (2004.65) (20.0 ft MSL).

The peak PMF flow in the Mississippi River at WSES was 1,800,000 cfs, and the peak PMF flow in the Atchafalaya floodplain at WSES is 5,875,000 cfs. The collective HEC-RAS computed PMF peak flow rate in the Mississippi River and Atchafalaya River (and adjoining floodplain) for this flow split was 7,675,000 cfs.

3.2.2.1.5 Perform Sensitivity Analyses

Sensitivity analyses were performed to evaluate the sensitivity of the HEC-RAS computed flood elevations to the downstream boundary condition and to the weir coefficient used for computing flow overtopping the lateral structure.

The sensitivity of the calculated PMF elevations at WSES to the energy slope used in computing the normal depth downstream boundary condition showed that the calculated PMF elevations are not very sensitive to the downstream boundary condition used.

The sensitivity of the calculated PMF elevations at WSES to the weir coefficient used for computing the overtopping flow rates over the right descending levees indicated no change in water surface elevation at WSES the Atchafalaya River and a decrease in the calculated water surface elevation at WSES in the Mississippi River. The model does not demonstrate significant sensitivity to the weir coefficient (used for computing flow overtopping the lateral structure).

3.2.3 Conclusions

The total PMF peak flow rate in the Mississippi River and Atchafalaya River (and adjoining floodplain) is approximately 7.7 million cfs (i.e., 1.8 million cfs in the Mississippi River at WSES and 5.9 million cfs in the Atchafalaya River and floodplain at WSES). The peak PMF water surface elevation in the Mississippi River at WSES is approximately 28.5 ft, NAVD88 (2004.65) (29.9 ft MSL). The peak water surface elevation on the Mississippi River channel resulting from the PMF is slightly below the top elevation of the levee of about 28.6 ft, NAVD88 (2004.65) (30.0 ft MSL). The peak PMF water surface elevation in the Atchafalaya floodplain at WSES is approximately 18.6 ft, NAVD88 (2004.65) (20.0 ft MSL).

3.2.4 References

AREVA, 2015. AREVA Document No. 38-9226996-000, "Waterford Steam Electric Station Flooding Hazard Re-evaluation – Probable Maximum Flood," GZA GeoEnvironmental, Inc., 2015.

Chow et al, 1964. "Applied Hydrology", Ven Te Chow, David R. Maidment, and Larry W. Mays, McGraw-Hill, New York, 1964.

HEC, 2010. "HEC-RAS River Analysis System Hydraulic Reference Manual – CPD-69", Version 4.1, USACE Institute of Water Resources – Hydrologic Engineering Center, January 2010.

LOSCO, 2004. Louisiana Digital Elevation Dataset from LDEQ source data, UTM Zone 15 NAD83, LOSCO (2004) [24KDEM_LDEQ_2004], Louisiana Department of Environmental Quality and Louisiana Oil Spill Coordinator's Office, April 23, 2001, Baton Rouge, LA.

MRC, 2007a. "The Mississippi River and Tributaries Project: Floodways", Information Paper, Mississippi River Commission, 2007.

MRC, 2007b. "The Mississippi River & Tributaries Project: Controlling the Project Flood", Information Paper, Mississippi River Commission, 2007.

MRC, 2008. "The Mississippi River & Tributaries Project: Designing the Project Flood", Information Paper, Mississippi River Commission, 2008.

NRC, 2011. "Design Basis Flood Estimation for Site Characterization at Nuclear Power Plants - NUREG/CR-7046", United States Nuclear Regulatory Commission, November 2011.

NSMG, 2004. "The Louisiana Statewide LiDAR Project," Natural Systems Modeling Group, Louisiana Oil Spill Coordinators Office, and The Spatial Data Company, http://atlas.lsu.edu/lidar/, published 2004, date accessed October 7, 2014

USACE, 2006. Levees in Louisiana, Geographic NAD83, USACE (2006) [levees_usace_2006], U.S. Army Corps of Engineers, 2006.

USACE, 2009. "Old River Control", Brochure, U.S. Army Corps of Engineers, New Orleans District, January, 2009.

USACE, 2013a. "Discharge Measurements - Mississippi River @ Natchez, MS", U.S. Army Corps of Engineers Vicksburg District – Water Control Center, http://rivergages.mvr.usace.army.mil/WaterControl/stationinfo2.cfm?sid=CE4103F4&fid=NTZM6&dt=S, date accessed October 11, 2013, date updated October 11, 2013

USACE, 2013b. "2013 Multibeam Survey of Mississippi River", U.S. Army Corps of Engineers New Orleans District, published 2013, date accessed September 10, 2013.

USGS, 1999. "National Elevation Dataset", Wilkinson County, MS, U.S. Geological Survey, EROS Data Center, published 1999.

USGS, 2014. "USGS 07374000 Mississippi River at Baton Rouge, LA – Discharge", U.S. Geological Survey, http://waterdata.usgs.gov/nwis/uv?site_no=07374000, date accessed September 1, 2014, date updated September 1, 2014.

WSES, 2012. "Document Mississippi River Levee Elevation at RM130 Near WF3 from the USACE per CR-WF3-2010-3232", EC0000041205, Revision 0. See AREVA Document No. 38-9243507-000.

WSES, 2013. WSES Updated Final Safety Analysis Report, 2013. See AREVA Document No. 38-9243507-000.

Figure 3-23: Hydraulic Control Structures in the Lower Mississippi River Basin

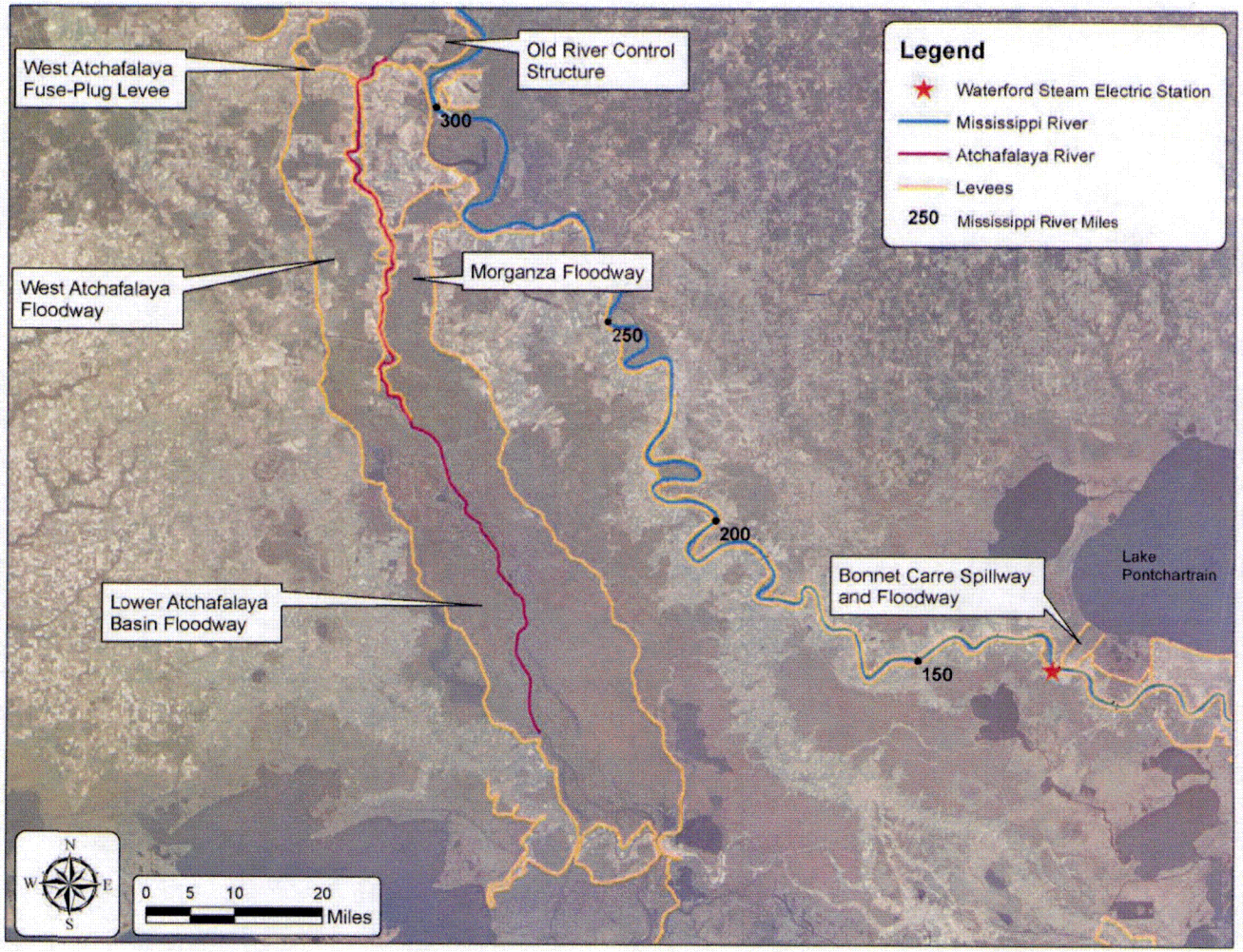

Any illegible text or features in this figure are not pertinent to the technical purposes of this document.

Figure 3-24: Project Design Flood for the Lower Mississippi River Basin

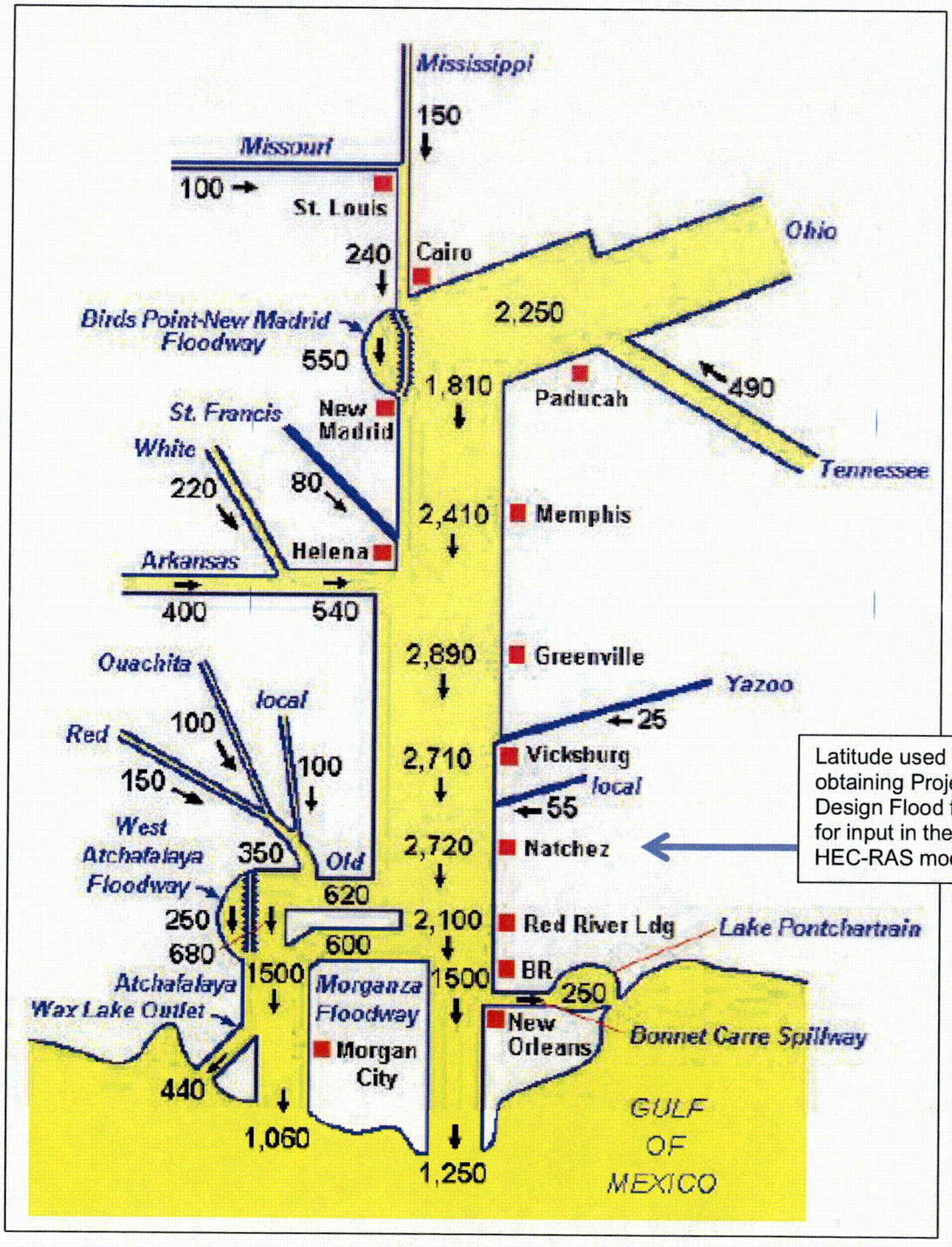

Figure from MRC, 2008.

Figure 3-25: HEC-RAS Cross Sections

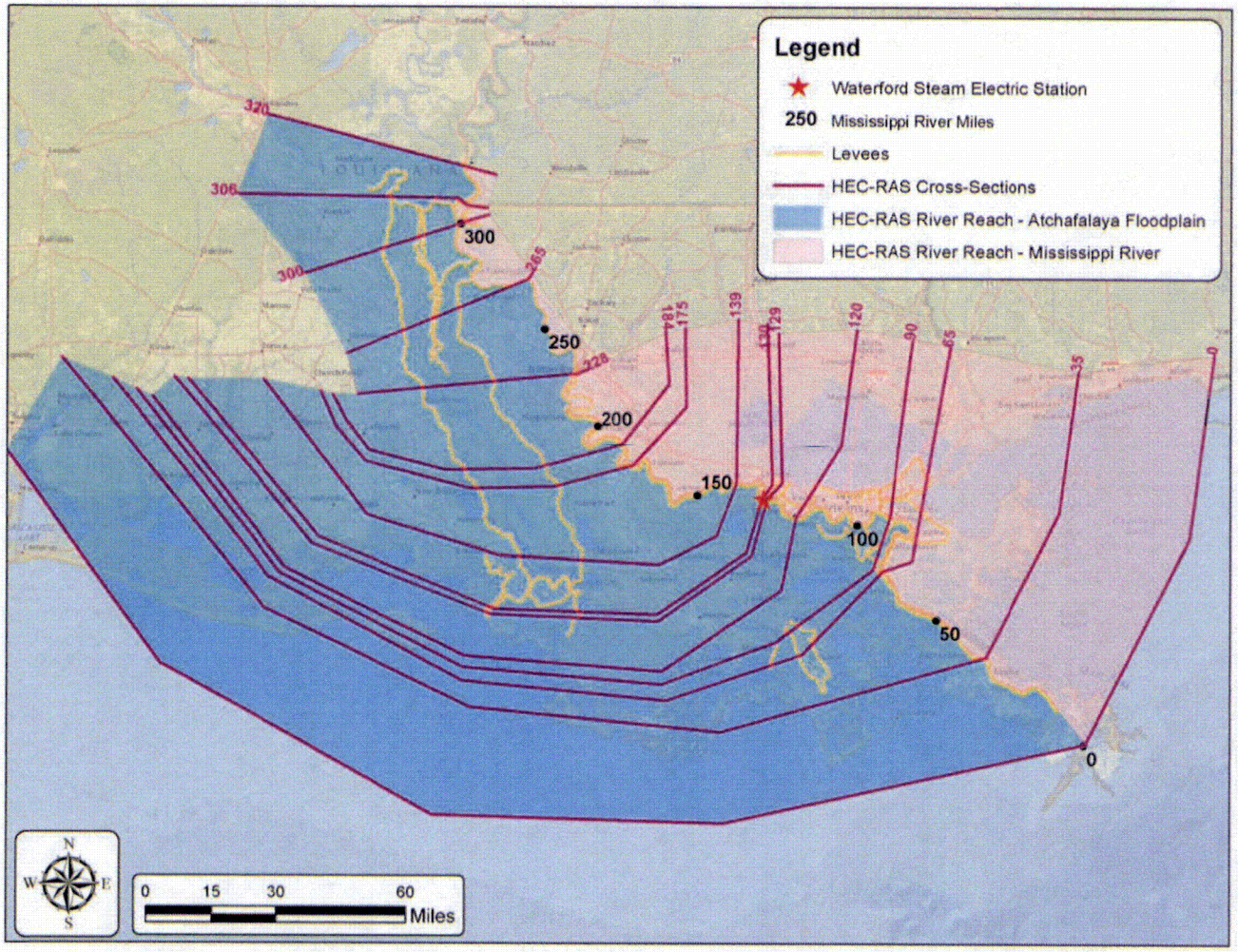

Any illegible text or features in this figure are not pertinent to the technical purposes of this document.

Figure 3-26: Levees in Southern Louisiana

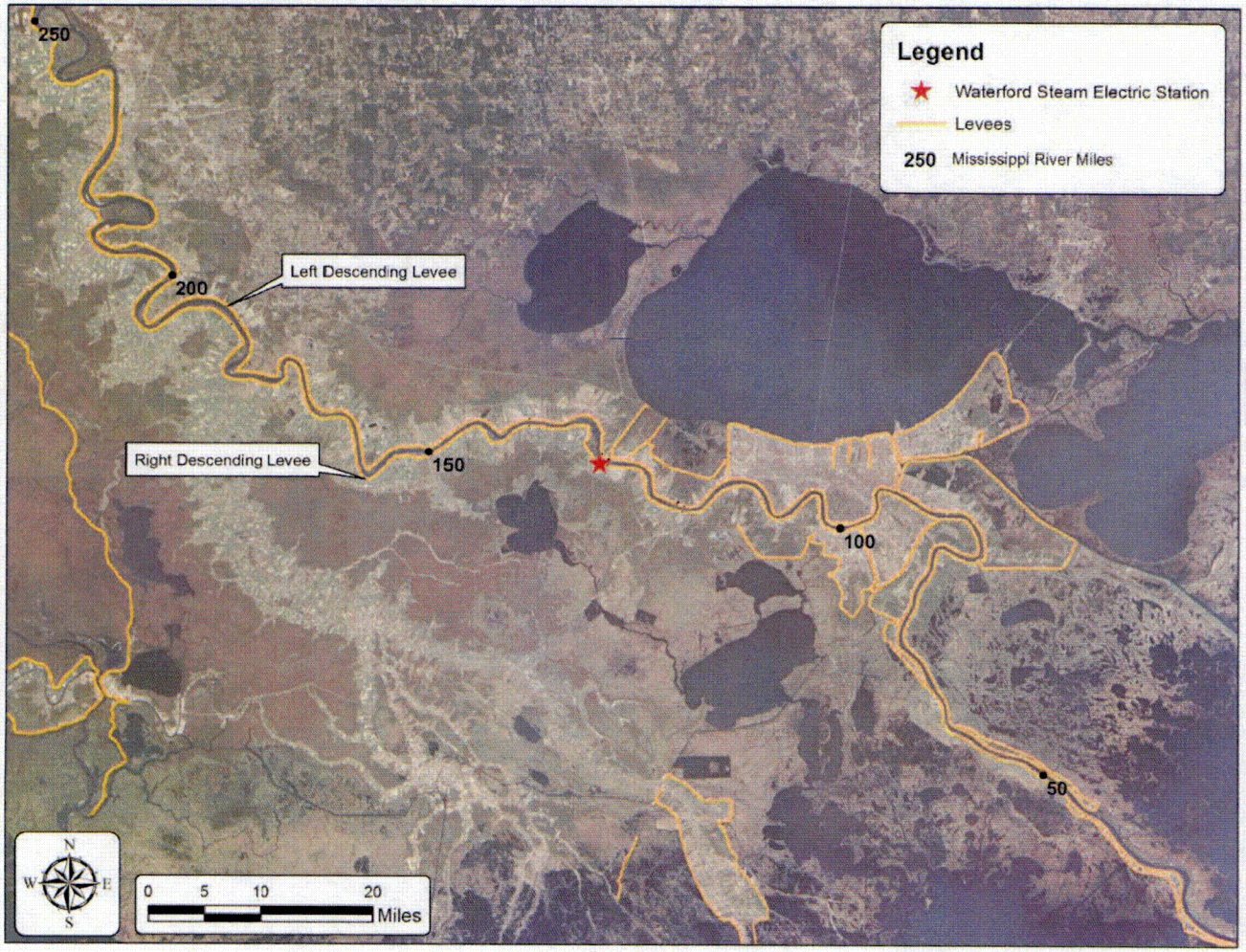

Any illegible text or features in this figure are not pertinent to the technical purposes of this document.

3.3 Dam Breaches and Failures

This section addresses the effect of upstream dam failures in the Mississippi River and Atchafalaya River watersheds on the PMF water surface elevations at WSES. Dam breaches and failures may cause flood waves that impact the PMF level of the receiving water body.

There are no dams on the Mississippi River or Atchafalaya River within 100 river miles upstream of WSES. The hypothetical failures of the largest dams closest to WSES in the Mississippi River and Atchafalaya River watersheds were used in this analysis.

This section summarizes the Dam Failure evaluations performed in AREVA Calculation No. 32-9226999-000 (AREVA, 2015a). The failure of the man-made levees along the Mississippi River was addressed in the Combined Effects Calculation (AREVA, 2015b) and is discussed in Section 3.9.

3.3.1 Method

The HHA approach described in NUREG/CR-7046 (NRC, 2011) was used for the evaluation of the effects of the dam failure flood at WSES. Additional guidance was provided by JLD-ISG-2013-01 - Interim Staff Guidance Japan Lessons-Learned Project Directorate - Guidance For Assessment of Flooding Hazards Due to Dam Failure (NRC, 2013).

Upstream dam failures may result from a hydrologic event (i.e. PMF), a seismic event, or embankment failure due to piping through the embankment (Sunny Day failure). As per Appendix D of NUREG/CR-7046 (NRC, 2011), the PMF scenario discussed below bounds Sunny Day and Seismic failure modes from a water surface elevation standpoint.

The criteria for evaluating flooding from dam breaches and failures is provided in NUREG/CR-7046, Appendix D (NRC, 2011). Two scenarios of dam failures are recommended and discussed including:

1. Failure of individual dams (i.e., group of dams not domino-like failures) upstream of the site; and
2. Cascading or domino-like failures of dams upstream of the site.

Due to the large number of dams upstream of WSES, the application of the two scenarios discussed above is not realistic for all dams. The drainage area of the Mississippi River encompasses all or parts of 31 US states and 2 Canadian provinces. Accounting for all the dams within the Mississippi River watershed is unrealistic because the effect of dam breach within the upstream subwatersheds of the Mississippi River are unlikely to have any effect on water surface elevations at WSES due to the long distance the breach outflows will have to travel before reaching the site. Dams within the upstream subwatersheds of the Mississippi River are far enough from the site such that the effects of dam failure could be expected to have been significantly attenuated before reaching the site.

WSES is located on the lower reach of the Mississippi River within the Lower Mississippi Region watershed. The Red River becomes the Atchafalaya River, which is interconnected with the Mississippi River by the ORCS and the Morganza Floodway and Spillway (see Figure 3-27). The Arkansas-White-Red Region watershed's outlet is the Red River, which flows into the Lower Mississippi Region watershed. Therefore, dams within the two most downstream watersheds of the Mississippi River (i.e., the Lower Mississippi Region and Arkansas-White-Red Region watersheds) were used for this analysis (USGS, 2013; See HUCs 8 and 11 in Figure 3-28).

The methodology adopted in this calculation is based on the NRC's ISG for Assessment of Flooding Hazards Due to Dam Failure (NRC, 2013) and involves the use of hypothetical dams, which represent the major dams upstream of the hypothetical dam. The hypothetical dams are located at the geographical locations of the most downstream major dam within the hypothetical dam's watershed. The hypothetical dam's storage equals the total storage volume of all major dams upstream of the hypothetical dam. The hypothetical dam's height was conservatively assumed to be the height of the tallest major dam upstream of the hypothetical dam.

The map layer "Major Dams of the United States" (DOI, 2014) was used as the source of data on dams within the Lower Mississippi Region and Arkansas-White-Red Region watersheds. The "Major Dams of the United States" map layer is a subset of the 2005 National Inventory of Dams (NID), within the National Atlas of the United States. As stated by the National Atlas, the "map layer [The National Atlas Major Dams layer] portrays major dams of the United States, including Puerto Rico and the U.S. Virgin Islands. The map layer was created by extracting dams 50 ft or more in height, or with a normal storage capacity of 5,000 acre-ft or more, or with a maximum storage capacity of 25,000 acre-ft or more, from the 79,777 dams in the U.S. Army Corps of Engineers National Inventory of Dams" (DOI, 2014). The Major Dams map layer only includes dams that fulfill at least one of the three criteria (for height, normal storage, or maximum storage) listed above.

The use of the "Major Dams of the United States" map layer served to screen inconsequential dams as recommended in the NRC's dam failure ISG (NRC, 2013). All "Major Dams" upstream of the WSES site and within the Lower Mississippi Region and Arkansas-White-Red Region watersheds were included in the model. Inconsequential dams, defined as dams whose failure poses no danger to life and property, or dams whose failure would only cause damage to property of the dam owner, were not included in this analyses. Dams which do not meet the technical definition of "inconsequential" contained in the ISG, but are not included on the "Major Dams" list were also not explicitly considered in this analysis. The vast majority of such non-major dams within the Lower Mississippi Region and the Arkansas-White-Red Region watersheds are far enough from the site such that the effects of dam failure could be expected to have been attenuated before reaching the site. The effects of closer non-major dams is accounted for in the inherent conservatism included in the assumptions regarding the storage volume, height, and location of the hypothetical dams used in the dam failure model.

The peak breach outflows from each hypothetical dam were calculated using regression equations referenced in the ISG (NRC, 2013). The Froehlich (Froehlich, 1995), MacDonald and Langridge-Monopolis (MacDonald, 1984), and Costa (Costa, 1985) peak dam breach outflow regression equations were evaluated using the storage volume and height parameters of the hypothetical dams. The peak breach outflow regression equation resulting in the highest breach flow was conservatively used to calculate the attenuated breach flow at WSES. The (United States Bureau of Reclamation (USBR) attenuation method discussed in the ISG (NRC, 2013) was used to account for the potential attenuation of the peak breach wave along the river and floodplain after failure (USBR, 1982).

The estimated PMF flow at WSES (AREVA, 2015c-also see Section 3.2) was combined with the estimated attenuated peak dam breach flow and used as an inflow to perform the steady-state HEC-RAS simulation.

3.3.2 Results

A total of 115 major dams were identified to be within the Lower Mississippi Region watershed upstream of WSES (Figure 3-29). A total of 777 major dams were identified to be within the Arkansas-White-Red Region watershed (Figure 3-30). These major dams were used to estimate the characteristics of two representative hypothetical dams, which were in turn used to calculate the peak dam breach outflow to be directly translated to WSES. The calculated storages and heights of the hypothetical dams are shown below:

Hypothetical Dam's Watershed	Number of Individual Dams	Total Storage (acre-ft)	Maximum Height (ft)
Lower Mississippi Region Upstream of WSES	115	24,573,000	243
Arkansas-White-Red Region	777	82,562,000	325

The peak breach outflow from the Froehlich equation resulted in the greatest estimated breach flow for both the Lower Mississippi Region and Arkansas-White-Red Region watersheds at approximately 5,510,000 cfs and 11,300,000 cfs, respectively.

The closest upstream major dam to WSES in the Lower Mississippi Region watershed is the False River Drainage Structure which is located approximately 129 river miles upstream (Figure 3-31). The closest upstream major dam to WSES in the Arkansas-White-Red Region watershed is Cotile Lake Dam which is located approximately 252 miles upstream (Figure 3-32). These locations were used as surrogates for the hypothetical dams representing their respective watershed.

The USBR attenuation method used is appropriate for the WSES hydrological setting. Within the Lower Mississippi Region watershed alone, the Mississippi River is over eight hundred miles long (USGS, 2012; USGS, 2013), which provides a large distance to attenuate peak dam breach outflows. In addition, there is significant floodplain attenuation anticipated due to the low-lying areas adjacent to the Mississippi River with little topographic relief. The Mississippi River floodplain is approximately 30 miles wide at Red River's confluence with the Atchafalaya River and expands to approximately 50 miles wide at the Gulf of Mexico coast (LOSCO, 2004). The vast floodplain extends for about 50 miles in the north-south direction and varies in average floodplain elevation from about 50 ft at the north end to 0 ft at the Gulf of Mexico coast (LOSCO, 2004).

After attenuation using the USBR method, the peak dam breach flow in the Lower Mississippi Region watershed upstream of WSES was calculated at 280,000 cfs. The attenuated peak dam breach flow in the Arkansas-White-Red Region watershed was calculated at 34,000 cfs. The total dam breach peak flow at WSES is 314,000 cfs.

The dam breach flows were initially distributed to the respective rivers of their upstream watersheds. The Arkansas-White-Red Region peak breach flow was added to the HEC-RAS model's upstream end of the Atchafalaya Floodplain and the Lower Mississippi Region peak breach flow was added to the HEC-RAS model's upstream end of the Mississippi River. However, adding flow in excess of the PMF inflow for the Mississippi River resulted in HEC-RAS model instabilities. For example, the HEC-RAS model demonstrated a decrease in elevations along the Mississippi River (i.e., the elevations in the Mississippi River when the PMF flow plus dam breach flow were added were lower than the elevations in the Mississippi River when only the PMF flow was added). Therefore, all calculated dam breach flows were added directly to the Atchafalaya Floodplain, which results in a more conservative water-surface elevation at WSES.

The peak stage resulting from the combined dam failure and PMF peak flow rate was calculated to be 28.5 ft NAVD88 (2004.65) at WSES in the Mississippi River and 19.1 ft NAVD88 (2004.65) at WSES in the Atchafalaya River and floodplain.

3.3.3 Conclusions

Based on the re-evaluation of upstream dam failures on the Mississippi River and Atchafalaya River, the peak water surface elevations on the Mississippi River and within the Atchafalaya Floodplain at WSES resulting from the failure of upstream dams and the PMF is below the top elevation of the NPIS of 29.18 ft MSL. This is well above the flood elevation calculated for the Atchafalaya River and floodplain of 19.1 ft NAVD88 (2004.65) (20.5 ft MSL).

3.3.4 References

AREVA, 2015a. AREVA Document No. 32-9226999-000, "Waterford Steam Electric Station Flooding Hazard Re-Evaluation – Dam Failure," GZA, GeoEnvironmental, Inc., 2015.

AREVA, 2015b. AREVA Document No. 32-9227036-000, "Waterford Steam Electric Station Flooding Hazard Re-Evaluation – Combined Effects," GZA, GeoEnvironmental, Inc., 2015.

AREVA, 2015c. AREVA Document No. 32-9226996-000, "Waterford Steam Electric Station Flooding Hazard Re-Evaluation – Probable Maximum Flood," GZA GeoEnvironmental, Inc., 2015.

Costa, 1985. "Floods from Dam Failures", Costa, J.E., U.S. Geological Survey, Open-File Report 85-560, 1985.

DOI, 2014. Major Dams of the United States map layer by the National Atlas of the United States. (http://nationalatlas.gov/mld/dams00x.html), Date published: March 2006, Date accessed: September 15, 2014.

Froehlich, 1995. Peak Outflow from Breached Embankment Dam. Froehlich, D.C. 1995. Journal of Water Resources Planning and Management, vol. 121, no. 1, p. 90-97.

LOSCO, 2004. Louisiana Digital Elevation Dataset from LDEQ source data, UTM Zone 15 NAD83, LOSCO (2004) [24KDEM_LDEQ_2004], Louisiana Department of Environmental Quality and Louisiana Oil Spill Coordinator's Office, April 23, 2001, Baton Rouge, LA.

MacDonald, 1984. "Breaching Characteristics of Dam Failures", MacDonald, T.C. and Langridge-Monopolis, J., Journal of Hydraulic Engineering, Vol. 110, No. 5, May 1984.

NRC, 2011. NUREG/CR-7046: Design-Basis Flood Estimation for Site Characterization at Nuclear Power Plants in the United States of America", U.S. Nuclear Regulatory Commission, Springfield, VA, National Technical Information Service, 2011.

NRC, 2013. JLD-ISG-2013-01: Interim Staff Guidance Japan Lessons-Learned Project Directorate - Guidance For Assessment of Flooding Hazards Due to Dam Failure, Revision 0, U.S. Nuclear Regulatory Commission, July 2013.

USBR, 1982. "Guidelines for defining inundated areas downstream from Bureau of Reclamation dams." Reclamation Planning Instruction No. 82-11, U.S. Bureau of Reclamation (USBR). June 15, 1982.

USGS, 2012. National Hydrography Dataset, United States Geological Survey, (http://nhd.usgs.gov), Date published: 2001, Date accessed: October 30, 2012.

USGS, 2013. "U.S Subwatershed Boundaries (HUC) Shapefiles," United States Geologic Survey, (http://water.usgs.gov/GIS/huc.html), Date modified: July 2013, Date accessed: November 5, 2013.

WSES, 2013. WSES Updated Final Safety Analysis Report, 2013, See AREVA Document No. 38-9243507-000.

Figure 3-27: Regional Locus Map of Hydraulic Structures

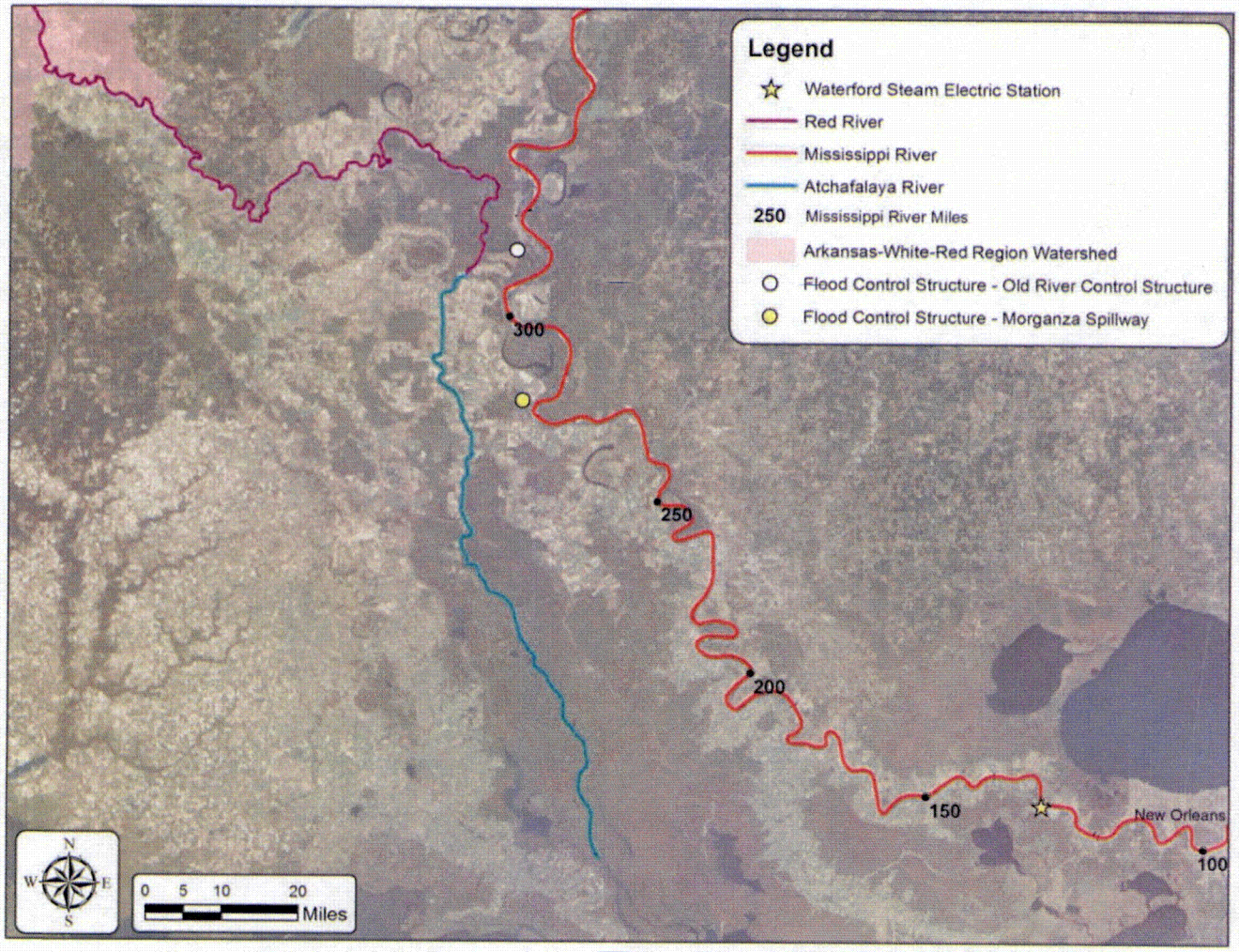

Any illegible text or features in this figure are not pertinent to the technical purposes of this document.

Figure 3-28: USGS HUC Watershed Boundaries

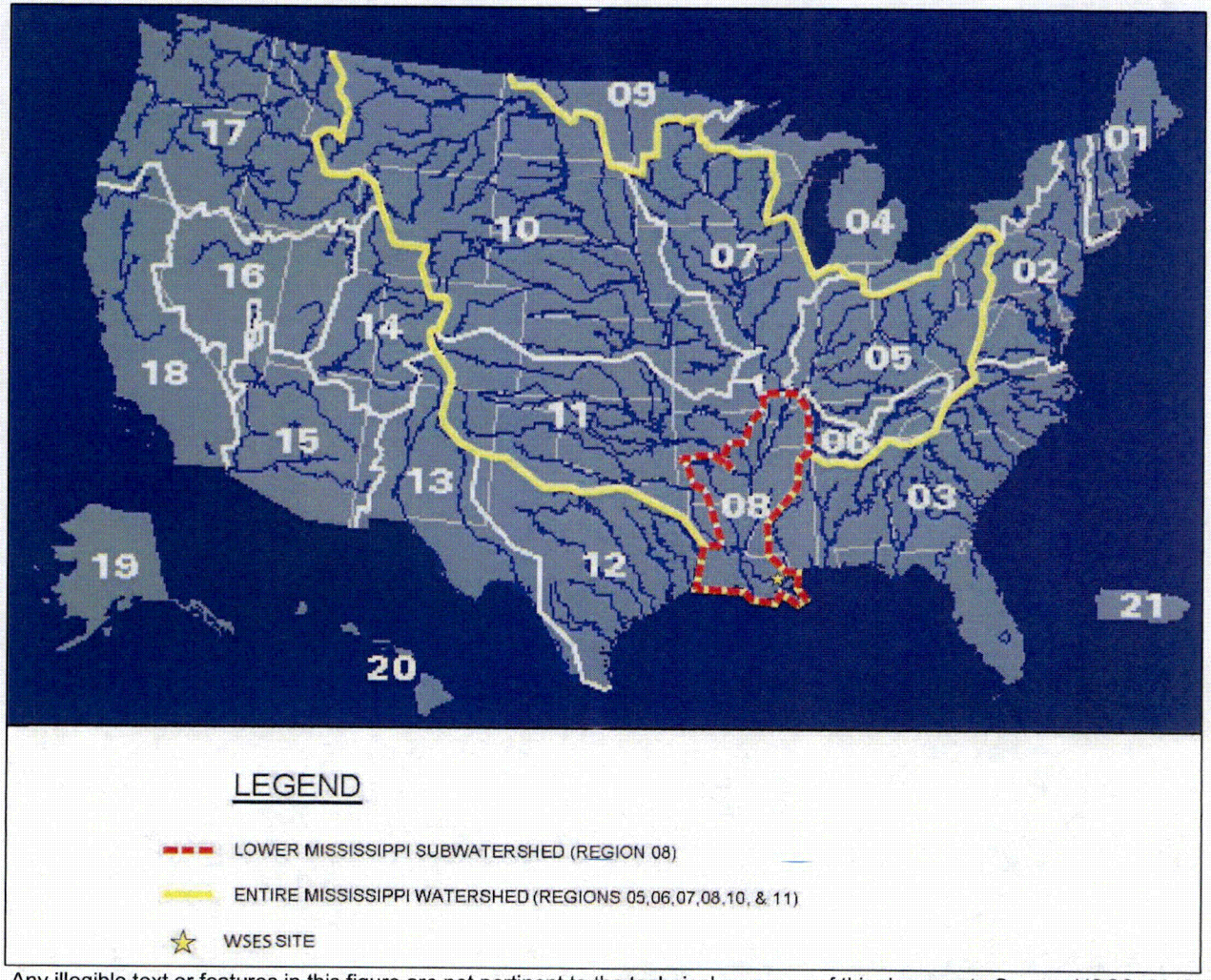

Any illegible text or features in this figure are not pertinent to the technical purposes of this document. Source: USGS, 2013

Figure 3-29: Major Dams in Lower Mississippi Region Watershed Upstream of WSES

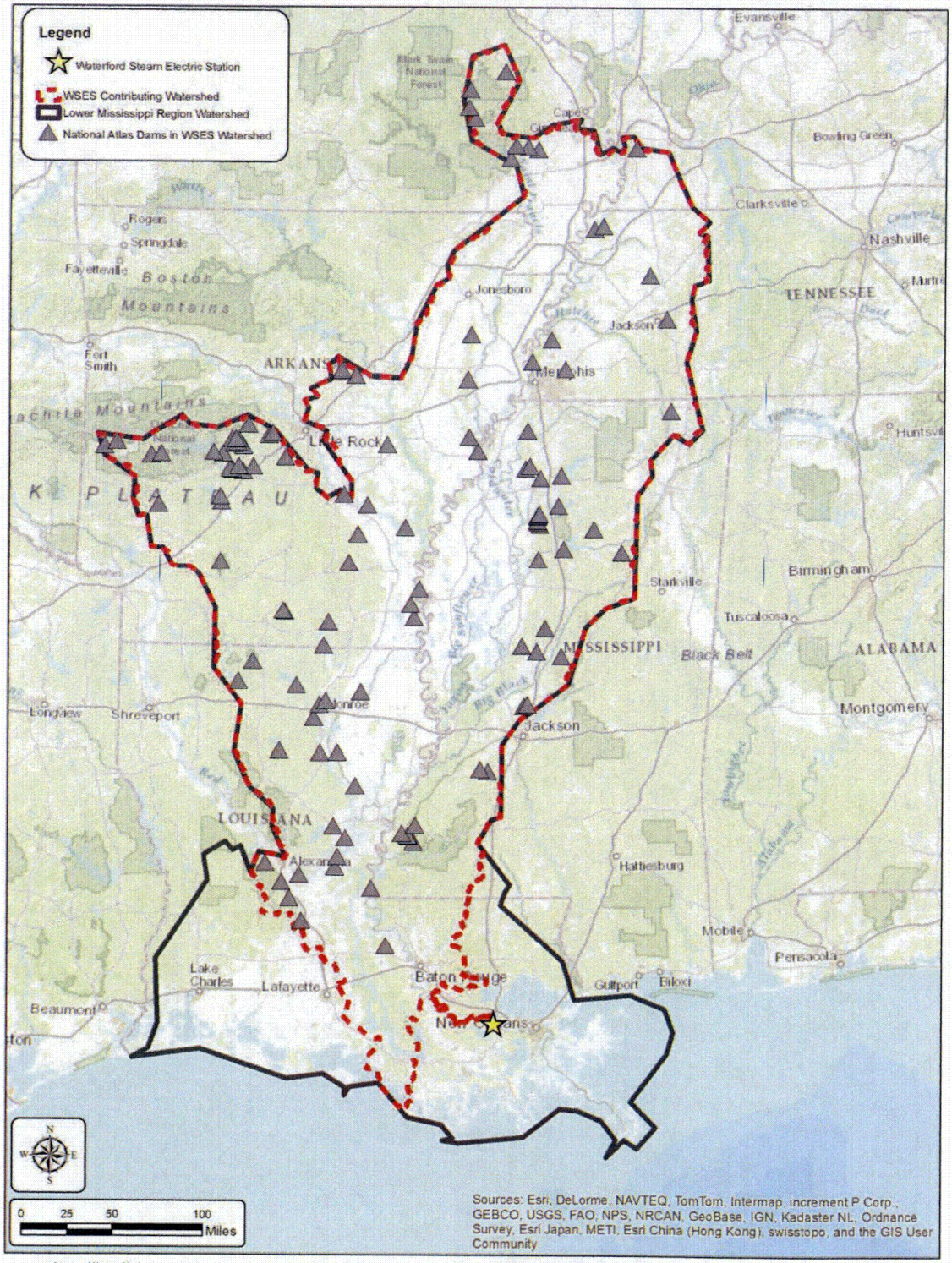

Any illegible text or features in this figure are not pertinent to the technical purposes of this document.

Figure 3-30: Major Dams in Arkansas-White-Red Region Watershed

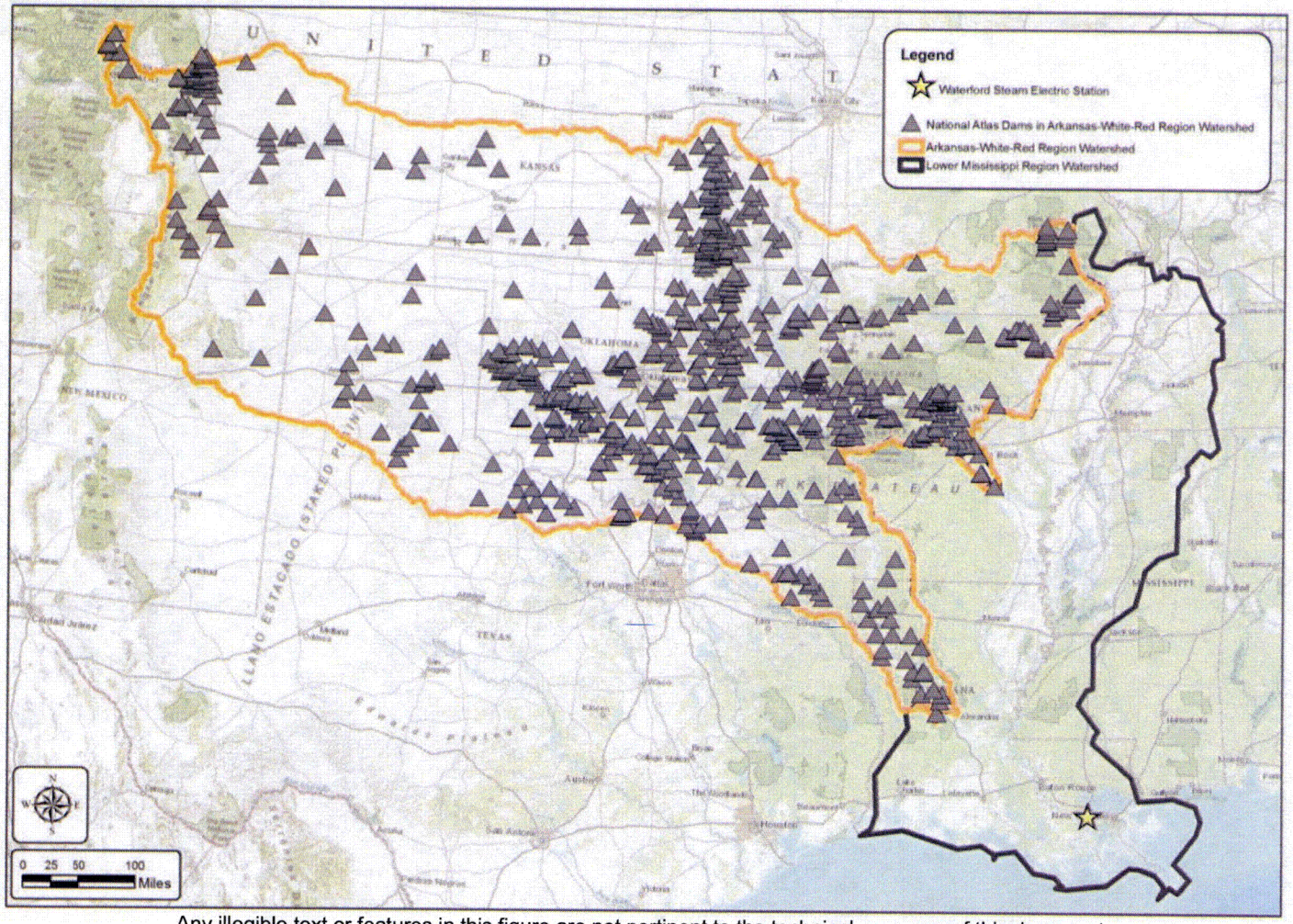

Any illegible text or features in this figure are not pertinent to the technical purposes of this document.

Figure 3-31: Distance to Closest Upstream Dam in Lower Mississippi Region Watershed

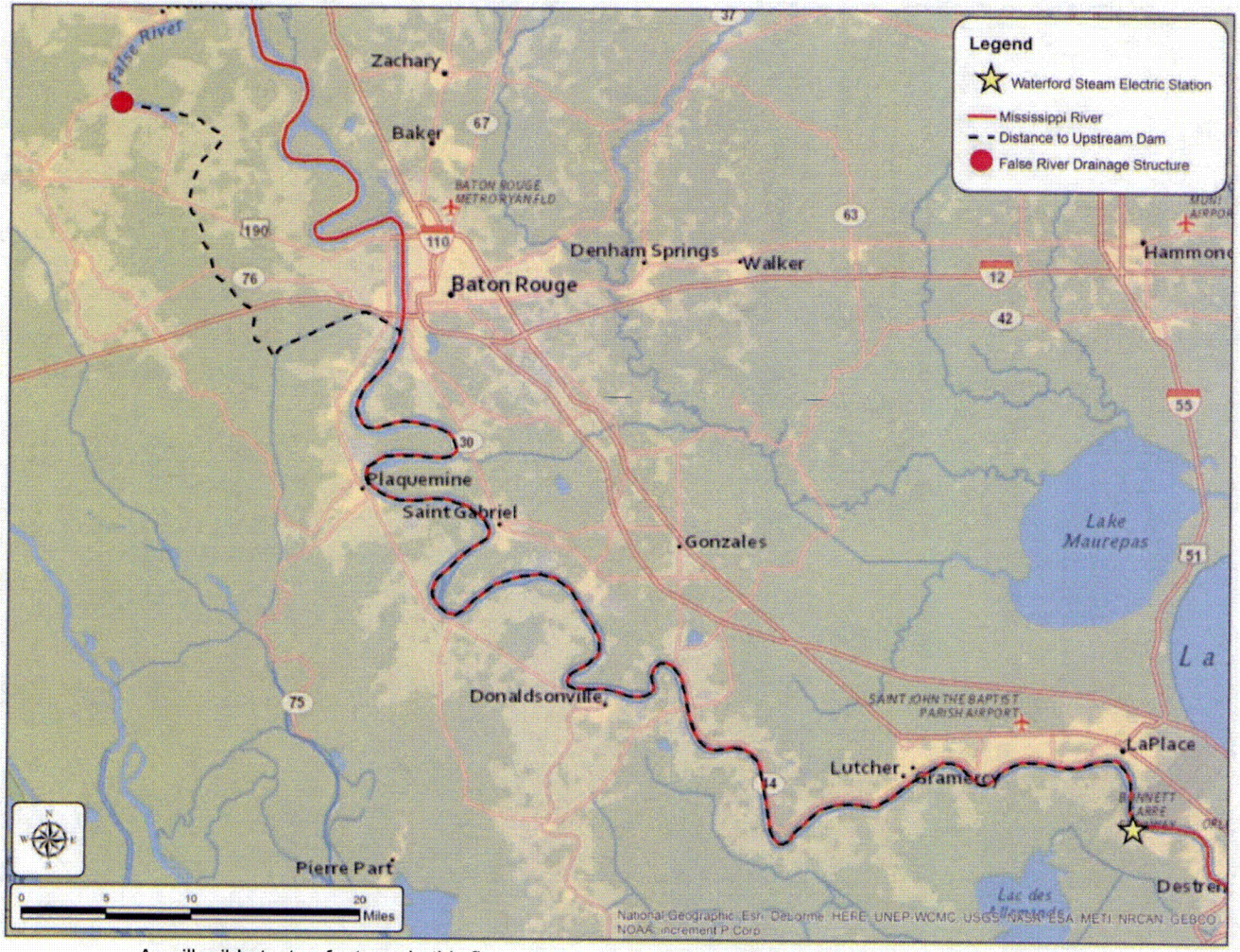

Any illegible text or features in this figure are not pertinent to the technical purposes of this document.

Figure 3-32: Distance to Closest Upstream Dam in Arkansas-White-Red Region Watershed

Any illegible text or features in this figure are not pertinent to the technical purposes of this document.

3.4 Storm Surge

A deterministic evaluation of the PMSS flood hazard at WSES was performed in a manner consistent with the HHA approach described in NUREG/CR-7046 (NRC, 2011, Section 2). The PMSS is "that surge that results from a combination of meteorological parameters of a Probable Maximum Hurricane, or a moving squall line and has virtually no probability of being exceeded in the region involved" (NRC, 2011). The evaluation of the PMH was performed in the AREVA calculation "Waterford Steam Electric Station Flooding Hazard Re-Evaluation – Probable Maximum Hurricane" (AREVA, 2015a) and the evaluation of the PMSS stillwater elevation was performed in the AREVA calculation "Waterford Steam Electric Station Flooding Hazard Re-Evaluation – Probable Maximum Storm Surge" (AREVA, 2015b). These calculations contain complete details of the evaluations.

The methodology, results and conclusions associated with these calculations are summarized below.

3.4.1 Location and Hydrologic Setting

WSES is located in Southern Louisiana, at Latitude 29.995° and Longitude -90.471° (°indicates decimal degrees). WSES is located south and west of, and adjacent to, the Mississippi River and about 7 miles southwest of Lake Pontchartrain. Lake Pontchartrain, not truly a lake but part of the estuary system, is hydraulically connected to the Gulf of Mexico (GoM) through Lake Borgne. WSES is also located about 60 miles to the north and about 80-miles to the west of the GoM. The area south of WSES (between WSES and the GoM) is a low-lying coastal floodplain with numerous interconnected estuaries, saltwater marshes, wetlands, channels and lakes, and much of the area around New Orleans lies near or below sea level (USACE, 2006). The coastal floodplain is located immediately adjacent to a broad (about 20 to about 80 miles in width) continental shelf (within the GoM). A large delta has been formed at the mouth of the Mississippi River from the deposition of river sediment which extends nearly to the continental shelf break. The low-lying topography and numerous water bodies make the region very susceptible to flooding from hurricane storm surge. The regional setting makes it conducive for hurricane surges to propagate rapidly across the floodplain, and from many track directions (FEMA, 2008).

An extensive levee system has been constructed in southeast Louisiana. The levee system and hydraulic control structures are owned and maintained by the USACE and interconnect the Mississippi River floodplain with the Atchafalaya River floodplain for the purposes of maintaining channel stability, navigation and flood control (MRC, 2007). The USACE structures along the Mississippi River and Atchafalaya River were designed based on the Mississippi River and Tributaries PDF. In the past few years (subsequent to Hurricane Katrina in 2004), a new round of levee repairs and improvement projects have been completed, which are referred to as the Greater New Orleans Hurricane and Storm Damage Risk Reduction System (HSDRRS) (USACE, 2012; USACE, 2013; USACE, 2014). The existing levee system plays an important role in protecting the area from both riverine and coastal floods (USACE, 2014).

Due to the topographic characteristics of the area and the proximity of the Mississippi River and Lake Pontchartrain, WSES is principally vulnerable to storms and storm surges that approach from the following three paths:

a) northerly bearing storm tracks (including storms from the southwest, south and southeast) making landfall along the coast of the GoM to the west of WSES, with storm surges encroaching through the low-lying coastal marshes and estuaries (such as Barataria Bay, Little Lake and Lake Salvador). The Mississippi River levee system does not provide significant protection for WSES from extreme storm surges coming from this southerly direction. Flooding in the vicinity of WSES, due to storm surges encroaching from the south, is primarily a function of the available storage provided by the marshes/wetlands/estuaries. This group of storm tracks represents a likely direction for a PMH track for storms intensities near the maximum potential intensity (MPI) limit (AREVA, 2015a).

b) northwesterly bearing storm track, with storm surges encroaching from the southeast and propagating toward WSES from the southwestern portion of Lake Pontchartrain. When a westerly, very intense storm

creates large surges along the coast, the storm surge propagates into Lake Borgne and Lake Pontchartrain. If the water volume accumulates within Lake Pontchartrain such that the water level exceeds the crest elevation of the north river levee, the levee is overtopped with discharge into the Mississippi River. Dependent upon the coincident capacity and water level within the river, the south river levee (northeast of WSES) could also be overtopped, thereby directly flooding WSES. Dependent upon the landfall location, storms with a northwesterly bearing can also contribute to flooding within the Mississippi River and to the west of the Mississippi River in the vicinity of WSES.

c) "Upriver" storm bearing, with coastal surges encroaching on the GoM shoreline such that a significant surge propagates up the Mississippi River. Under extreme storm surge scenarios, the surge within the river could result in overtopping of both river levees, causing flooding at WSES.

Southern Louisiana is a region that is changing significantly over time due to natural morphological evolution (such as ground subsidence and sea level rise [SLR]), and due to modifications of manmade features such as levees and dredged channels (FEMA, 2008). The amount and rate of ground subsidence varies spatially. Therefore, adjustments to account for the relative sea level rise (including the combination of global sea level rise and local ground subsidence) are required. Based on these published documents, the subsidence rate at different locations within the region ranges from zero (no subsidence) to over 20 millimeters per year (mm/yr) in the general area of southern Louisiana. The long-term, global average rate of SLR has been determined to be 1.7 to 1.8 mm/yr (NOAA, 2014d). Variations in regional SLR rates, relative to global sea level rise, are due significantly to local land subsidence or heave (NOAA, 2014d).

3.4.2 Methodology

The following sections summarize the methodology used to evaluate the PMH and the PMSS stillwater elevation at WSES. Figure 3-33 presents an overview of the process used to calculate the coastal flood potential at WSES.

3.4.2.1 Probable Maximum Hurricane

A step-wise approach consistent with the HHA approach described in NUREG/CR-7046 (NRC, 2011, Section 2) was used to establish the range of hurricane meteorological parameters representative of the PMH. The PMH meteorological parameter ranges applicable to WSES were initially developed using the National Weather Service (NWS) "Meteorological Criteria for Standard Project Hurricane and Probable Maximum Hurricane Windfields, Gulf and East Coast of the United States, Technical Report FT" (FT) (NOAA, 1979). A site and region-specific hurricane climatology study was then performed to evaluate the conservatism of the PMH parameter ranges presented in FT based on the current state of knowledge and in consideration of recent, strong hurricanes that have been recorded in the region since the publication of FT (i.e., Hurricane Katrina (2005), Hurricane Rita (2005), etc.).

The site and region-specific hurricane climatology study involved analyses of historical storm surge and hurricane data that are characteristic of the site region – which includes the northern GoM in the vicinity of the Louisiana coastline. The site and region-specific hurricane climatological study performed the following:

1. Evaluated historical extreme storm surge water levels based on observed tide gauge data and recorded high water marks;
2. Evaluated the historic hurricane tracks, landfalls, life cycle of hurricanes in the GoM, and observed surge elevations;
3. Evaluated other characteristics of GoM hurricanes that affect hurricane meteorological parameters including:
    a. Wind field geometry;
    b. Hurricane dynamics, including hurricane intensification and weakening and the effects of the Loop Current in the GoM;

c. Seasonal and climatic trends, including landfall climatic trends;

d. Hurricane landfall probabilities, including determination of the annual, omni-directional hurricane frequency (λ) for the site region.

4. Statistical analysis of the hurricane meteorological parameter data, consistent with the current science and available meteorological data:

a. Compilation of historic hurricane meteorological parameter data within a defined data capture zone, based on the published best track database, HURDAT, by National Oceanic Atmospheric Administration (NOAA), and Extended Best Track Data provided by Regional and Mesoscale Meteorology Branch (RAMMB) of NOAA and the National Environmental Satellite, Data, and Information Service (NESDIS). Original HURDAT and Extended Best Track 6-hourly data were interpolated at 1-hourly intervals to provide more resolution of the evolution of storm intensity and characteristics. The interpolation process does not change the magnitude of the original observed best track data. The hourly data points simply represent the best-estimated possible storm parameters between the 6-hourly data points.

b. Development of PDFs and CDFs for key hurricane meteorological parameters, including:

i. Core Intensity:

a) Central Pressure Deficit (ΔP), which is the difference of P_w and P_o;

b) V_{maxs} (spline smoothed hourly maximum wind speeds);

ii. Storm track bearing (θ), defined as the direction that the storm is tracking toward (in degrees [°]) from true north (track direction and track bearing used interchangeably in this calculation);

iii. V_f;

iv. R_{max} (also referred to as storm core size).

Several parametric distribution functions and a non-parametric distribution (kernel) method were used. Appendix A of the PMH Calculation (AREVA, 2015a) presents the probability distributions used.

c. Statistical correlation between key parameters.

d. Comparison of the results to parameter characteristics of landfall hurricanes for the GoM region presented in Jacobsen, 2013.

5. Identification of the MPI applicable to the region based on published values.

3.4.2.2 Probable Maximum Storm Surge

A step-wise approach consistent with the HHA approach described in NUREG/CR-7046 (NRC, 2011, Section 2) was used to deterministically evaluate the PMSS stillwater elevation (i.e., the resulting surface water elevation in the absence of waves, wave set-up and river flood) at WSES. The method of analysis is described as follows:

1. Generation of the Initial Storm Set: An Initial Storm Set was developed based on the range of meteorological parameters representative of the PMH. As a first step in defining the hurricanes included in the Initial Storm Set, each potential storm bearing (θ) was combined with a potential landfall location to create a set of storm tracks as shown in Figure 3-34. Ten potential landfall locations spanning the distance between FT Mile Posts 550 and 750 (NOAA, 1979) in 20 or 25 nm intervals were used (Figure 3-34). The coordinates of these landfall locations are provided in Table 3-16. One hundred storm tracks were created, based on ten potential bearings (-80° to +10° at 10° intervals) and ten potential landfall locations (Figure 3-35). Each track was then assigned three maximum wind speeds, up to an initial, assumed maximum 1-minute, 10-meter wind speed for screening purposes of 160 knots (kt) (AREVA,

2015a). Lastly, the tracks were assigned to unique pairings of the remaining, discretized parameters (i.e., four radii of maximum winds and four forward speeds) to create the Initial Storm Set of 4,800 hypothetical events:

10 (Landfall Points) x 10 (0) x 3 (V_{max}) x 4 (R_{max}) x 4 (V_f) = 4,800

Each track was assigned with a unique storm identification (STORMID) number ranging from 1 through 4,800.

2. Calculation of the Antecedent Water Level: In accordance with NUREG/CR-7046 (NRC, 2011), the PMSS is evaluated coincident with an Antecedant Water Level (AWL) equal to the 10 percent exceedance high tide plus long term sea level rise (NRC, 2013). The 10 percent exceedance high tide is defined as the high tide level that is equaled or exceeded by 10 percent of the maximum monthly tides over a continuous 21 year period (ANS, 1992). The 10 percent exceedance high tide was statistically calculated using National Oceanic and Atmospheric Administration / National Ocean Service / Center for Operational Oceanographic Products and Services (NOAA/NOS/CO-OPS) using observed monthly maximum high tides from the NOAA/NOS/CO-OPS Grand Isle tide gage (Station 8761724, NOAA, 2014a), Dauphin Island tide gage (Station 8735180, NOAA, 2014b) and Eugene Island tide gage (Station 8764311, NOAA, 2014c), and the Weibull plotting position equation (Stedinger et al., 1993).

   Long-term sea level rise over a projected 30-year period was calculated based on recorded, long-term sea level trends data from the NOAA CO-OPS Tide Gage at Pensacola, Florida. This station was selected since it is located in an area with little or no observed ground subsidence (NOAA, 2014d). The sea level trend observed at Pensacola is assumed to be representative for the coastline of interest for this calculation, i.e., central-northern GoM.

   The initial water level in the ADCIRC model was increased prior to the simulations to convert the water levels in ADCIRC from local mean sea level (LMSL) to NAVD88-2004.65 (elevation datum used in the ADCIRC model) and also to account for the seasonal fluctuations in sea level in the GoM due to thermal expansion and other natural processes (steric water level adjustment). The component of the 10-percent exceedance high tide due to the seasonal fluctuation in sea level in the GoM was calculated separately based on long-term tidal data at NOAA stations at Pensacola, Dauphin Island, Grand Isle, Galveston Pier, Eugene Island, and Sabine Pass. The adjustment was based on the average of the largest seasonal (monthly) thermal expansion of the GoM as indicated in recorded seasonal mean seal levels at these gages. The AWL with SLR and datum adjustment is calculated as:

   $AWL = Tide_{10\%}$ (including steric water level adjustment) + SLR_{30year} + LMSL to NAVD88-2004.65 adjustment

   These adjustments do not account for future ground subsidence. Projected ground subsidence in the vicinity of WSES was accounted for after the simulations as a post-processing step.

3. PMH Parameter Combination Sensitivity Analysis: Simulations were performed using the SLOSH model and the Initial Storm Set to identify: 1) the sensitivity of storm surge at WSES to different storm parameters (i.e., storm track, radius of maximum winds, etc.) as constrained by the PMH calculation; and 2) the specific combinations of storm parameters and storm tracks that result in the largest predicted storm surges at WSES. The simulations assumed steady-state conditions (i.e., storm parameters were not varied from the initial specifications). The results of the sensitivity analysis done using SLOSH were verified in ADCIRC using a smaller set of storms before the selection of the final PMSS storm set.

4. ADCIRC Model Validation: ADCIRC is a state-of-the-art two-dimensional, depth-integrated, barotropic time-dependent long wave, hydrodynamic circulation model. ADCIRC is a highly developed computer program for solving the equations of motion for a moving fluid on a rotating earth. ADCIRC uses non-structured, finite element grids with variable grid resolution.

The finite element grid used in the calculation of the PMSS is the Southern Louisiana (SL16) mesh. The SL16 mesh is an improved version of the southeast Louisiana Federal Emergency Management Agency (FEMA) Flood Insurance Study (FIS) model (SL15) (FEMA, 2008). The SL15 mesh was validated and used by FEMA in the southeast Louisiana FIS (FEMA, 2008). The SL15 grid was refined locally to resolve features such as inlets, rivers, navigation channels, levee systems, and local topography and/or bathymetry. The resolution in the wave breaking zones and inland is less than 200m to improve the wave breaking and the transfer of wave radiation stress gradients to ADCIRC. In the small-scale channels and passes, such as the Mississippi River and its distributaries, the Mississippi River Gulf Outlet (MRGO), and the Rigolets and Chef Menteur passes, the resolution is 20 to 50m (Dietrich et al., 2011). The increased resolution in the SL16 mesh, compared to the SL15 mesh, is mainly within Southeastern Louisiana and the Mississippi River. Validation of the SL16 mesh and nodal attributes using historical hurricanes (Hurricanes Katrina and Rita (2005) and Gustav and Ike (2008)) is provided in the 2012 publication on the performance of the SWAN+ADCIRC model in computing hurricane waves and surge (Dietrich et al., 2012). No modifications to the SL16 mesh were made as part of this re-evaluation.

5. Tidal, River and Meteorological Input: Input to the ADCIRC model for the PMSS simulations included tidal potential, river flowrates, and meteorological parameters from the hurricane wind field. Seven tidal potential constituents (including K1, K2, M2, N2, O1, Q1 and S2) from the LeProvost tide database (LeProvost et al., 1994) were used to simulate the tides. Tidal simulations (without storm meteorological parameters) were performed to demonstrate consistency between the simulated and predicted tidal phasing, range and amplitude. River flows were specified for the Mississippi and Atchafalaya Rivers at Baton Rouge and Simmesport, Louisiana, respectively. A steady flow boundary condition, equal to the highest mean monthly flow rate from August to October, was applied for each river. The months of August, September and October were selected for determination of the representative "normal" river flow conditions because they are the months for peak hurricane activity (AREVA, 2015a). River flow rates were determined from the U.S. Geological Survey (USGS) stream gage stations at Baton Rouge and Simmesport (USGS, 2014a). Wind fields were developed for input to the ADCIRC model using the Dynamic Holland Model (Fleming et al., 2008). Storm parameters used in developing the wind field include latitude of the cyclone eye in decimal degrees, longitude of the cyclone eye in decimal degrees, maximum 10-meter altitude, 1-minute sustained wind speed in knots, minimum sea level pressure in millibars, radius of maximum winds in nautical miles, and date/time.

6. PMSS Simulation/Calculation: ADCIRC simulations were performed for hurricanes that are consistent with the range of meteorological parameters representative of the PMH (AREVA, 2015a). The storms were selected based on the results of the screening-level assessment done using SLOSH. However, due to the limitations of the SLOSH model in simulating the complex site condition between the coast and WSES, a preliminary set of ADCIRC simulations were performed to further characterize flood sensitivity to parameter variation, followed by the final PMSS set of storm surge simulations. The storms were simulated such that they made landfall coincident with the high tide elevation (antecedent water level condition at the coast). Each storm track was simulated for a minimum of 31 days, with each storm making landfall on day 30. The meteorological input representing the hurricane parameters was applied in the model three days prior to landfall with the meteorological input being "ramped up" over the first 24-hour period to ensure that the full meteorological input is in effect at least two days prior to landfall. The ADCIRC simulation was restarted at the time of application of the meteorological input from day 27, with conditions representative of the steady flow rates in the rivers and full tidal input. Simulations were performed assuming steady conditions.

7. Projected Subsidence and AWL Adjustment: Predicted ground subsidence at WSES was calculated based on historic and current topographic surveys at WSES. Previously and currently measured elevations at select locations (reference points) were compared. The differences between the two sets of survey data represent ground settlement at the site over this time period. The calculated subsidence rate was compared to regional subsidence rates from publicly available sources (e.g., USGS, 2001) to check for

consistency. The ADCIRC modeling results (water levels) were adjusted for projected land subsidence using linear superposition, based on the calculated projected subsidence rate at WSES. The simulated elevations were also adjusted for differences in the calculated and simulated antecedent water levels. This approach is consistent with the method used by USACE for the Louisiana Coastal Protection and Restoration Project to account for relative, future sea level rise (USACE, 2009).

3.4.3 Assumptions

The following justified assumptions were made as part of this re-evaluation:

PMH Calculation (AREVA, 2015a)

1. The capture zone(s) used for this calculation was assumed to represent an area representative of the PMH parameters at WSES because it: (a) provides an adequate sample for calculations; (b) represents the surge-producing area for WSES; (c) captures the meteorological effects of the Gulf of Mexico Loop Current, and (d) produces limited latitudinal variations in storm parameters.
2. Interpolated storm parameters (at 1-hour intervals) from the compiled tropical cyclone storm set were conservatively assumed equally likely to occur at any location within the defined capture zone.
3. The spline interpolation was assumed to better represent the evolution of the hurricane parameters than the raw HURDAT 6-hourly data, thereby filling in the temporal gaps, because it provides a smoother transition between the 6-hourly values.
4. For certain calculations, a peripheral pressure (P_w) value of 1,015 millibars (mb) was used to calculate pressure deficit (ΔP) based on observed central pressure data. This value was selected based on analysis of the observed data and represents a conservative 95-percent upper confidence level for the peripheral pressure in the study region, as described in the PMH calculation (AREVA, 2015a).

PMSS Calculation (AREVA, 2015b)

1. Per regulatory guidelines (ANS, 1992; NRC, 2011; NRC, 2013), the observed sea level rise trend at Pensacola, FL was used. The mean, sea level rise rate observed at Pensacola, FL was assumed to be a representative water level change for the southeast Louisiana coast, because Pensacola is often used as a control/reference gage for calculating land subsidence rate at other locations along the GoM coast (Gonzalez and Tornqvist, 2006; USGS, 2014b).
2. An average value for the highest monthly thermal expansion of water/steric water level adjustment along the GoM coastline was used.
3. Thirty years of remaining WSES plant life were conservatively used for the calculation of sea level rise and projected subsidence.
4. Future ground subsidence rates are assumed to be the consistent with observed rates.
5. Projected subsidence was not accounted for in elevation data in the SL16 ADCIRC model mesh. An elevation adjustment equal to the calculated projected subsidence at WSES was applied to the calculated storm surge elevations.
6. Recently constructed (post 2010) HSDRRS structures/modifications are not included in the SL16 ADCIRC model mesh. The new HSDRRS is capable of defending against up to a 100–year level of storm surge (USACE, 2014). The PMSS is considerably larger than the 100-year surge and hence these new structures will likely be overwhelmed by the PMSS.

3.4.4 Results

The following sections describe the results of the PMH and PMSS evaluations at WSES.

3.4.4.1 Probable Maximum Hurricane

Initial calculation of PMH parameters using FT based on the site location are provided in Table 3-17. The FT PMH was further evaluated using the results of the site and region specific hurricane climatology study.

The following provides a summary of the the results of the site and region specific hurricane climatology study. Full descriptions of the study methods, calculations, and results are described in the PMH calculation (AREVA, 2015a).

The GOM coast experiences an average of one storm surge $\geq$ 16.4 ft (5 meters) per decade, which is the second highest rate in the world (Needham, 2014). Figure 3-36 indicates the 10 highest storm surge/storm tide levels observed in the region since 1880 and Table 3-18 provides detailed information on each event. WSES is impacted by storm surges that approach from the southwest, south, southeast and northeast. Surges approaching from the northeast propagate from the southwestern portion of Lake Pontchartrain. Surges from the southwest approach WSES from eastern Vermillion Bay, near Morgan City. Surges from the south propagate from Southern Terrebonne and Lafourche Parish. Surges from the southeast approach WSES from Jefferson Parish, near Grand Isle.

The tracks of major hurricanes that have occurred in the Atlantic Basin (including the GoM) from 1851 through 2010 are shown in Figure 3-37 (NOAA, 2014a). The tracks show the entire life of each cyclone, with the yellow portion the period of major hurricane intensity, the solid red indicating the period of tropical cyclone of less than Category 3 intensity, and the dashed red indicating the formative or dissipating stage.

The following characteristics are apparent from the tracks shown in Figure 3-37:

- Nearly all major hurricanes form over the tropical Atlantic, Caribbean or southern GoM and reach major hurricane status in those areas.
- The predominant direction of motion is westward at latitudes south of the Florida peninsula.
- Across the latitudes that span Florida, major hurricanes typically have or develop a strong northward component of motion.
- Storms increase in intensity as they pass the warm GoM water (in particular, the areas of the Loop Current and warm-water eddies).

The presence of warm-water currents within the GoM can cause hurricanes to intensify as they track over the warm water. These currents serve as the mechanism to transport heat and energy within the GoM, and can be both horizontal (across the surface) and vertical (from the surface of the water to depth and vice-versa). The most important current in the GoM is the Loop Current (Figure 3-38), which is an extension/diversion of the Gulf Stream. It forms where water is warmed as it travels through the Caribbean, and then enters the Gulf through the Yucatan Channel – between the Yucatan Peninsula and Cuba. From there, it loops into the GoM in a clockwise direction forming a horseshoe shaped current, and exits the GoM between Cuba and Florida. It brings very warm water (at depth) into the GoM. The presence of the relatively warm water causes storms to intensify as they travel over the current and also to weaken at a lower rate since warm water, rather than cooler water, is brought to the surface from the turbulence at the water surface that occurs beneath the hurricane (i.e., upwelling). Warm-water eddies that can take months to dissipate are also present outside the main current.

Hurricane Katrina of 2005 provides an example of the Loop Current's influence on hurricane intensification. When the storm track passed over the warm waters associated with the Loop Current, it experienced rapid intensification to a strong Category 5 strength between 170-175 mph. As the hurricane moved closer to shore, it moved over cooler water, which decreased its intensity before landfall. Hurricane Rita made a similar pass over the Loop Current a few weeks after Katrina and it also intensified at that time.

Hurricanes making landfall along the northern Gulf Coast generally traverse the GoM in less than 4 days and, during that time, their intensity size and wind field geometry undergo major changes (Jacobsen, 2013). The conditions most affecting these changes include (Jacobsen, 2013):

- Land Masses: Hurricanes which avoid the mountainous Caribbean islands typically emerge into the GoM with stronger circulation centers.
- SSTs: As discussed previously, hurricanes which track over the Yucatan Straight or the waters near western Cuba experience the effects of the Loop Current. Hurricanes lose intensity as they leave these relatively warm water areas and traverse cooler water. Storm intensity is correlated with SSTs for intense hurricanes. Also, the correlation may be greater with depth-averaged sea temperatures rather than SSTs, as evidenced by storm intensification over the Loop Current which has warm water at depth.
- Atmospheric Conditions: Hurricane stability and growth are inhibited by encounters with: 1) masses of cool dry air; 2) regional environments of high wind shear; and 3) interfering upper level pressure systems.

Significantly, the ocean (through its heat and moisture fluxes) governs the behavior of tropical cyclones in the GoM. Most major hurricanes reached their peak intensity over the central GoM over the Loop Current and warm-water eddies (Rappaport et al., 2010). These deep heat reservoirs are also more resistant to cooling by hurricane-induced turbulent mixing. Increases in hurricane intensity suggest a lag of about 12 to 15 hours upon encountering these deep warm water reservoirs.

Intense hurricanes lose strength and symmetry as they approach landfall and move onshore (i.e., increase in central pressure, a process called "filling") both due to frictional resistance over land and to the presence of cooler water. Along the northern Gulf Coast, the SST drop due to turbulent mixing is about 1°C (Rappaport et al., 2010). On average, Category 1 to 2 hurricanes strengthen and Category 3 to 5 hurricanes weaken by landfall. Weakening in the last 6 to 24 hours prior to landfall was also characterized by an increase in R_{max} and decrease in Holland B (Resio, 2007).

GoM hurricanes typically undergo pronounced decay with landfall approach, based on "best track" data for the study period of 1979 to 2008 (Rappaport et al., 2010). Landfall refers to the time when the center of the tropical cyclone crosses the coast. Eighty-nine U.S. Gulf Coast tropical cyclone landfalls occurred during the 30 year study period. Thirty-four out of the 89 tropical cyclones were classified as hurricanes. The amount and sign of intensity change in hurricanes are strong functions of the initial intensity, with the strongest hurricanes weakening the most (AREVA, 2015a).

Estimates of hurricane intensity decay upon landfall are presented in Kaplan and DeMaria (1995). Kaplan and DeMaria (1995) used maximum sustained wind speeds, in which the maximum wind speed after landfall was approximated as an exponential decay function in time. The study was based on observed historical data south of 37°N Latitude. The analysis results suggest that the average reduction in maximum sustained wind speed is approximately 60 percent of its wind speed at landfall 12 hours after landfall and 70 percent 24 hours after landfall for major hurricanes (i.e., Category 3 and higher). Most storms experience significant intensity decay during the first 6 hours upon landfall, i.e., decrease in wind speed and increase in central pressure (sometimes called "filling").

An analysis was performed to statistically characterize the meteorological hurricane parameters for the region. The results of the statistical analyses were used to support appropriate ranges of PMH parameters for WSES. Data sources for this analysis include both the complete 1851-2013 storm data from HURDAT, including the 1979-2012 subset containing central pressure data and the complete 1988-2013 storm data from the Extended Best Track Database (RAMMB, 2014). A second data set was developed for this calculation to increase the quantity of data for the purpose of creating univariate probability distributions of the parameters, using synthetic data available from Florida State University (FSU). The synthetic data was created by FSU by interpolation of the 6-hourly HURDAT and Extended Best Track Data storm data. Specifically, 1-hourly interpolated HURDAT and Extended Best Track Data were developed for the time period from 1851-2013 (FSU, 2014). The methodology used by FSU to develop the interpolated hourly HURDAT database is presented in Elsner and Jagger, 2013.

A cutoff threshold of 63 kt was used to remove data points associated with a V_{max} value less than 63 kt from the data set. That is, the data analyzed represents data for tropical cyclones that are of Category 1 Hurricane intensity

or greater, and does not include tropical storms or tropical depressions. The purpose of the threshold of 63 kt was to exclude tropical storms with weak intensity that is not representative of the PMH.

Two capture zones (primary and subset capture zones) were used for statistical analysis of the hurricane data. The limits of the first, primary data capture zone used for this calculation are shown in Figure 3-44. The rationale used to select the limits of the capture zone includes:

1) to have limits broad enough that an adequate amount of data is available to perform statistical analysis;
2) to limit the bounds of the storm tracks to a distance from landfall that is approximately and conservatively representative of the surge-producing zone;
3) to capture the effects of the Loop Current on the hurricane parameters within the surge-producing zone; and
4) to limit the southern extent of the capture zone within the GoM such that latitudinal variations in storm parameters are small.

Each data point represents a distinctive condition in time and space and includes the following hurricane parameters:

- Time of observation, including year, month, day, hour in coordinated universal time (UTC);
- Location, latitude and longitude in decimal degrees;
- Vmax, observed maximum wind speed in kt;
- P_o, observed minimum central pressure in millibars (mb);
- P_w, observed peripheral pressure in mb;
- ΔP, calculated central pressure deficit in mb, where $\Delta P = P_w - P_o$;
- Rmax, observed radius of maximum wind in kt;
- Vf, calculated forward (translational) speed in kt;
- F_{dir} (θ), calculated forward direction or bearing in degrees (°).

A second, sub-set data capture zone was also analyzed (sub-capture zone). This sub-capture zone was developed to better assess parameter correlations and ranges for the hurricanes expected to generate extreme storm surge at in the vicinity of WSES (e.g., hurricanes making landfall or bypassing close enough to the coastline to generate extreme storm surges). The new sub-capture zone (labeled "Lat N26+", indicating north of latitude 26°N) is shown in Figure 3-45. This data set is a subset of the primary capture zone dataset (LSU, 2014). The data subset was developed by removing data points south of Latitude 26° N.

Datasets from both the primary and sub-set capture zones are plotted for comparison. Figure 3-46 and Figure 3-47 presents an overall view to the parameter correlations in a "matrix" format.

The principal differences indicated for the subset versus primary data capture zones are:

1. The maximum wind speed within the sub-capture zone is up to 149 kt, approximately 11 kt less than the maximum wind speed (160 kt) in the primary capture zone.
2. The combination of a very intense wind speed (e.g., 160 kt) and a very slow moving forward speed (e.g., 5 to 6 kt) is not present in the sub-capture zone.
3. The combination of a very intense wind speed (e.g., 153 kt) and a very large radius (e.g., 25 nm) is not present in the sub-capture zone.

4. Decrease in intensity for the sub-capture zone is also valid in terms of pressure deficit.

Based on these differences, the PMH parameters can be defined more accurately to represent the storm characteristics for the storm surge analysis.

Based on the results of the site and region specific hurricane climatology study, certain hurricane parameters generated using FT were revised to reflect the current state of knowledge. The environmental setting in the GoM is conducive to the generation of intense hurricanes, including the potential for hurricanes to briefly reach the regional MPI (maximum wind speeds of 175 kt) over open water. However, the theoretical MPI of 175 kt is not sustainable as the storm approaches the coast and moves away from the warmest ocean water in the GoM Loop Current. Further, non-steady state storms above Category 3 reflect weakening as hurricanes landfall or approach landfall. The ranges of PMH parameters recommended for use in calculating the PMSS for WSES are based on the sub-capture zone data and are presented in Table 3-17 and below:

Peripheral Pressure (P_w): Observed peripheral pressure (P_w) data is available for the period of 1988 to current. For this period, the mean observed P_w for all the hurricanes within the defined capture zone is 1,009.5 mb with a standard deviation of 2.5 mb. The recommended peripheral pressure of 1,015 mb is about 2 standard deviations away from the mean P_w and approximately represents the upper 95 percent confidence level for P_w based on the historical data.

Central Pressure (P_o): Observed central pressure (P_o) data is available for the period of 1852 to current. For this period, the mean observed P_o for all the hurricanes within the defined capture zone is 962.5 mb with a standard deviation of 21.6 mb. The recommended minimum central pressure of 883 mb is more than 3 standard deviations away from the mean P_o and conservatively represents the upper 99 percent confidence level for P_o, assuming the normal distribution. This value is also 9 mb smaller than the minimum central pressure value of 892 mb, observed during the Labor Day Hurricane 1935. Using the univariate GEV distribution, the non-exceedance probability for P_o of 883 mb is approximately 0.001. Using the frequency analysis results with annual maxima data for P_o, the annual non-exceedance probability for P_o of 883 mb is approximately 0.006.

Central Pressure Deficit (ΔP): Calculated central pressure deficit (ΔP) data is available for the period of 1852 to current, assuming a peripheral pressure of 1,015 mb. For this period, the mean observed ΔP for all the hurricanes within the defined capture zone is 52.5 mb with a standard deviation of 21.6 mb. The recommended central pressure deficit of 132 mb is more than 3 standard deviations away from the mean ΔP and conservatively represents the upper 99 percent confidence level for ΔP, assuming the normal distribution. This value is 9 mb higher than the maximum historical value of 123 mb with a peripheral pressure of 1,015 mb, recorded during the Labor Day Hurricane 1935. Using the univariate GEV fit, the exceedance probability for the recommended maximum pressure deficit of 132 mb is approximately 0.002. Using the frequency analysis results with annual minima data, the annual exceedance probability for ΔP of 132 mb is approximately 0.004. This recommended value is also consistent with the MPI values from published sources (Bister and Emanuel, 2014; USACE, 2009) (Figure 3-39).

Maximum Sustained Wind Speed (V_{maxs}): Calculated maximum wind speed (V_{maxs}) data is available for the period of 1851 to current. V_{maxs} scatter plots for maximum wind speed are presented in Figure 3-40 through Figure 3-43. Datasets from both capture zones (Figure 3-44 and Figure 3-45) are plotted for comparison. FT maximum wind speeds for four different bounding conditions and published MPI values are also shown for reference. The MPI of a tropical cyclone is the theoretical limit of the strength of a tropical cyclone.

Using the same approach adopted by FT, V_{max} values for four bounding scenarios are selected and presented in Table 3-17. The mean observed V_{maxs} for all the hurricanes within the defined capture zone (Figure 3-44) is 88.1 kt with a standard deviation of 18.7 kt. The recommended maximum wind speed of 160 kt is more than 3 standard deviations away from the mean V_{maxs} and conservatively represents the upper 99 percent confidence interval for V_{maxs}, assuming the normal distribution. The 160-kt value is also more conservative than the highest V_{max}

predicted using FT methodology (158 knots). Using the univariate GEV fit, the exceedance probability for the recommended maximum sustained wind speed of 160 kt is approximately 0.004. Using the frequency analysis results with annual maxima data, the annual exceedance probability for V_{maxs} of 160 kt is approximately 0.012.

FT V_{max} values were adopted for the other three scenarios and were judged to be conservative compared with historical data. For example, the lowest V_{max} of 149 kt is conservative compared to the historical data for the subset data capture zone for an R_{max} of 25 nm (Figure 3-42). For the dataset from the full capture zone, the equivalent circular wind speed V_{max}* of 143 kt (total wind speed – forward speed =149 kt – 6 kt) for an R_{max} of 25 nm is 2 kt lower than one of the historical data points of 145 kt (total wind speed – forward speed = 153 kt – 8 kt) for an R_{max} of 25 nm. The full capture zone includes the data from the entire GoM and is judged to be unrealistic for landfalling or near-shore hurricanes in the vicinity of WSES. Therefore, the FT V_{max} of 149 kt is recommended in combination with an R_{max} of 25 nm (large) and a V_f of 6 kt (slow).

Radius of Maximum Winds (R_{max}): Calculated radius of maximum winds (R_{max}) data is available for the period of 1992 to current. For this period, the mean observed R_{max} for all hurricanes within the defined capture zone is 22.6 nm with a standard deviation of 12.3 nm. However, R_{max} is significantly negatively correlated to storm intensity for intense hurricanes (i.e., major hurricanes), with R_{max} values not exceeding (based on the historical data) 25 nm for storms with intensities consistent with the PMH. This value of 25 nm is conservative compared to the upper bound of 22 nm as defined in FT (NOAA, 1979). The R_{max} upper bound was increased to 25 nm and is capped to represent meteorological limitations of very intense hurricanes (Figures 3-49 and 3-42). The R_{max} value of 25 nm is approximately the 96th percentile for a ΔP of 132 mb based on the functional fit proposed by Toro, 2008 (Figure 3-50). Therefore, it approximately represents the upper 92 percent confidence level (calculation provided in the notes for Figure 3-50).

Forward Speed (V_f): Calculated forward speed (V_f) data is available for the period of 1851 to current. For this period, the mean observed V_f for all the hurricanes within the defined capture zone is 9.0 kt with a standard deviation of 4.1 kt. The recommended upper bound V_f value of 20 kt is 2.7 standard deviations away from the mean and conservatively represents the upper 99 percent confidence interval, assuming the normal distribution. Using the non-parametric kernel fit, the exceedance probability for the recommended upper bound V_f of 20 kt is approximately 0.025. The data also indicates that very intense storms can occur with slow translational speeds (as low as about 5 kt, as shown on Figure 3-51) for the dataset within the full capture zone. In Figure 3-41, there are three data points above 140 kt in the range of 5 to 7 kt in forward speed. These three points were from Hurricane Carla 1961. In a recent re-analysis study (Delgato, 2014), these wind speeds were found to be in the range of 120 to 125 kt, rather than 140. The revisions proposed by Delgato are expected to be considered and incorporated in the next version of the publicly available HURDAT database. The lower bound of 6 kt as specified by FT (NOAA, 1979) is conservative relative to the observed data within the sub-capture zone. Figure 3-41 indicates that the very intense storms move at faster speeds (around 10 kt) in the sub-capture zone.

Storm Bearing (θ): Calculated storm bearing (θ) data is available for the period of 1851 to current. For this period, the mean observed θ for all the hurricanes within the defined capture zone is -21.9 degrees with a standard deviation of 51.8 degrees. Using the non-parametric kernel fit, the recommended range of -80 to 10 degrees approximately represents 60 percent of the all possible track directions. Also, hurricanes with a more westward bearing would: 1) experience decay over land; or 2) are not likely to result in a PMSS. The scatter plot shown in Figure 3-46 indicates that this selected bearing range is conservative for the data within the sub-capture zone.

Holland B: Holland B for major hurricanes, based on review of the data within the capture zone, ranges approximately from 1 to 1.5. The very intense hurricanes indicate a Holland B parameter close to 1.3 to 1.5 based on the historical record. The proposed PMH parameter combinations are consistent with the FT parameters and reasonably conservative in terms of calculated Holland B parameters ranging from 1.1 to 1.3, which indicate a relatively flat, wide wind profile. Note that the vertical axis is maximum wind speed for stationary storm (V_{maxs}*), which was approximated by subtracting V_f from V_{maxs}.

Offshore Decay: The total central pressure increase (filling) due to offshore intensity decay (over the distance of 90 nm from shore) was calculated as:

25 – 6 = 19 mb

For the offshore Rmax = 25 nm. The maximum central pressure increase for the offshore decay phase recommended by IPET (Resio, 2007) is 18 mb; therefore, an 18 mb central pressure increase was linearly applied along the track from 90 nm offshore to landfall (or 1 hour past landfall). The forward PMH translational storm speed is 6 kt; therefore, the offshore decay was initiated at about 15 hours before landfall and ended at landfall (or 1 hour after landfall). The corresponding maximum wind speeds (V_{max}) were calculated using the regression analysis results for V_{max} vs ΔP (AREVA, 2015a). The increased central pressures were converted to pressure deficit (ΔP) assuming a peripheral pressure of 1,015 mb.

Post-Landfall Decay: Analysis of the decay of historical GoM hurricanes shows that most intense hurricanes (Category 3 and higher) lose strength significantly after landfall (Figure 3-48). A conservative, post-landfall decay rate of -3 kt per hour for maximum wind speed and +2 mb per hour for central pressure is recommended for use in the PMSS calculation based on the post landfall decay rate of historical GoM hurricanes.

The conclusions relative to FT are:

1. No change to the FT values for ΔP is recommended.

2. A minor reduction of the FT P_w and P_o is recommended based on the analysis results of the historical hurricane data in the region.

3. A slightly larger range of R_{max} (to include PMH values of R_{max} up to 25 nm) is recommended based on the analysis results of the historical hurricane data in the region, as well as comparison to values used previously in the region for PMH analysis (Resio, 2007; USACE, 2009).

4. No change to the FT values for V_f is recommended because the FT bounds for V_f are consistent with the historical hurricane data in the region.

5. A larger range of hurricane bearing, θ, (to allow hurricanes with a more westerly bearing) is warranted based on the analysis results of the historical hurricane data in the region.

6. A slight increase to the FT value for V_{max} is recommended for the development of a steady-state wind field to be used in PMSS simulations for the upper V_f and lower R_{max} combination. No change to the FT values for V_{max} is recommended for other scenarios.

3.4.4.2 Probable Maximum Storm Surge

3.4.4.2.1 Development of the Antecedent Water Level

In accordance with NUREG/CR-7046 (NRC, 2011), the PMSS is required to be evaluated coincidentally with an AWL equal to the 10% exceedance high tide plus long term changes in sea level in addition to other adjustments unique to the GoM including steric water level and datum adjustment. The 10% exceedance high tide is defined as the high tide level that is equaled or exceeded by 10% of the maximum monthly tides over a continuous 21 year period. In accordance with ANSI/ANS-2.8-1992 (ANS, 1992), this tide can be determined from recorded tide data or from predicted astronomical tide tables.

The 10% exceedance high tide was calculated using recorded monthly maximum tide elevations from NOAA tidal gage stations at Grand Isle, Dauphin Island and Eugene Island. Using this approach, an average value of

2.21 ft, LMSL was obtained. Data at NOAA station at Pensacola, Florida indicates a relative sea level rise rate of 2.1 mm per year (NOAA, 2014d). The mean sea level rise rate observed at Pensacola, Florida was selected since the Pensacola does not experience significant ground subsidence and was often used as a control/reference gage for calculating land subsidence rates at other locations along the Gulf coast (Gonzalez and Tornqvist, 2006; USGS, 2014b). The projected 30 year SLR using the annual rate at the NOAA tidal gage station at Pensacola, Florida, the AWL was determined to be 0.3 ft.

The average LMSL to NAVD88-2004.65 adjustment for the South Louisiana region is calculated to be 0.135m (0.44 ft).

Long-term NOAA tidal station data at Stations along the Gulf Coast (Pensacola, Dauphin Island, Grand Isle, Galveston Pier, Eugene Island, and Sabine Pass) indicate that the largest average increase in water levels above MSL in the Gulf of Mexico occur in September. The average increase in water at these stations is 0.133 m (Table 3-19). A steric water level adjustment of 0.133 m (0.436 ft) was applied to the initial water levels in the ADCIRC model at the beginning of the simulations.

The total recommended AWL is calculated as:

$$HT_{10\%} \text{ (including steric water level adjustment)} + SLR + \text{Datum Adjustment}$$

$$= 2.21 \text{ ft} + 0.26\text{ft} + 0.44 \text{ ft}$$

$$= \underline{\mathbf{2.9 \text{ ft}}}, \text{ NAVD88-2004.65}$$

The datum adjustment, sea level rise adjustment and the steric water level adjustment were applied as adjustments to the initial water levels in ADCIRC. The 10-percent exceedance high tide was simulated in ADCIRC using tidal constituents. The total adjustment to the initial water levels in ADCIRC prior to the simulations is:

$$0.135 \text{ m (Datum Adjustment)} + 0.133 \text{ m (Steric Water Level Adjustment)} + 0.08 \text{ m (Sea Level Rise)}$$

$$= \underline{0.35\text{m (1.15 ft)}}$$

3.4.4.2.2 PMH Parameter Combination Sensitivity Analysis

A total of 4,800 simulations were performed using the NOAA SLOSH model. The operational New Orleans (ms7) SLOSH basin was used. SLOSH results in the form of simulated surge elevation time series for each simulation were extracted at locations within the New Orleans (ms7) basin, along the coastline and at WSES. The SLOSH parameter sensitivity analysis results indicate that storm surge at WSES is maximized by two scenarios:

(1) Storms which are large in size, slow-moving with a northwest bearing. These storms are capable of transporting a significant volume of water (from the coastal surge) into Lake Borgne and Lake Pontchartrain. Due to the location of the maximum winds within the simulated, idealized cyclones, simulated storm surge is also maximized by storms making landfall to the south of the Lake Borgne opening. These slow-moving storms are able to maintain momentum and significantly increase the water level in Lake Pontchartrain, with the potential to overtop the north bank of the Mississippi River levee.

(2) Storms which are large in size, relatively slow-moving with a northerly bearing. These storms are capable of transporting a significant volume of water (from the coastal surge) over the low-lying marsh areas to the south of WSES. The simulated storm surge is maximized by storms making landfall to the west of WSES.

3.4.4.2.3 ADCIRC Model Validation

The SL16 mesh has 5,035,113 nodes and 9,945,623 elements and extends to the mid-Atlantic Ocean. Levees, floodwalls, and raised coastal roads and railroads are represented in the mesh as internal boundaries (weirs). The

ADCIRC model grid is presented in Figure 3-52 and Figure 3-53. The model mesh elevation data are presented in Figure 3-54. The results of the hindcast simulations of Hurricanes Katrina, Rita, Gustav and Ike (Dietrich, et al., 2012), is presented in Table 3-20 to Table 3-23. Simulated peak surge elevations were compared to High Water Mark (HWM) elevations. These observed HWMs were from High Water Mark Collection reports after the storm in the States of Louisiana, Mississippi and Alabama (FEMA, 2006a, 2006b and 2006c) and the USACE (UASCE, 2006). The results of the hindcast simulations do not indicate a significant bias towards either over prediction or under prediction of surge elevations. No adjustments related to uncertainty in model prediction were applied to the calculated surge elevations using the SL16 grid (AREVA, 2015c).

3.4.4.2.4 Tidal, River and Meteorological Inputs

Tide Input

An analysis of the tide gage data at Grand Isle identified the occurrence of the highest astronomical high tide of 1.26 ft LMSL to be October 18, 1989 at 04:54. This documented, historical tide amplitude, although less than the calculated 10-percent exceedance high tide, was used to create tidal conditions for the storm surge simulations. An adjustment equal to the difference between the simulated antecedent water level and the calculated antecedent water level was added to the calculated surge values. The K1, K2, M2, N2, O1, Q1 and S2 tidal constituents were selected for the date of September 18, 1989 and the tidal flow was simulated in ADCIRC for a period of 30 (simulated) days. The tidal input was ramped up over a 24-hour period to avoid model instability. As demonstrated by the results of the tide simulation (Figure 3-55), the K1 (Luni-solar diurnal), K2 (Luni-solar semidiurnal), M2 (Principal lunar), N2 (Larger lunar elliptic), O1 (Principal lunar diurnal), Q1 (Larger lunar elliptic) and S2 (Principal solar) tidal constituents make up a significant portion of the tidal signal along the Gulf Coast. The results indicate that ADCIRC acceptably simulates the tidal amplitude and phasing.

River Flow

The highest monthly mean flow rates in the Mississippi and Atchafalaya Rivers during the peak hurricane months (August-October) occur in August. The August mean flow rate in the Mississippi River at Baton Rouge is 343,000 cubic ft per second (cfs) or 9,713 cubic meters per second (cms) and the August mean flow rate in the Atchafalaya River at Simmesport is 146,000 cfs or 4,134 cms. The monthly mean statistics for the Mississippi River at Baton Rouge and the Atchafalaya River at Simmesport from the USGS were used in the PMSS simulations for WSES.

Meteorological Inputs - Tropical Cyclone Wind Field

Meteorological input (fort.22) files were created based on the PMH parameters (Table 3-17) and the results of the PMH parameter combination sensitivity analysis done using SLOSH. Each fort.22 file represents a PMH parameter combination.

3.4.4.2.5 Probable Maximum Storm Surge Simulations

Antecedent Water Level/Tide Simulation

Table 3-24 and Figure 3-56 show the simulated water levels. Because dynamic tides were simulated based on astronomical/predicted tides (i.e., excluding meteorological effects), a final adjustment is made to linearly add the difference between the peak predicted tide and the simulated AWL. The simulated AWL is 2.5 ft, NAVD88-2004.65 compared to the targeted antecedent water level of 3.5 ft, NAVD88-2004.65. An adjustment to be applied to the simulated surge elevations is calculated as follows:

- Average ADCIRC simulated AWL along coastline = 2.5 ft, NAVD88-2004.65.
- Calculated AWL = 2.9 ft, NAVD88-2004.65.
- Linear Elevation Adjustment to Surge Elevations = 2.9 ft – 2.5 ft = 0.4 ft.

The linear adjustment to the surge elevations is due to the under prediction of the 10-percent exceedance high tide elevation. The high tide is a transient condition and thus a linear adjustment is appropriate (as opposed to sea level rise or steric water level adjustment).

ADCIRC Storm Surge Sensitivity Simulations

Based on the SLOSH results of the PMH parameter combination sensitivity analysis, eighteen storms to be simulated by ADCIRC were identified (numbered 1 through 11 and 101 through 107). These storms represented hurricane parameter combinations capable of creating the largest surge elevations at WSES. The input parameters for these storms are summarized in Table 3-25. Note that some parameter combinations were allowed to vary beyond the recommended PMH parameter bounds, to better assess parameter sensitivity and uncertainty. Two storms, 106 and 107, were formulated based on FT parameter ranges (NOAA, 1979). These storms were simulated in ADCIRC in combination with:

1. Tides and initial water level adjustments to represent antecedent water level conditions; and
2. Flow rates in the Mississippi and Atchafalaya Rivers equal to the mean August flow rates.

The simulated storm tracks are shown in Figure 3-57. The storms were simulated such that they made landfall coincident with high tide elevations representative of the calculated antecedent water level along the GoM coast.

The simulation results were evaluated at several, representative locations within the ADCIRC mesh, including WSES, within the Mississippi River near WSES and along the right descending levee near WSES, to further evaluate surge sensitivity to parameter and landfall variation. The results of the sensitivity analysis simulations in ADCIRC are presented in Table 3-25.

It is noted that the simulation results at and near WSES demonstrate a very high sensitivity to parameter and landfall variations, with minor variations often resulting in significant differences in the predicted storm surge elevations. This is due, principally, to the very complex hydrological setting which includes a complex system of levees and other flood control features. The hydrological setting is further complicated by the interaction between flooding among different hydrological features such as the lakes and the Mississippi River. Floodwaters exceeding crest elevations of levees separating these features can dramatically change the flood spatial distribution.

ADCIRC Probable Maximum Storm Surge Simulations

A total of ten final PMSS ADCIRC simulations, numbered 201 through 210 were identified and simulated based on the sensitivity results (Table 3-25). The results of the final simulation set identified the PMSS to result Storm 202. Storm 202 is a slow moving (forward speed of 6 kt), north tracking storm making landfall east of Eugene Island (Landfall Point 3 in Figure 3-58). Storm 202 has a CPD of 132mb, a bearing of 0°, a V_{max} of 149 kt and an R_{max} of 25 nm (Table 3-26). The resulting maximum unadjusted surge elevation from Storm 202, when offshore and post-landfall decay are not applied, is 22.4 ft NAVD88-2004.65 at WSES and 25.3 ft NAVD88-2004.65 in the Mississippi River near WSES (Table 3-26). Including offshore and inland post-landfall intensity decay for the Storm 202 results in an unadjusted maximum stillwater elevation at WSES of 19.5 ft, NAVD88-2004.65 (Table 3-27, Figure 3-59 and Figure 3-60). Time series of water levels at WSES, and in the Mississippi River near WSES are shown in Figure 3-61.

3.4.4.2.6 ADCIRC Simulated Water Elevation Adjustments

The adjustment for AWL is 0.4 foot and the adjustment for projected subsidence is 0.3 foot. The total adjustment to the ADCIRC simulated PMSS stillwater elevations at WSES is therefore:

Total Adjustment = 0.4 ft (AWL adjustment) + 0.3 ft (Projected Subsidence Adjustment) = 0.7 ft.

The ADCIRC-calculated storm surge water elevations were adjusted for antecedent water level and projected land subsidence upon completion of the numerical simulations. The adjusted water levels are presented in Table 3-28. The adjusted PMSS stillwater elevation at WSES is 23.1 ft NAVD88-2004.65 for Storm 202, the worst case for WSES due to the PMSS. Based on the preliminary PMSS results predicted in this calculation (i.e., PMSS stillwater elevation without waves and river flood conditions) for Storm 202, the coastal storm surges propagating from the south do not overtop the right descending levees in the vicinity of WSES; storm surges encroaching from the Lake Pontchartrain do not overtop the left descending levees in the vicinity of WSES. Including offshore and inland post-landfall intensity decay for the worst storm (Storm 202), the adjusted maximum PMSS stillwater elevation (without waves and river flood conditions) at WSES is 20.2 ft, NAVD88-2004.65 (Table 3-27).

3.4.5 Conclusions

With post-landfall and offshore decay applied to storm 202, the PMSS stillwater elevation at WSES is 20.2 ft NAVD88-2004.65 (21.6 ft, MSL Plant Datum).

3.4.6 References

ANS, 1992. American National Standard for Determining Design Basis Flooding at Power Reactor Sites (ANSI/ANS 2.8 – 1992).

AREVA, 2015a. AREVA Document No. 32-9227002-000, "Waterford Steam Electric Station Flooding Hazard Re-Evaluation – Probable Maximum Hurricane", 2015.

AREVA, 2015b. AREVA Document No. 32-9227005-000, "Waterford Steam Electric Station Flooding Hazard Re-Evaluation – Probable Maximum Storm Surge", 2015.

AREVA, 2015c. AREVA Document No. 32-9227036-000, "Waterford Steam Electric Station Flooding Hazard Re-Evaluation – Combined Effects," GZA GeoEnvironmental, Inc., 2015.

Bister and Emanuel, 2014. Hurricane Climatological Potential Intensity Maps and Tables, M. Bister and K. Emanuel, Program in Atmospheres, Oceans, and Climate, Massachusetts Institute of Technology. Available at http://wind.mit.edu/~emanuel/pcmin/climo.html. Accessed in September 2014. Last updated date not available. *

Delgado, 2014. Reanalysis of the 1954-1963 Atlantic Hurricane Seasons, S. Delgado, Florida International University, College of Arts and Sciences, FIU Electronic Theses and Dissertations, Paper 1511, http://digitalcommons.fiu.edu/etd/1511.

Dietrich et al., 2011. "Hurricane Gustav (2008) waves, storm surge and currents: hindcast and synoptic analysis in Southern Louisiana". Dietrich, J.C.,Westerink, J.J., Kennedy, A.B., Smith, J.M., Jensen, R.E., Zijlema, M., Holthuijsen, L.H., Dawson, C.N., Luettich, R.A. Jr., Powell, M.D., Cardone, V.J., Cox, A.T., Stone, G.W., Pourtaheri, H., Hope, M.E., Tanaka, S., Westerink, L.G., Westerink, H.J., Cobell, Z.: Mon. Weather Rev. (2011). doi:10.1175/2011MWR3611.1

Dietrich, et al., 2012. Performance of the Unstructured-Mesh, SWAN+ADCIRC Model in Computing Hurricane Waves and Surge, J.C. Dietrich, S. Tanaka, J.J. Westerink, C.N. Dawson, R.A. Luettich Jr., M. Zijlema, L.H. Holthuijsen, J.M. Smith, L.G. Westerink, H.J. Westerink, Journal of Scientific Computation, 52:468-497. DOI 10.1007/s10915-011-9555-6.

Elsner and Jagger, 2013. Hurricane climatology: a modern statistical guide using R, Elsner, J.B. and T.H. Jagger 2013. Oxford University Press, 430pp. Also available at http://www.hurricaneclimate.com/. Accessed in September 2014. Last updated in September 2014.

Emanuel, 2000. A Statistical Analysis of Tropical Cyclone Intensity, K. Emanuel, Monthly Weather Review, April 2000. Pp.1139-1152.

FEMA, 2006a. High Water Mark Collection for Hurricane Katrina in Louisiana, FEMA-1603-DR-LA, Task Orders 412 and 419, Federal Emergency Management Agency, March 2006.

FEMA, 2006b. Final Coastal and Riverine High Water Mark Collection for Hurricane Katrina in Mississippi, FEMA-1604-DR-MS, Task Orders 413 and 420, Federal Emergency Management Agency, March 2006.

FEMA, 2006c. High Water Mark Collection for Hurricane Katrina in Alabama, FEMA-1605-DR-AL, Task Orders 414 and 421, Federal Emergency Management Agency, April 2006.

FEMA, 2008. Flood Insurance Study: Southeastern Parishes, Louisiana, Intermediate Submission 2: Offshore Water Levels and Waves, Federal Emergency Management Agency and US Army Corps of Engineers, New Orleans District. Available on the web at: http://www3.nd.edu/~coast/reports_papers/SELA_2007_IDS_2_FinalDraft/Text%20SELA%202007%20IDS%202%20FINAL%20072808.pdf. Accessed in September 2014. Last updated in July 2008.

Fleming et al., 2008. "A Real Time Storm Surge Forecasting System using ADCIRC", Fleming, J.G., Fulcher, C.W., Luettich, R.A., Estrade, B.D., Allen, G.D. and Winer, H.S. 2008.

FSU, 2014. Interpolated Hourly HURDAT Data from 1851 to 2013, provided by J. B. Elsner and T. H. Jagger, Florida State University. Date accessed July 14, 2014. Date updated June 5, 2014. Available at http://myweb.fsu.edu/jelsner/data/best.interp.zip

Gonzalez and Tornqvist, 2006. Coastal Louisiana in Crisis: Subsidence or Sea Level Rise? EOS, Transactions, American Geophysical Union, Volume 87, Number 45, November 2006, 493-498. DOI: 10.1029/2006EO450001.

Jacobsen, 2013. Hurricane surge hazard analysis: the state of the practice and recent applications for southeast Louisiana, prepared for the Southeast Louisiana Flood Protection Authority – East, Task Order 02-03-006, by B. Jacobsen PE, LLC, Baton Rouge, Louisiana, May 2013.

Kaplan and DeMaria, 1995. A Simple Empirical Model for Predicting the Decay of Tropical Cyclone Winds after Landfall, J. Kaplan and M. DeMaria, Journal of Applied Meteorology, Vol. 34, November 1995. Pp 2499-2512.

LeProvost et al., 1994. "Spectroscopy of the ocean tides from a finite element hydrodynamic model", Le Provost, C., Genco, M.L., Lyard, F., Vincent, P. and Canceil, P., Journal of Geophysical Research, 99(C12):24777–24797, 1994.

LSU, 2014. Source data files containing hurricane parameters "Capture_Zone_Obs_HU_only_RAW.csv" and "Capture_Zone_Obs_HU_only.csv", Louisiana State University, August 2014.

MRC, 2007. "The Mississippi River and Tributaries Project: Controlling the Project Flood", information paper, Mississippi River Commission, 2007.

Needham, 2014. A Data-Driven Storm Surge Analysis for the U.S. Gulf Coast. Doctoral Dissertation, Needham, H.F., 2014, successfully defended March 31, 2014, Louisiana State University.

NOAA, 1979. Meteorological Criteria for Standard Project Hurricane and Probable Maximum Hurricane Windfields, Gulf and East Coast of the United States, Technical Report FT, Schwerdt, R.W., Ho, F.P., & Watkins, R.R.,. Washington D.C., National Oceanic and Atmospheric Administration, 1979.

NOAA, 2014a. Tides and Currents, Grand Isle, Louisiana, 8761724, National Oceanic and Atmospheric Administration. Data retrieved August 2014. Date modified August 2014. Available at http://tidesandcurrents.noaa.gov/stationhome.html?id=8761724 .

NOAA, 2014b. Tides and Currents, Grand Isle, Louisiana, 8761720, National Oceanic and Atmospheric Administration. Data retrieved August 2014. Date modified August 2014. Available at http://tidesandcurrents.noaa.gov/stationhome.html?id=8761720 .

NOAA, 2014c. Tides and Currents, Dauphin Island, Alabama, 8735180, National Oceanic and Atmospheric Administration. Data retrieved August 2014. Date modified August 2014. Available at: http://tidesandcurrents.noaa.gov/stationhome.html?id=8735180 .

NOAA, 2014d. Tides and Currents, Pensacola, Florida, 8729840, National Oceanic and Atmospheric Administration. Data retrieved in August 2014. Date modified August 2014. Available at http://tidesandcurrents.noaa.gov/sltrends/sltrends_station.shtml?stnid=8729840 .

NRC, 2011. "Design Basis Flood Estimation for Site Characterization at Nuclear Power Plants - NUREG/CR-7046", United States Nuclear Regulatory Commission, November 2011.

NRC, 2013. JLD-ISG-2012-06: Guidance for Performing a Tsunami, Surge, or Seiche Hazard Assessment", U.S. Nuclear Regulatory Commission, January 2013.

RAMMB, 2014. The Tropical Cyclone Extended Best Track Dataset, Regional and Mesoscale Meteorology Branch of NOAA/NESDIS, Colorado State University. Date accessed July 14, 2014, Date Updated February 2014. Available at ftp://rammftp.cira.colostate.edu/demaria/ebtrk/ebtrk_atlc.txt.

Rappaport et al., 2010. Tropical Cyclone Intensity Change before U.S. Gulf Coast Landfall, E. N. Rappaport, J. L. Franklin, A. B. Schumacher, M. DeMaria, L. K. Shay and E. J. Gibney, Weather and Forecasting, Vol. 25, October 2010, pp 1380-1396. DOI:10.1175/2010WAF2222369.1.

Resio, 2007. White Paper on Estimating Hurricane Inundation Probabilities, D. T. Resio, U.S. Army Corps of Engineers ERDC-CHL, May 7, 2007.

Stedinger et al., 1993. Chapter 18: Analysis and Modeling of Hydrologic Time Series, Stedinger, J., Vogel, R., & Foufoula-Georgiu, E., in *Handbook of Hydrology*. McGraw-Hill, 1993. *

SURGEDAT, 2014. SURGEDAT - The World's Storm Surge Data Center. Maps of the Top 10 Gulf Coast Storm Surges. Available on the Web at: http://surge.srcc.lsu.edu/historical_maps.html. Dated accessed August 2014.

Toro, 2008. Joint Probability Analysis of Hurricane Flood Hazards for Mississippi, Final Report prepared for URS Group, Tallahassee, FL in support of the FEMA-HMTAP flood study of the State Mississippi by G. R. Toro, Risk Engineering, Inc., Revision 1, June 23, 2008.

USACE, 2006. Performance Evaluation of the New Orleans and Southeast Louisiana Hurricane Protection System, Draft Final Report of the Interagency Performance Evaluation Task Force, June 2006, U.S. Army Corps of Engineers.

USACE, 2009. Louisiana Coastal Protection and Restoration (LACPR) Final Technical Report, U.S. Army Corps of Engineers, New Orleans District Mississippi Valley Division, June 2009.

USACE, 2012. Hurricane and Storm Damage Risk Reduction System Design Guidelines, New Orleans District Engineering Division, Revision June 2012, United States Army Corps of Engineers.

USACE, 2013. Map titled "Greater New Orleans Hurricane and Storm Damage Risk Reduction System", dated June 2013, map produced by United States Army Corps of Engineers - New Orleans

USACE, 2014. United States Army Corps of Engineers, New Orleans District. http://www.mvn.usace.army.mil/Missions/HSDRRS/RiskReductionPlan.aspx. Date accessed November, 2014. Date last modified not available. Web page maintained by USACE.

USGS, 2001. U. S. Geological Survey Subsidence Interest Group Conference, Proceedings of the Technical Meeting, Galveston, Texas, November 27-29, 2001, Open-File Report 03-308. Sea-Level Rise and Subsidence: Implications for Flooding in New Orleans, Louisiana, V. R. Burkett, D. B. Zilkoski and D. A. Hart. 63-70.

USGS, 2014a. USGS Surface Water Monthly Statistics for the Nation. http://waterdata.usgs.gov/nwis/monthly/?search_site_no=07374000&agency_cd=USGS&referred_module=sw&format=sites_selection_links and http://waterdata.usgs.gov/la/nwis/monthly/?search_site_no=07381490&agency_cd=USGS&referred_module=sw&format=sites_selection_links.

USGS, 2014b. Subsidence and Wetland Loss Related to Fluid Energy Production, Gulf Coast Basin – Induced Subsidence Related to Hydrocarbon Production, U.S. Geological Survey, St. Petersburg Coastal and Marine Science Center. Accessed in November, 2014. Last modified in April, 2014. Available at http://coastal.er.usgs.gov/gc-subsidence/induced-subsidence.html.

Table 3-16: Summary of Landfall Locations

Point No.	FT Mile Post (nautical miles)	Latitude (degrees)	Longitude (degrees)
1	550	29.633	-91.600
2	575	29.275	-91.314
3a	604	29.046	-90.842
3	600	29.046	-90.909
3b	590	29.085	-91.079
5	640	29.125	-90.158
6	660	29.307	-89.856
7	680	29.220	-89.497
4	620	29.078	-90.531
8	700	28.947	-89.387
9	725	29.163	-89.011
10	750	29.640	-88.973
11	715	29.068	-89.084

Table 3-17: PMH Parameter Ranges for WSES

Parameter	Units	Recommended PMH Parameters for WSES	Reference Range per NOAA FT
Peripheral Pressure P_w	(mb)	1015	1020
Central Pressure P_o	(mb)	883	888
Pressure Deficit ΔP	(mb)	132	132
Radius of Maximum Winds R_{max}	(nm)	6 to 25	6 to 22
Forward Speed V_f	(kt)	6 to 20	6 to 20
Bearing θ	(°)	-80 to +10	-60 to +10
Maximum Wind V_{max}	(kt)	V_f | R_{max}: 6 nm, 25 nm 6 kt | 152 | 149 20 kt | 160 | 156	V_f | R_{max}: 6 nm, 22 nm 6 kt | 152 (VLL) | 149 (VUL) 20 kt | 158 (VLU) | 156 (VUU)
Holland B	(--)	1.0 to 1.5	Not Included
Offshore Intensity Decay	(--)	Accounted for. See Note 4	Not Included

Notes:

1. mb = millibars; kt = knots; nm = nautical miles; ° = degrees; yr = years.
2. V_{max} values are presented in the form of "VLU", "VLL", "VUU" and "VUL" as used in FT (NOAA, 1979), where V stands for maximum wind speed, L stands for lower bound, U stands for upper bound. The middle letter denotes radius and the last letter denotes forward speed.
3. Maximum wind speed values were converted from 10-minute average (FT) to 1-minute average (this table) with a multiplication factor of 1/0.88 (Fleming et al, 2008), consistent with the ADCIRC model.

Table 3-18: Top 10 extreme water levels from storm surge/ storm tide along the U.S. Gulf: Coast from 1880-2013 from SURGEDAT database.

Rank	Year	Storm Name	Storm Surge (ft)	Storm Tide (ft)	Datum	Location	State
1	2005	Katrina	--	28	NGVD29	Hancock County EOC	MS
2	1969	Camille	--	24.6	Unknown	Pass Christian	MS
3	1961	Carla	--	22	Mean Sea Level	Port Lavaca	TX
4	1900	Galveston	--	20	Unknown	Galveston	TX
5	1975	Eloise	--	18.2	Mean Sea Level	Dune Allen Beach	FL
6	1935	Labor Day	--	18	Unknown	Lower Matecumbe Key	FL
6	1967	Beulah	18	--	Above Predicted Tide	South Padre Island	TX
8	2005	Rita	--	17.8	NAVD88	Cameron Parish	LA
9	2008	Ike	--	17.5	NAVD88	Chambers County	TX
10	1915	New Orleans	--	17	Unknown	S. of New Orleans	LA

Note: "--" denotes data not available.

Table 3-19: Steric Water Level Adjustment

Station	Highest Mean Monthly Seasonal Change in meters (MSL)
Pensacola	0.129
Dauphin Island	0.126
Grand Isle	0.137
Galveston Pier	0.153
Eugene Island	0.118
Sabine Pass	0.132
Average	**0.133**

Table 3-20: Comparison of ADCIRC Simulated Results and Observed High Water Marks – Hurricane Katrina (2005)

Data Source	Lat	Long	Description	ADCIRC (m)	HWM (m)	Error (m)
FEMA	29.260584	-89.96317	Gulf Coast near Grand Isle State Park	2.54	2.32	0.22
USACE	29.387619	-89.59742	On MS River near Adams Bay	1.58	4.39	-2.81
USACE	29.86083	-89.90774	On MS River near St. Bernard	4.17	3.36	0.81
USACE	29.999022	-90.28475	Inland near Kenner	3.79	1.68	2.11
USACE	30.003	-89.9607	Lake Pontchartrain coast near Laplace	4.68	4.72	-0.04
FEMA	30.02101	-90.12297	Coast of Lake Pontchartrain near Lakeview	3.4	3.32	0.08
FEMA	30.03679	-90.01701	Coast of Lake Pontchartrain near New Orleans East Area	3.57	3.47	0.1
FEMA	30.040939	-90.23858	Coast of Lake Pontchartrain near Kenner	3.1	2.01	1.09
USACE	30.1067	-90.4241	Lake Pontchartrain coast near Laplace	2.41	2.16	0.25
USACE	30.219233	-89.81995	Lake Pontchartrain coast near Eden Isle	4.62	4.02	0.6
USACE	30.3052	-89.3356	Gulf Coast near Bay St. Louis	8.05	7.89	0.16
FEMA	30.314344	-89.25115	Gulf Coast near Pass Christian	7.76	7.62	0.14
FEMA	30.364817	-88.632	Gulf Coast near Pascagoula Bay	5.11	6.43	-1.32
FEMA	30.366902	-89.09876	Gulf Coast near Gulfport	7.52	7.41	0.11
USACE	30.4008	-88.8956	Gulf Coast near Biloxi	6.1	6.25	-0.15
USACE	30.05	-90.3678	Lake Pontchartrain coast near Norco	2.89	1.83	1.06
					Average Error	+0.15

Note: Elevations refer to NAVD88-2004.65.

Table 3-21: Comparison of ADCIRC Simulated Results and Observed High Water Marks – Hurricane Rita (2005)

Lat	Long	Description	ADCIRC (m)	HWM (m)	Error (m)
29.261	-89.9632	Gulf Coast near Grand Isle State Park	1.11	1.26	-0.16
29.731	-90.123	Inland near Lake Salvador	1.47	1.1	0.37
30.297	-89.9536	Coast of Lake Pontchartrain near Lacombe	1.99	1.59	0.4
29.627	-89.9515	Off MS River near Round Lake	1.59	1.27	0.32
				Average Error	+0.23

Note: Elevations refer to NAVD88-2004.65.

Table 3-22: Comparison of ADCIRC Simulated Results and Observed High Water Marks – Hurricane Gustav (2008)

Lat	Long	Description	ADCIRC (m)	HWM (m)	Error (m)
30.0936	-90.4379	Near Coast of Lake Pontchartrain near Laplace	1.3	1.4	-0.1
30.0214	-90.1432	Coast of Lake Pontchartrain near Lakeview	1.73	1.62	0.11
29.8603	-89.9073	On MS River near St. Bernard	2.65	2.74	-0.09
29.4169	-89.6179	On MS River near Adams Bay	1.73	1.89	-0.16
29.2626	-89.9621	Gulf Coast near Grand Isle State Park	1.61	1.49	0.12
29.9199	-90.6221	West coast of Lac des Allemands	0.72	0.79	-0.07
29.8625	-90.4545	Inland near Paradis	0.68	0.82	-0.14
				Average Error	-0.05

Note: Elevations refer to NAVD88-2004.65.

Table 3-23: Comparison of ADCIRC Simulated Results and Observed High Water Marks – Hurricane Ike (2008)

Lat	Long	Description	ADCIRC (m)	HWM (m)	Error (m)
29.559	-91.5251	Gulf Coast near West Cote Blanche Bay	2.15	2.47	-0.32
29.2532	-90.66	Inland near Bay Chaland	1.69	2.32	-0.63
29.6533	-90.1063	Inland near Lake Salvador	1.39	1.58	-0.19
				Average Absolute Error	-0.38

Note: Elevations refer to NAVD88-2004.65.

Table 3-24: ADCIRC Simulated Antecedent High Water Level

Location	Maximum Water Level (m, NAVD88-2004.65)	Maximum Water Level (ft, NAVD88-2004.65)
Eugene Island	0.75	2.5
Grand Isle	0.75	2.5
Dauphin Island	0.75	2.5
Average along Coastline	**0.75**	**2.5**

Table 3-25: ADCIRC Storm Parameter Sensitivity Simulations

									ADCIRC Results at WSES (ft, NAVD88-2004.65)		
Storm #	**ΔP (mb)**	**V_{max} (kt)**	**Bearing (deg from N)**	**V_f (kt)**	**R_{max} (nm)**	**Landfall Point**	**Landfall Lat. (°)**	**Landfall Lon. (°)**	**WSES**	**Mississippi River near WSES**	**Left Descending Levee near WSES**
1	158	160	-50	5	28	7	29.22	-89.5	22.7	33.4	39.5
2	158	160	10	15	28	2	29.27	-91.31	dry	19.5	dry
3	158	160	-30	5	28	5	29.12	-90.16	27.2	30.6	32.4
4	132	150	-80	6	26	10	29.64	-88.97	dry	18.5	28
5	132	150	-70	6	26	9	29.16	-89.01	dry	28	31.6
6	132	150	-60	6	26	9	29.16	-89.01	dry	26.4	31.8
7	132	150	-60	6	26	7	29.22	-89.5	16.6	28.9	32.1
8	132	150	-40	6	26	6	29.31	-89.86	dry	27.9	31.3
9	132	160	-30	6	18	5	29.12	-90.16	dry	24.8	dry
10	132	150	-30	6	26	5	29.12	-90.16	16.5	29.1	22.5
11	132	160	10	6	18	3	29.05	-90.91	dry	17.4	dry
101	132	160	-70	5	30	9	29.16	-89.01	21.1	31.7	36.0
102	132	160	-60	5	30	7	29.22	-89.5	22.9	32.3	37.0
103	132	160	-40	5	30	5	29.12	-90.16	27.6	30.7	28.7
104	132	160	0	5	30	3	29.05	-90.91	30.0	30.0	dry
105	132	160	10	15	30	2	29.27	-91.31	dry	15.8	dry
106	132	158	-40	6	22	5	29.12	-90.16	18.3	25.4	15.7
107	132	158	0	6	22	3	29.05	-90.91	18.2	21.0	dry

Notes:

1. "Dry" refers to the condition where the modeled surge elevation is below the general site grade elevation of approximately 15.1 ft, NAVD88 (2004.65).
2. Some storm parameter combinations (V_f, R_{max} and V_{max}) exceeded the recommended PMH ranges for the sensitivity analysis.
3. ° denotes decimal degrees.

Table 3-26: Final PMSS Storm Set and ADCIRC-Simulated Results

									ADCIRC Results at WSES (ft, NAVD88-2004.65)		
Storm #	ΔP (mb)	V_{max} (kt)	Bearing (deg from N)	V_f (kt)	R_{max} (nm)	Landfall Point	Landfall Lat. (°)	Landfall Lon. (°)	WSES	Mississippi River near WSES	Left Descending Levee near WSES
201	132	149	-40	6	25	5	29.12	-90.16	21.0	28.9	21.2
202	132	149	0	6	25	3	29.05	-90.91	22.4	25.3	dry
203	132	160	-45	20	6	6	29.31	-89.86	dry	10.3	dry
204	132	156	-40	20	25	5	29.12	-90.16	dry	18.1	dry
205	132	149	-60	6	25	7	29.22	-89.50	17.4	28.7	30.6
206	132	149*	-60	6	25	7	29.22	-89.50	dry	27.7	27.1
207	132	149	0	6	22	3a	29.05	-90.84	19.1	24.8	dry
208	132	149	10	6	25	3b	29.08	-91.08	21.0	25.4	dry
209	132	149	-60	6	25	9	29.16	-89.01	dry	26.4	31.4
210	132	149	-60	6	22	11	29.07	-89.08	dry	27.6	30.4

Notes:

1. "Dry" refers to the condition where the modeled surge elevation is below the general site grade elevation of 15.1 ft, NAVD88 (2004.65).
2. Input for Storm 206 included post-landfall intensity decay. A constant decay rate of -3 kt per hour and +2 mb per hour was applied to maximum wind speed (V_{max}) and minimum central pressure (P_o), respectively. Other tracks (201 through 205 and 207 through 210) are steady-state storms.

Table 3-27: ADCIRC Simulated Results – With Offshore and Post-Landfall Decay

Storm #	CPD (mb)	V_{max} (kt)	Bearing (deg from N)	Forward Speed (kts)	Rmax (nm)	Elevation at WSES (ft, NAVD88-2004.65)		Mississippi River near WSES (ft, NAVD88-2004.65)	Left Descending Levee near WSES (ft, NAVD88-2004.65)
						Unadjusted	Adjusted (1)		
Storm 202 with offshore and post-landfall decay	132	149	0	6	25	19.5	20.2	20.1	No Flooding

Notes:

1. Adjustment for difference in calculated and simulated antecedent water level is 0.9 ft (AREVA, 2015b).
2. Post-landfall decay is calculated in the WSES PMH calculation (AREVA, 2015a).
3. Off-shore decay is calculated in the WSES Combined Effect Calculation (AREVA, 2015b).

Table 3-28: ADCIRC Simulated Results – Adjusted for Antecedent Water Level and Projected Subsidence

Storm #	ADCIRC Results at WSES (ft, NAVD88-2004.65)		
	WSES	Mississippi River near WSES	Left Descending Levee near WSES
201	21.7	29.6	21.9
202	23.1	26.0	dry
203	dry	11.0	dry
204	dry	18.8	dry
205	18.1	29.4	31.3
206	dry	28.4	27.8
207	19.8	25.5	dry
208	21.7	26.1	dry
209	dry	27.1	32.1
210	dry	28.3	31.1

Note: Water levels presented in this table were calculated by adding 0.7 ft to the values presented in Table 3-26.

Figure 3-33: Overview of Process for Coastal Flooding Calculations

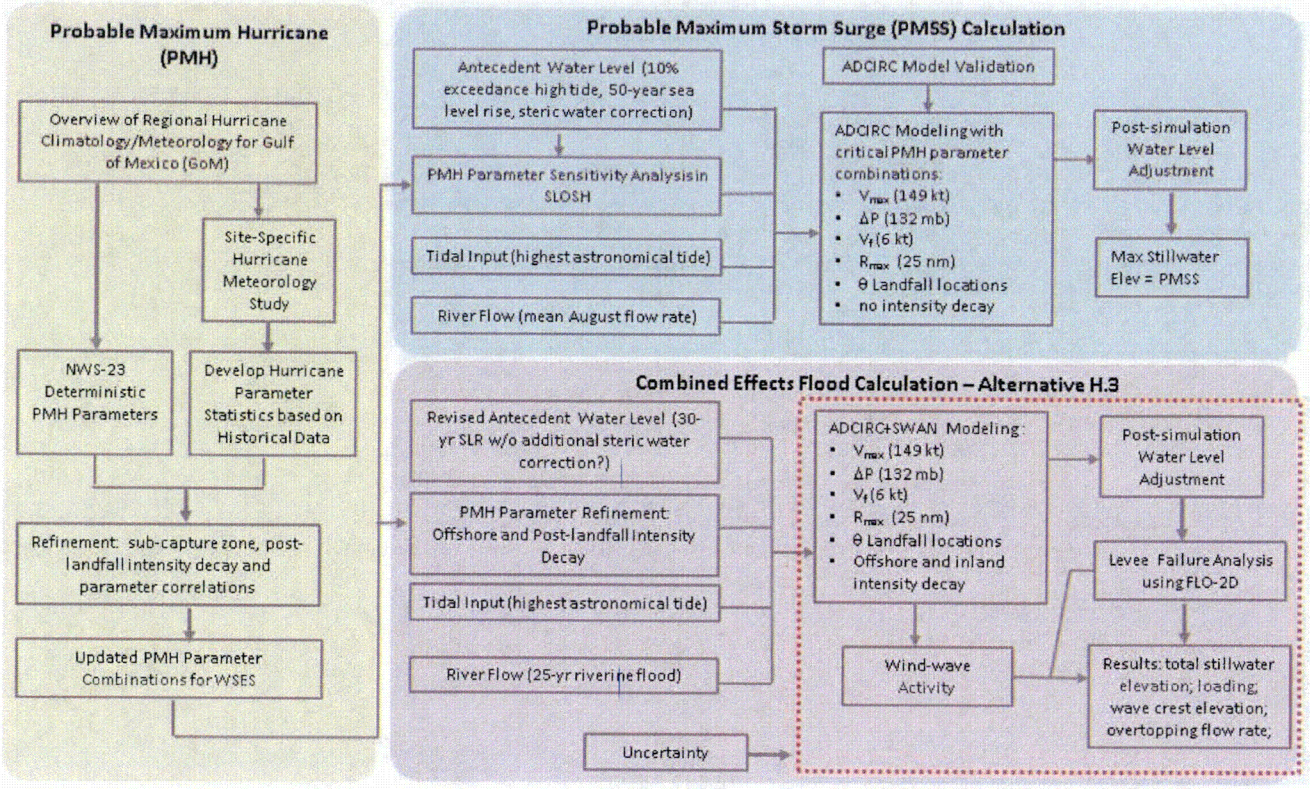

Figure 3-34: Deterministic SLOSH Simulations – Storm Tracks

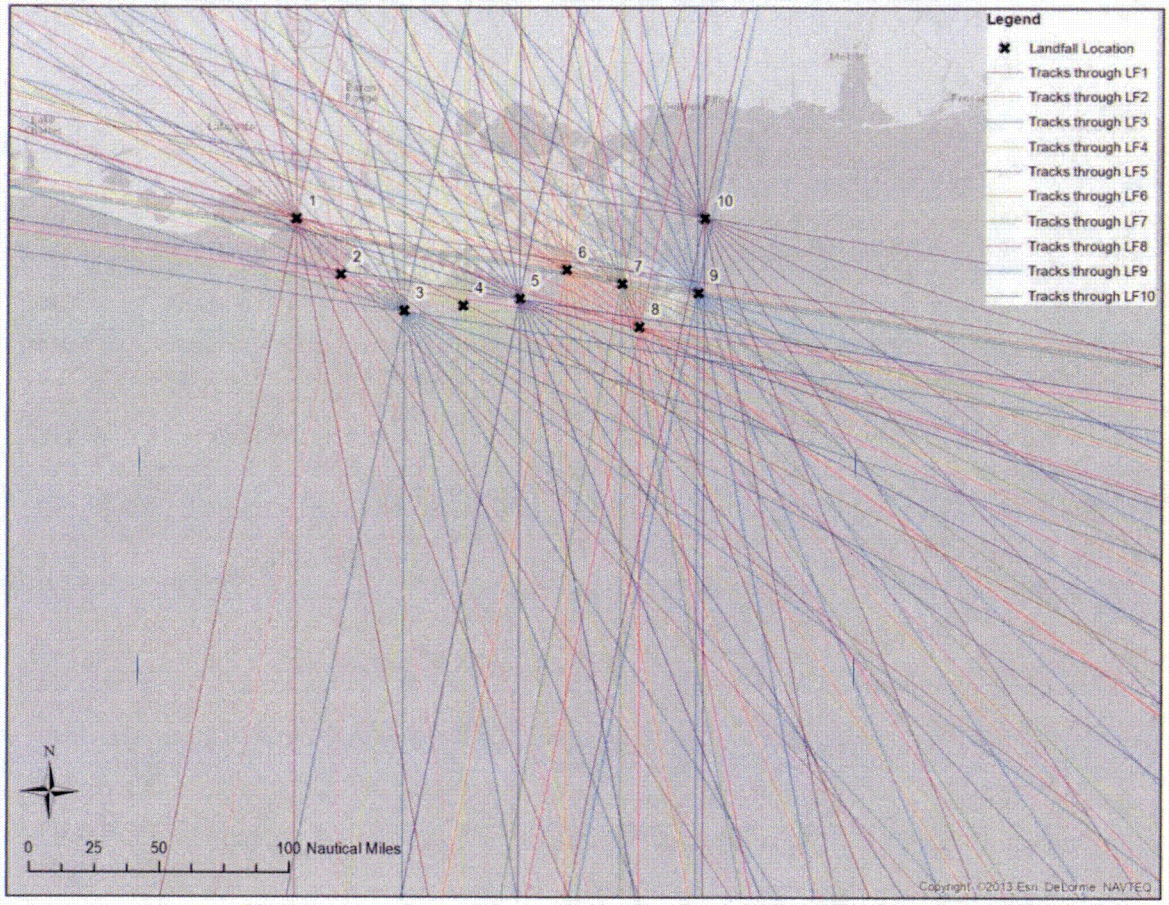

Figure 3-35: Deterministic SLOSH Simulations - Landfall Location Map

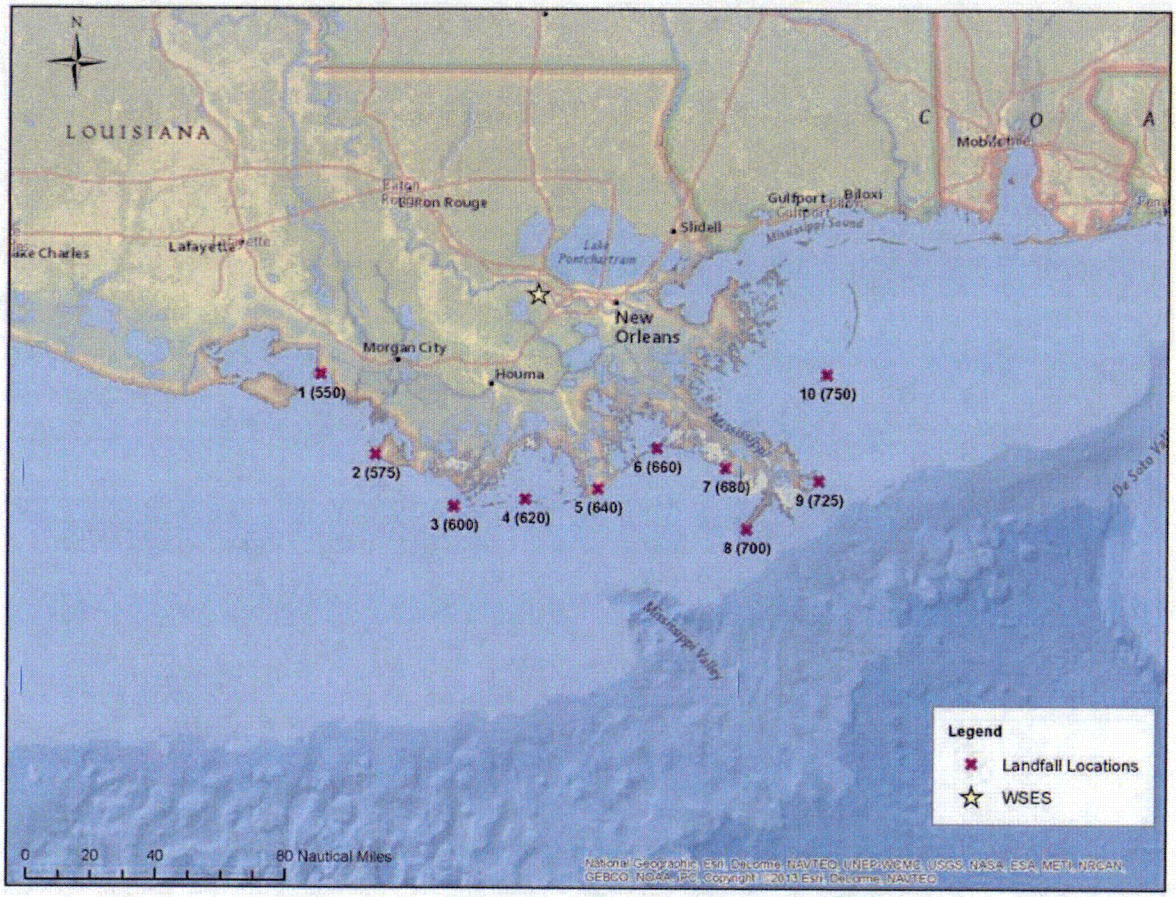

Note: "(550)" denotes FT mile post (in nautical miles) for each landfall point.

Figure 3-36: Highest Storm Tide Water Levels along the U.S. Gulf Coast from 1880 to 2013 (SURGEDAT, 2014)

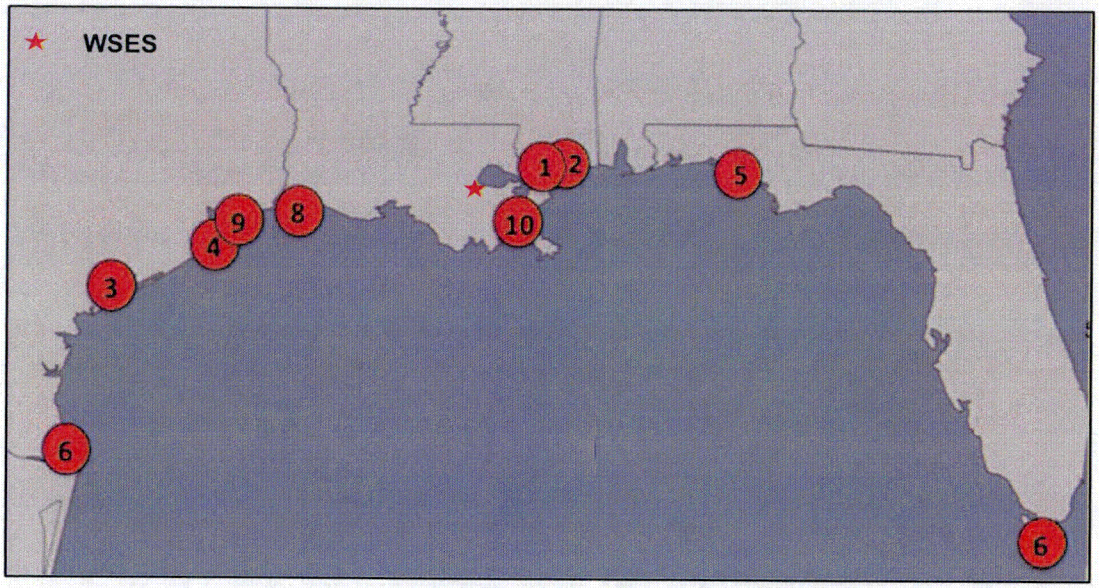

Note: The location of the top 10 highest storm surge/ storm tide levels along the U.S. Gulf Coast from 1880-2013. Each number refers to the storm rank in Table 3-18. Two storms tie for 6 (e.g., there is no 7).

Figure 3-37: Tracks of Major Hurricanes from 1851 - 2010

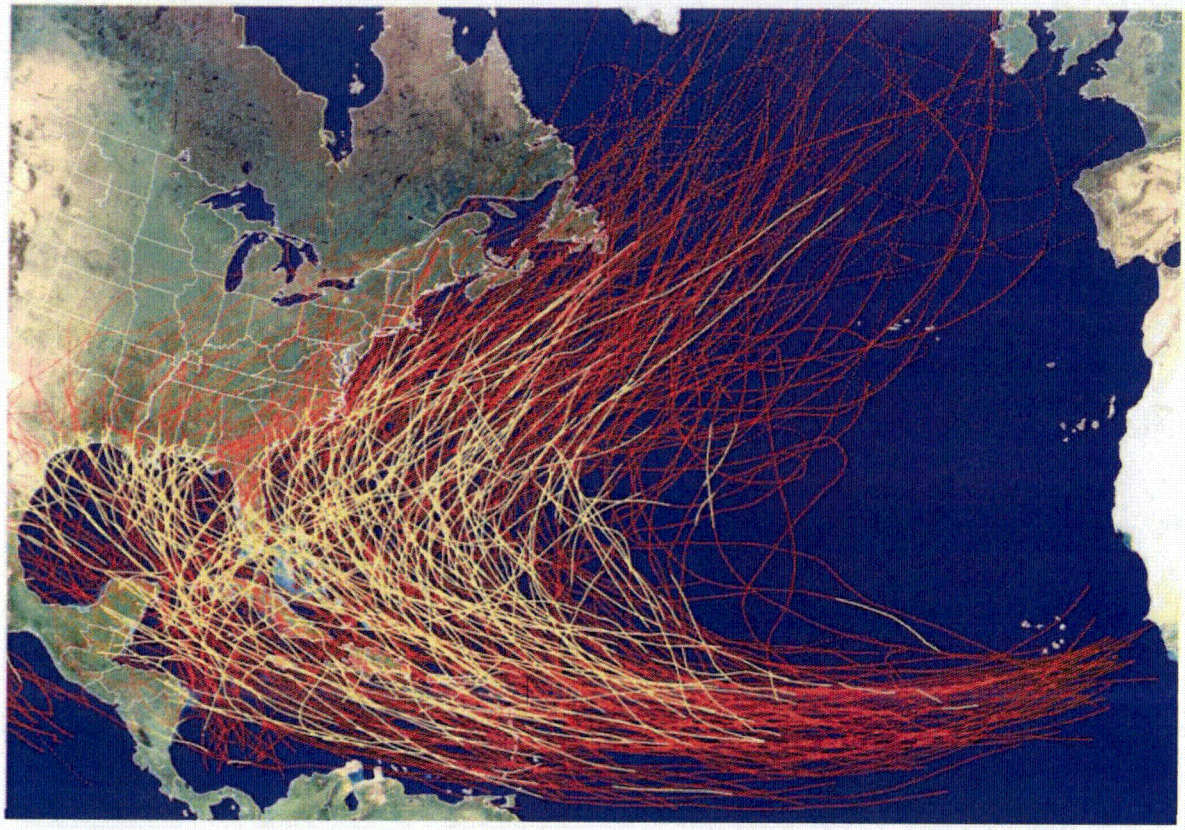

Note: Tracks of Major Hurricanes from 1851-2010. Yellow indicates portion of track when cyclone was of major hurricane intensity (i.e., Category 3 and higher). Solid red portion when the storm was classified as a tropical cyclone, but of less than Category 3 intensity. Dashed red indicates the formative or dissipative stage. Source: NOAA, 2014a.

Figure 3-38: Chronology of the Loop Current

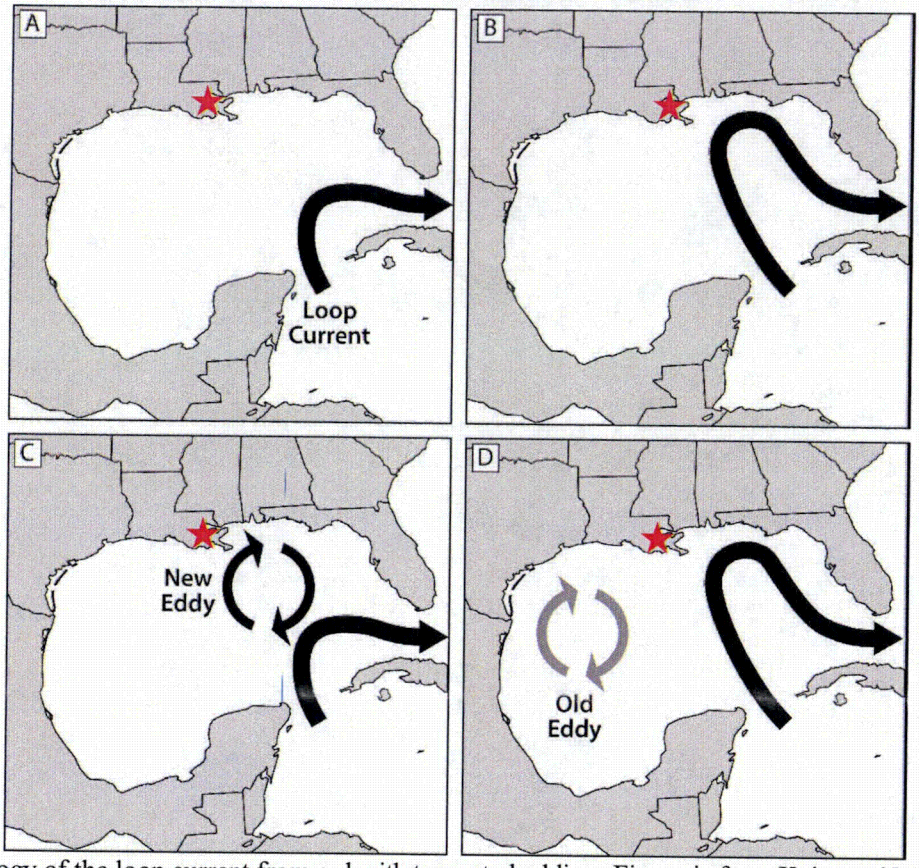

Note: Chronology of the loop current from a-d with truncated eddies. Figure is from Keim and Muller (2009).
★ WSES Location

Figure 3-39: Scatter Plot - DP versus R_{max}

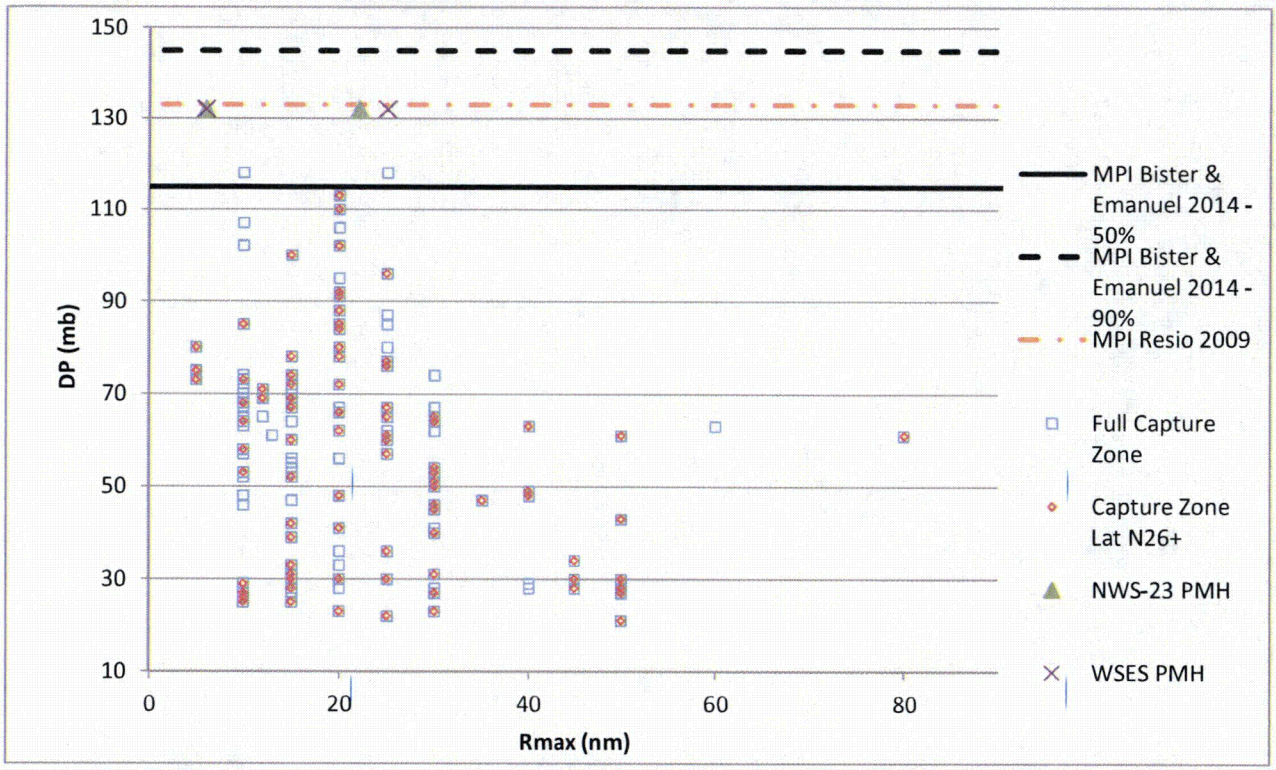

Notes:

1. "MPI Resio 2009" refers to Annex B in the Louisiana Coastal Protection and Restoration Final Technical Report – Hydraulics and Hydrology Appendix, June 2009 (USACE, 2009). Annex B is titled "The Maximum Possible Intensity and Its Use for Coastal Hazard Estimation" by D. Resio, 2009.
2. The proposed minimum central pressure is 880 mb. Assuming a peripheral pressure of 1,013 mb (commonly used by Dr. Resio, refer to his recent paper "The effect of uncertainty on estimates of hurricane surge hazards", Resio et al., 2013), the central pressure deficit is therefore calculated as:

$$1{,}013 \text{ mb} - 880 \text{ mb} = 133 \text{ mb}.$$

Figure 3-40: Scatter Plot - V_{maxs} versus Bearing

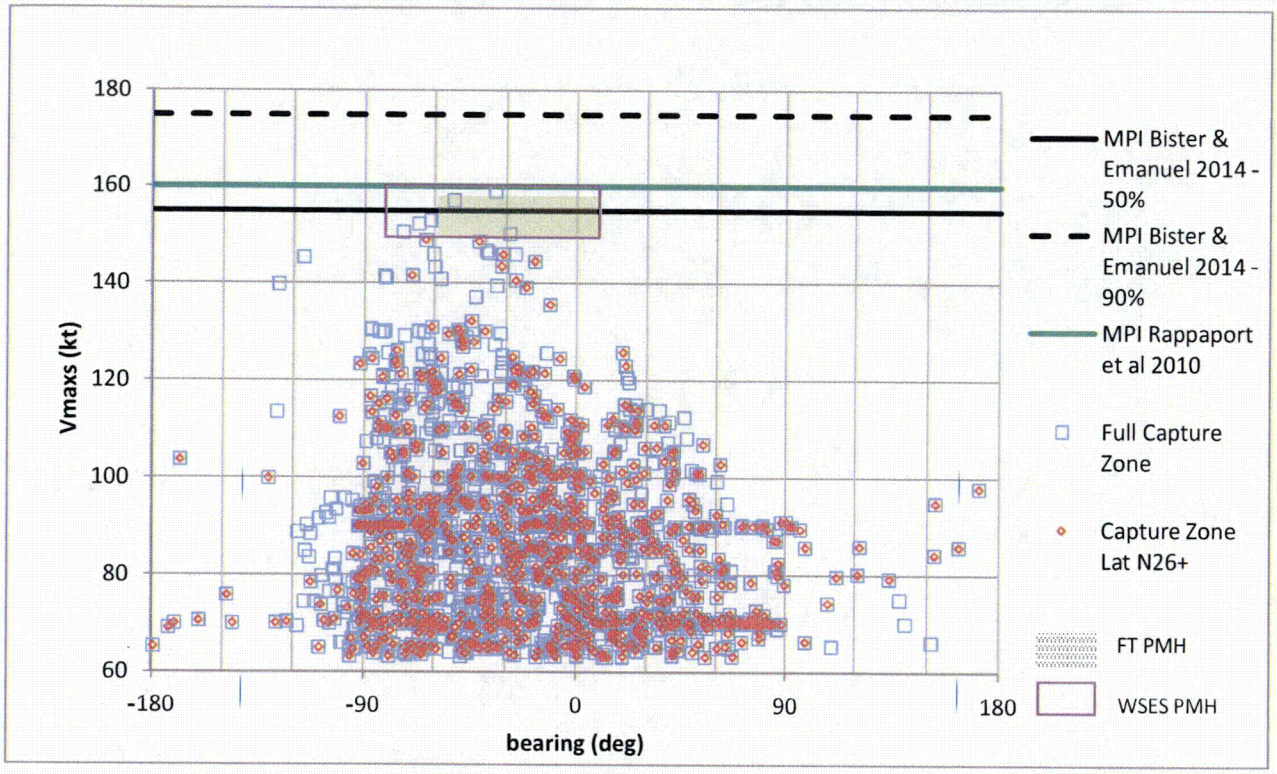

Figure 3-41: Scatter Plot - V_{maxs} versus V_f

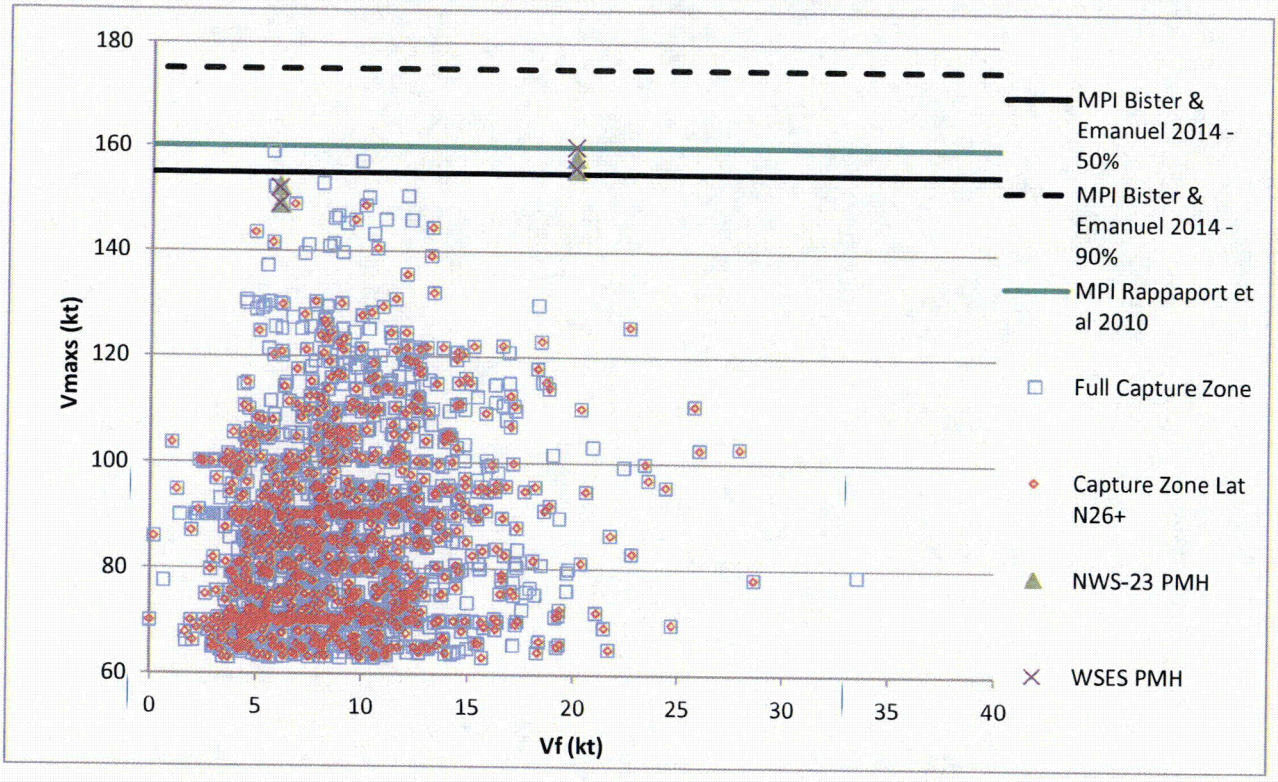

Note:

The three data points located between V_f of 5 to 7 kt and V_{max} of 140 to 150 kt have been found to be in the 120-kt range by a recent study (Delgato, 2014).

Figure 3-42: Scatter Plot - V_{maxs} versus R_{max}

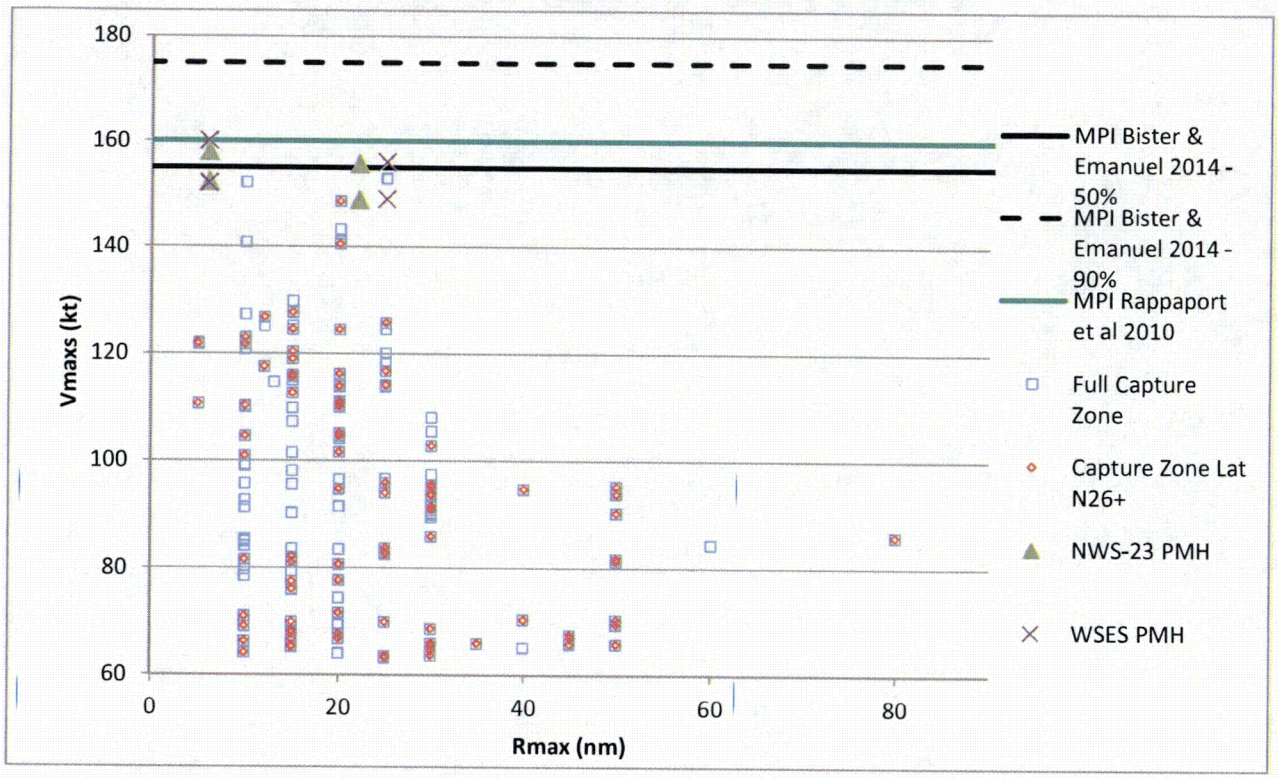

Figure 3-43: Scatter Plot - Vmaxs versus ΔP

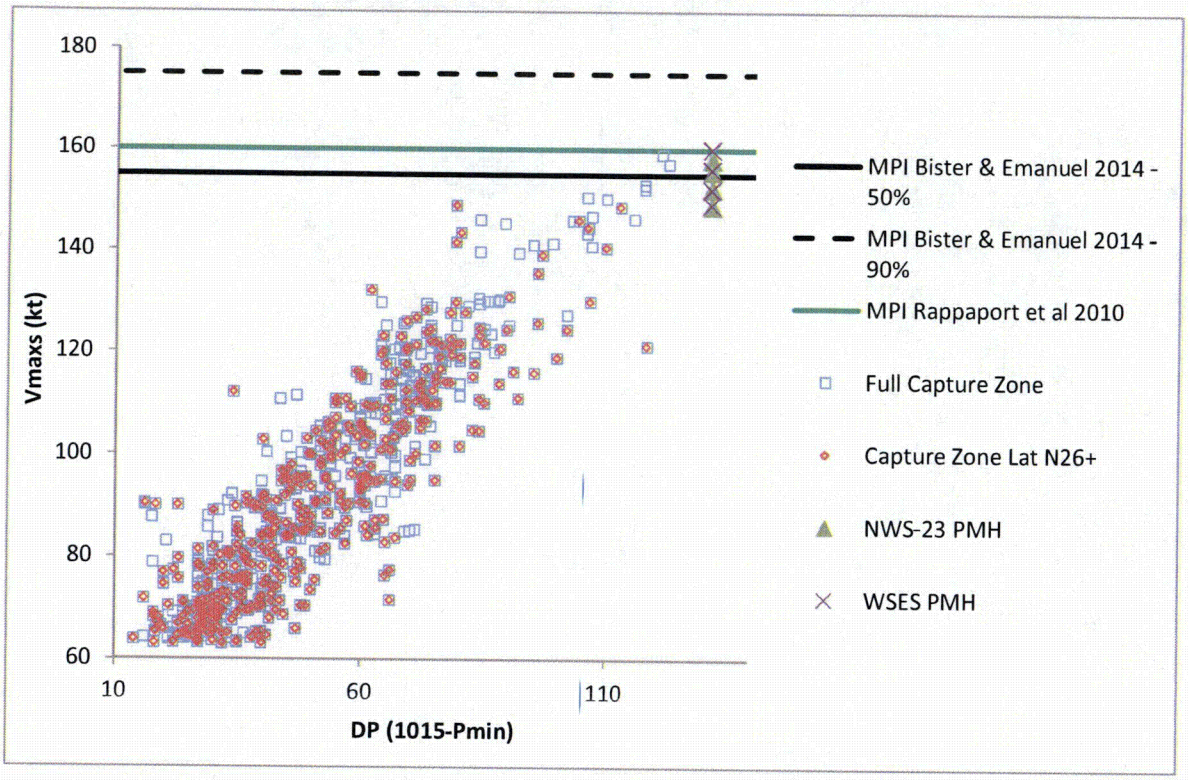

Figure 3-44: Hurricane Data Capture Zone for WSES

Figure 3-45: Full Capture Zone (GoM) versus Sub-Capture Zone (Lat N26+)

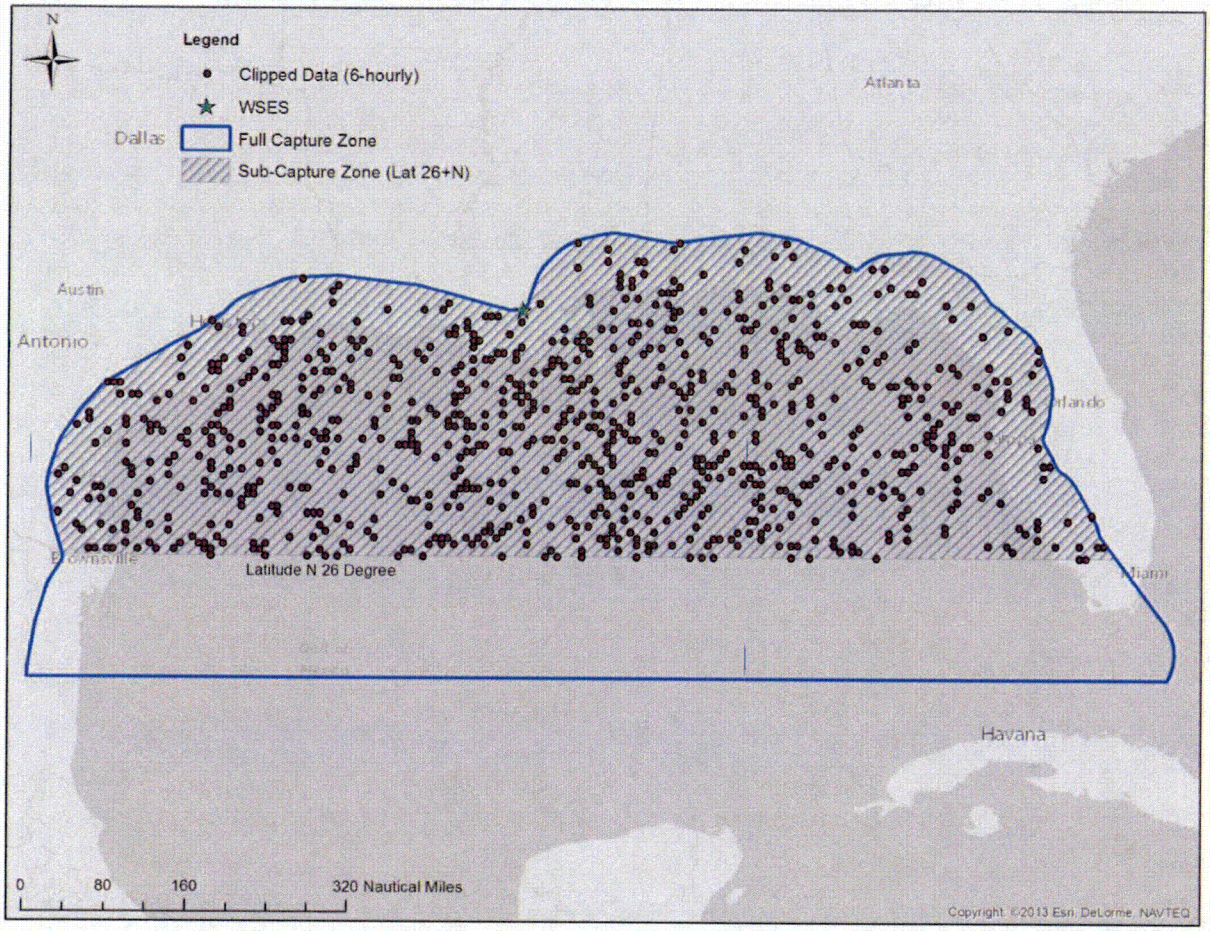

Notes:

1. The sub-capture zone is north of Latitude 26° N. This sub-capture zone is more representative for the surge creating hurricane parameters for WSES.
2. A total of 924 6-hourly data points (e.g., latitude, longitude, wind speed, forward speed and bearing) are located within this sub-capture zone. A total of 1353 6-hourly data points are located in the full capture zone.

Figure 3-46: Matrix Scatter Plot – Full Capture Zone

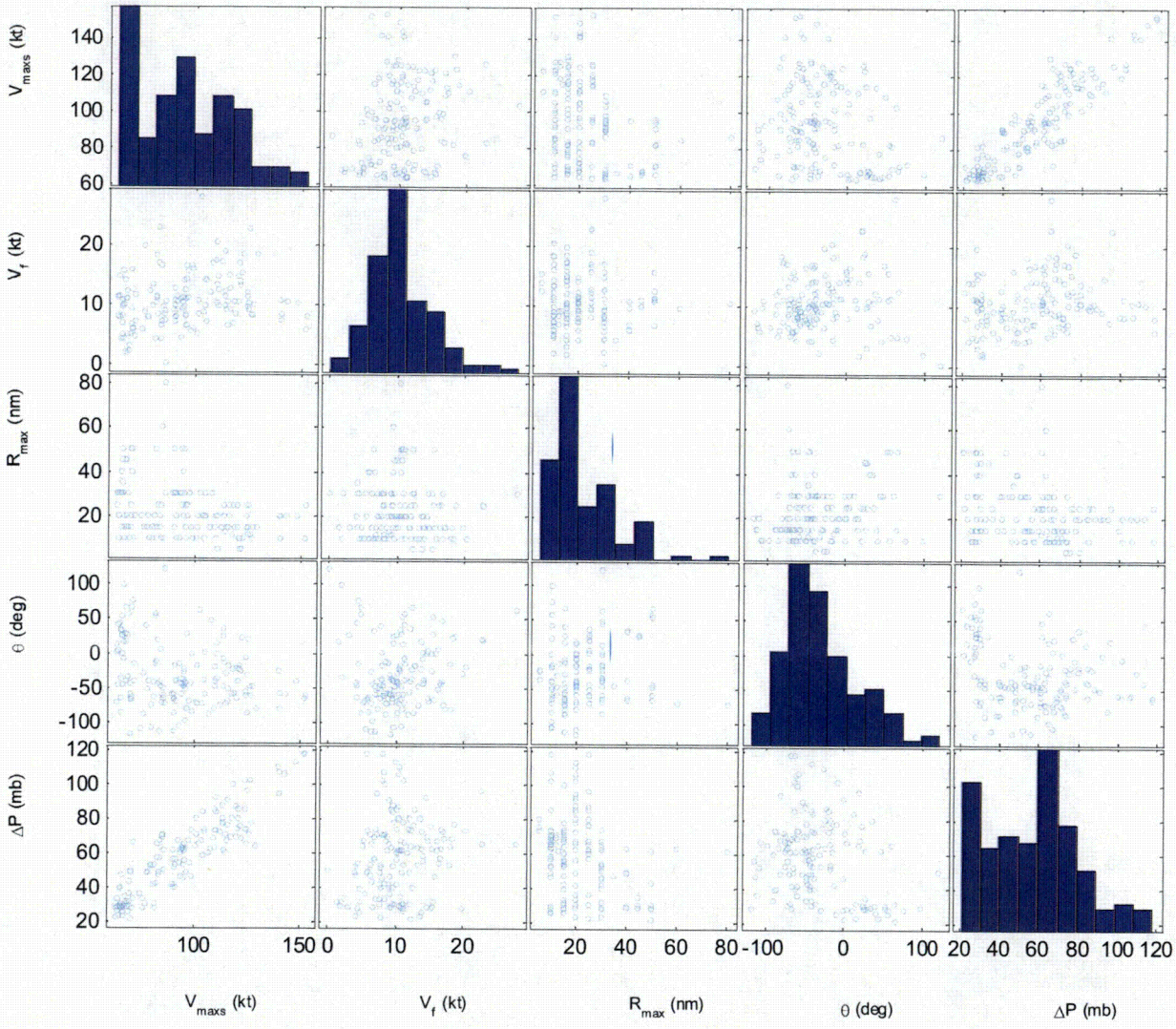

Notes:

1. The diagonal squares of this plot are histograms for each individual parameter.
2. This plot uses a total of 151 data points that have R_{max} values within the full capture zone (GoM).

Figure 3-47: Matrix Scatter Plot – Subset Data Capture Zone

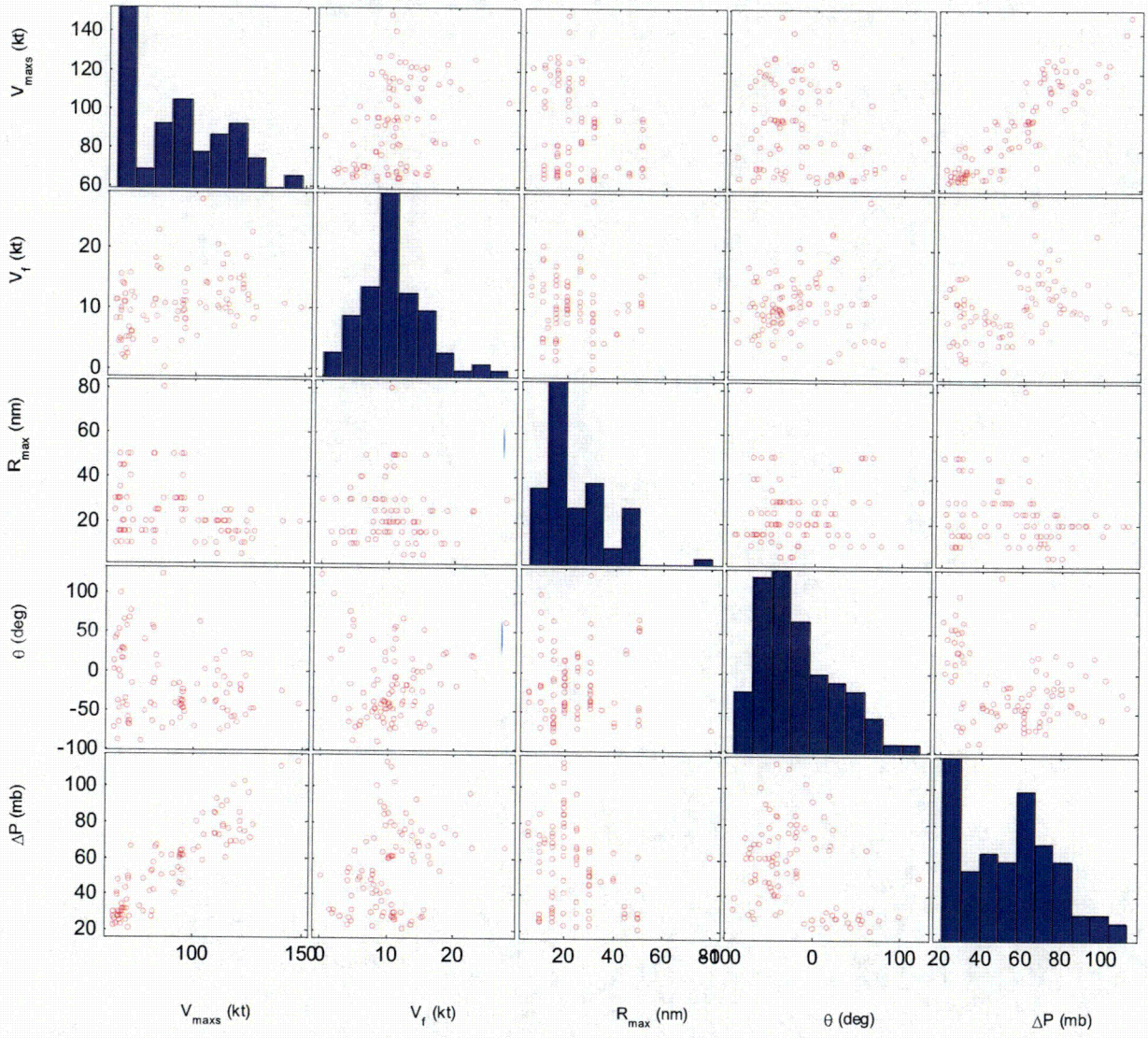

Notes:

1. The diagonal squares of this plot are histograms for each individual parameter.
2. This plot uses a total of 61 data points that have R_{max} values within the sub-capture zone (Lat N26+).

Figure 3-48: Post-landfall Decay of Selected Historical Hurricanes

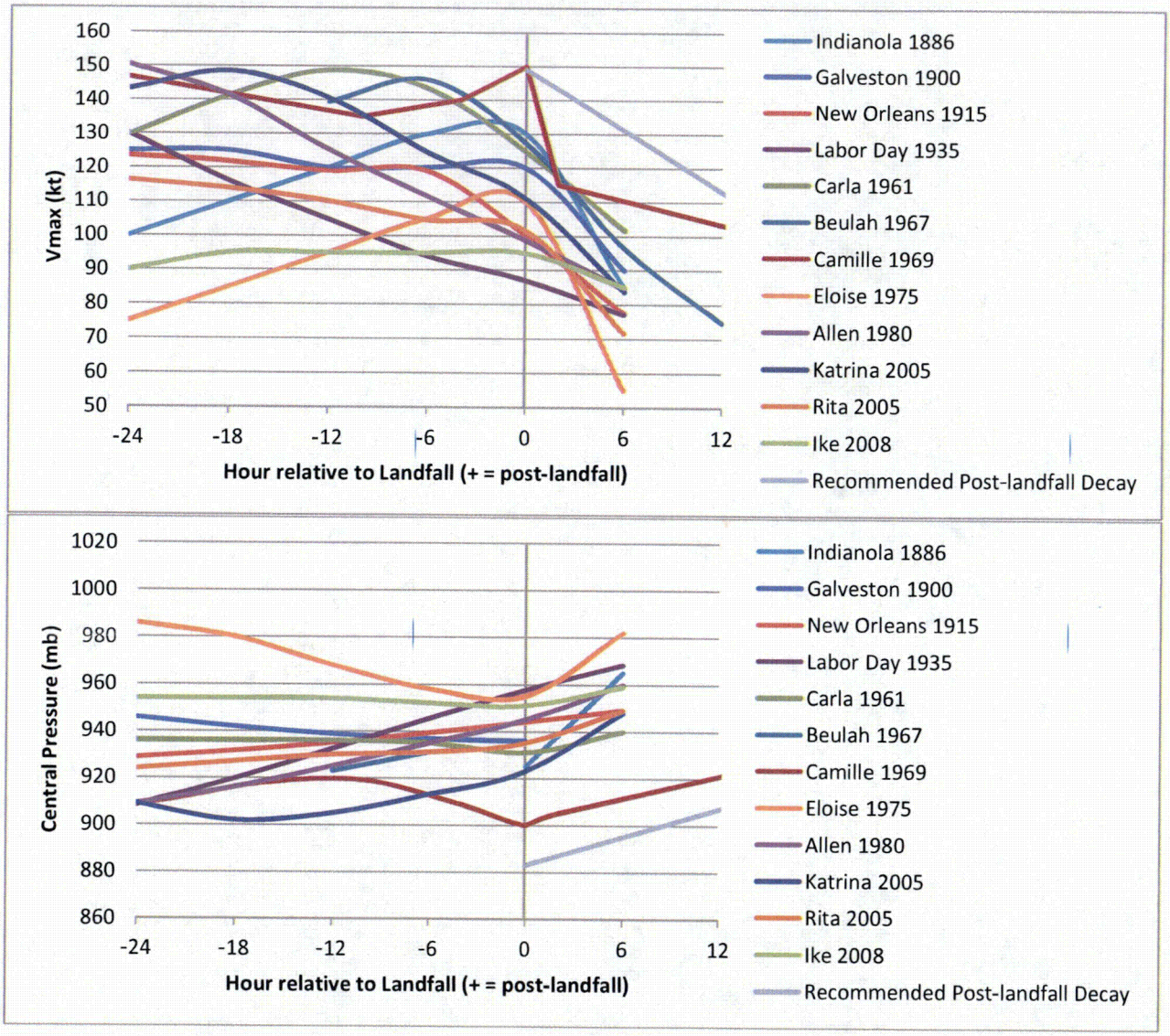

Notes:

1. The primary source for the data plotted is the 6-hourly central pressure (P_o) and smoothed wind (V_{maxs}) (LSU, 2014).
2. For storms (Galveston 1900, Indianola 1886 and Eloise 1975) where the first post-landfall data point is located outside the full capture zone (GoM), HURDAT data was used as a supplement. The reanalysis results on Camille 1969 were incorporated into the HURDAT2 database.
3. Recommended decay rates (-3 kt/hr for V_{max} and +2 mb/hr for P_o) are conservative (flatter than the overall observed trend) and determined based on the data of the selected storms.
4. "0 hour" on the x-axis denotes landfall; "-" denotes before landfall and "+" denotes after landfall.

Figure 3-49: Pressure Deficit versus Radius of Maximum Winds for Vmaxs >= 96 knots

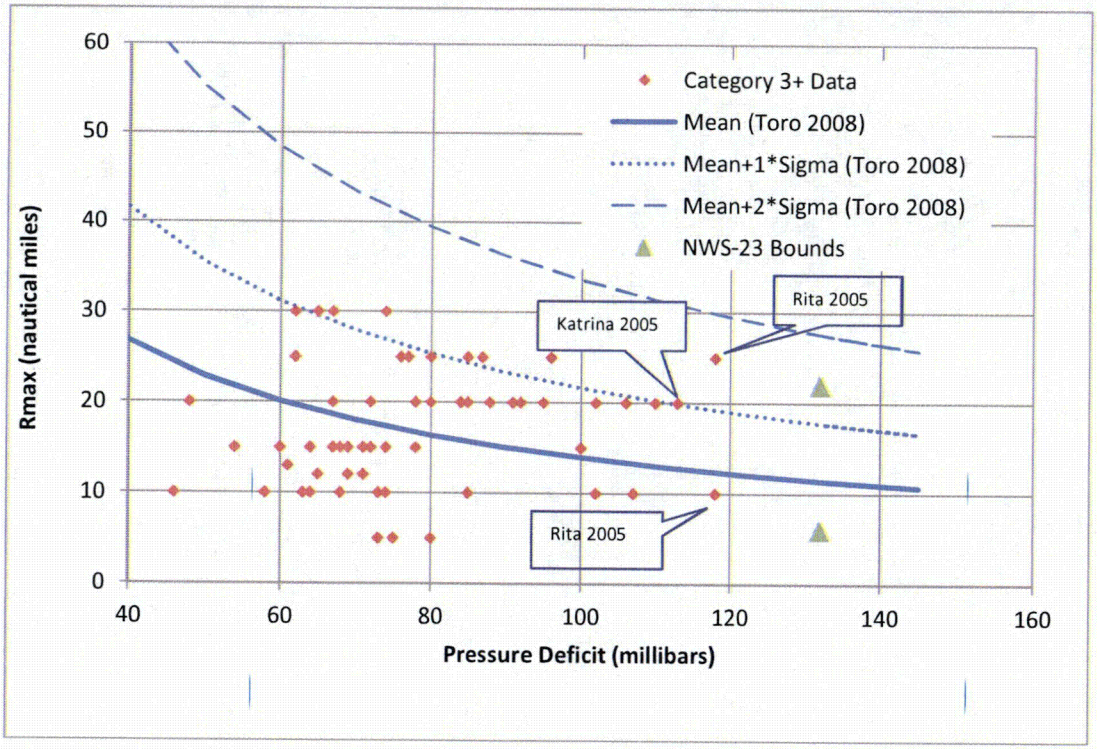

Notes:

1. This figure shows the data with a minimum value of 96 knots for V_{maxs}, i.e., the lower bound for Category 3 intensity.
2. Curves using $\ln(y) = 5.91 - 0.711 * \ln(x)\,; sigma\ for\ \ln(y) = 0.44$ based on Figure 3.7 in Toro, 2008. $y = R_{max}$; $x = \Delta P$.

Figure 3-50: Scatter Plot - R_{max} versus ΔP

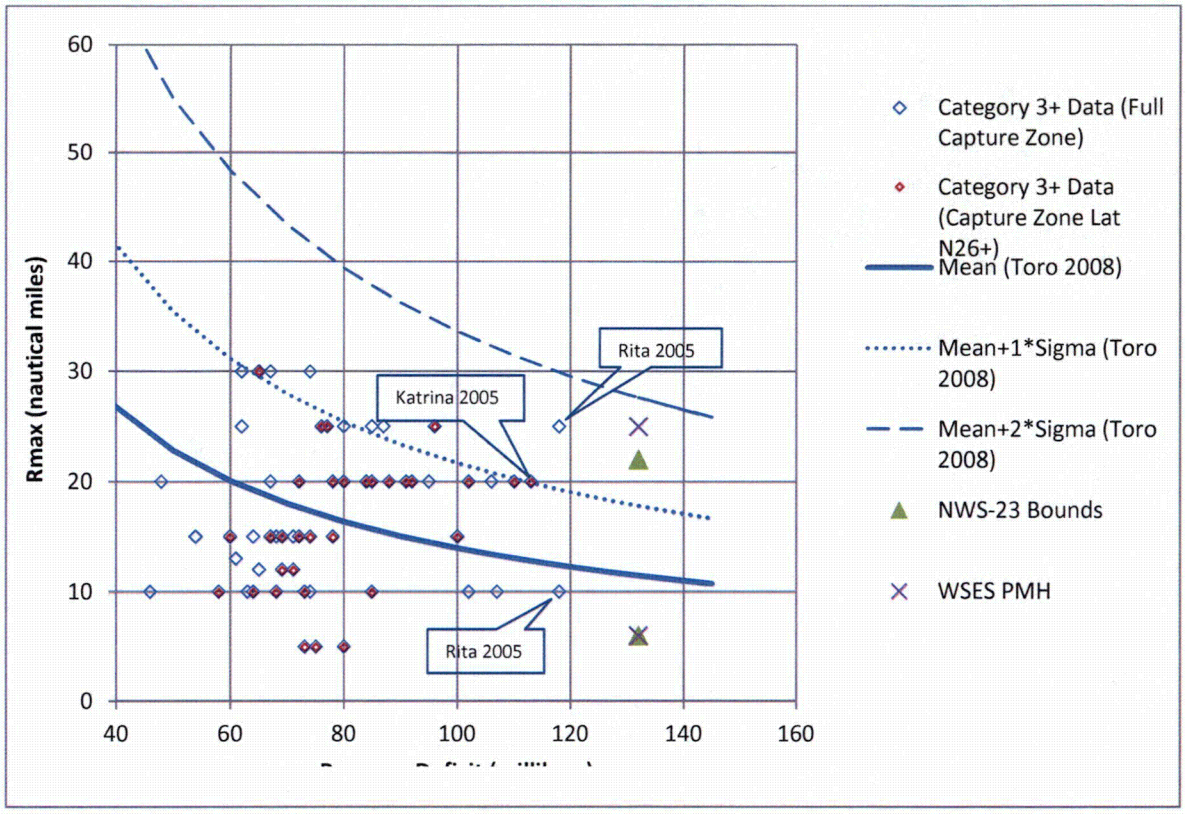

Notes:

1. This figure was developed base on Figure 74.
2. Curves using $\ln(y) = 5.91 - 0.711 * \ln(x)$; $sigma\ for\ \ln(y) = 0.44$ based on Figure 3.7 in Toro, 2008. $y = R_{max}$; $x = \Delta P$.
3. The recommended combination for the upper Rmax of 25 nm and maximum □P of 132 mb is approximately 1.77 standard deviation (sigma) from the mean (Toro, 2008). Given x = 132 (mb), ln(y)=2.44 and y = 11.45 (nm),

$$\frac{\ln(25) - \ln(y)}{0.44} = \frac{\ln(25) - 2.44}{0.44} = \frac{0.781}{0.44} = 1.77$$

   1. This represents the upper 96th percentile or the upper 92 percent confidence interval (CI). For the standard normal distribution (□=0, □=1), z equal to 1.645 for the upper 90 percent CI and 1.96 for the upper 95 percent CI.

Figure 3-51: Hurricane Intensity versus Forward Speed

(a) V_{maxs} vs. V_f

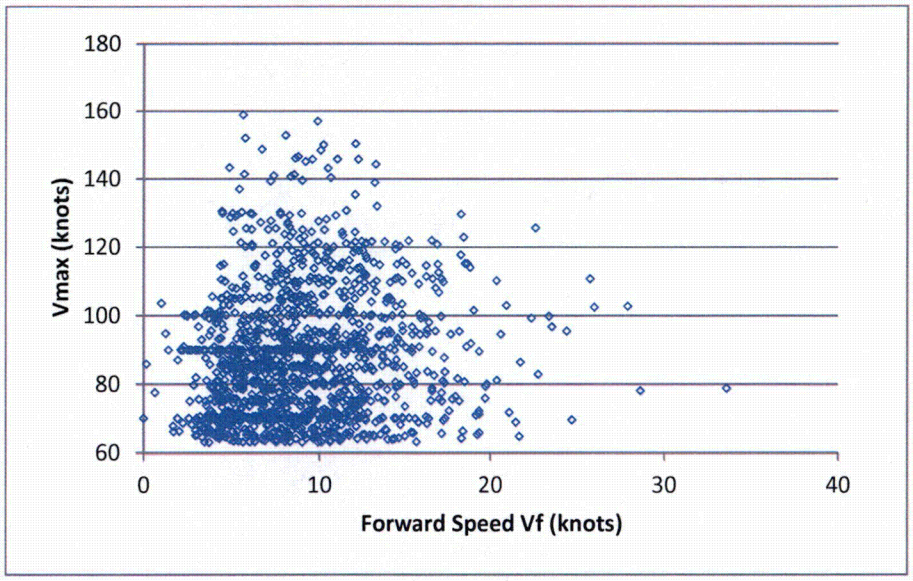

(b) □P vs. V_f

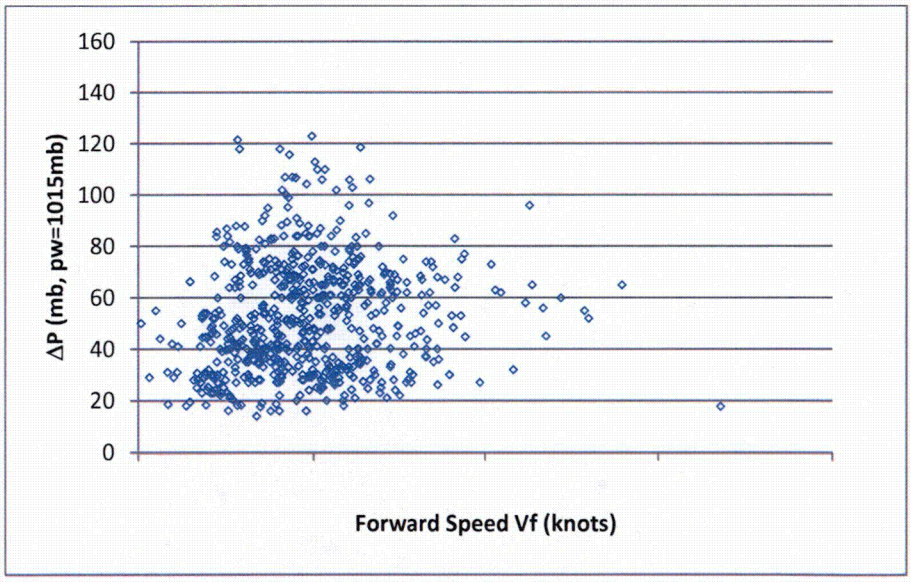

Note: ΔP was calculated using a peripheral pressure of 1,015 mb.

Figure 3-55: Comparison of Tide Phase and Amplitude along Coastline

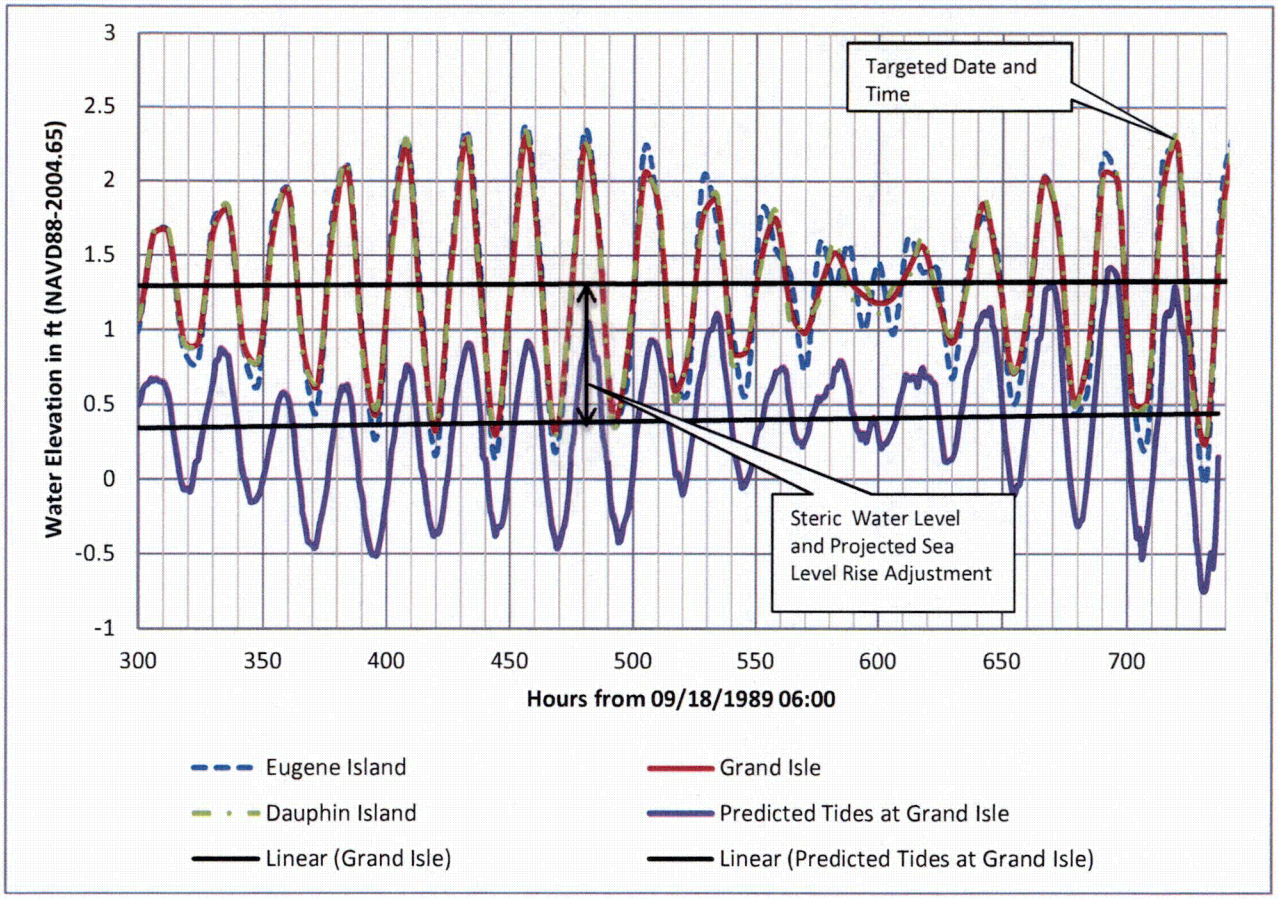

Note: Time series are at hourly intervals and may not reflect the absolute peak elevations

Figure 3-57: Storm Tracks of ADCIRC Sensitivity Simulations

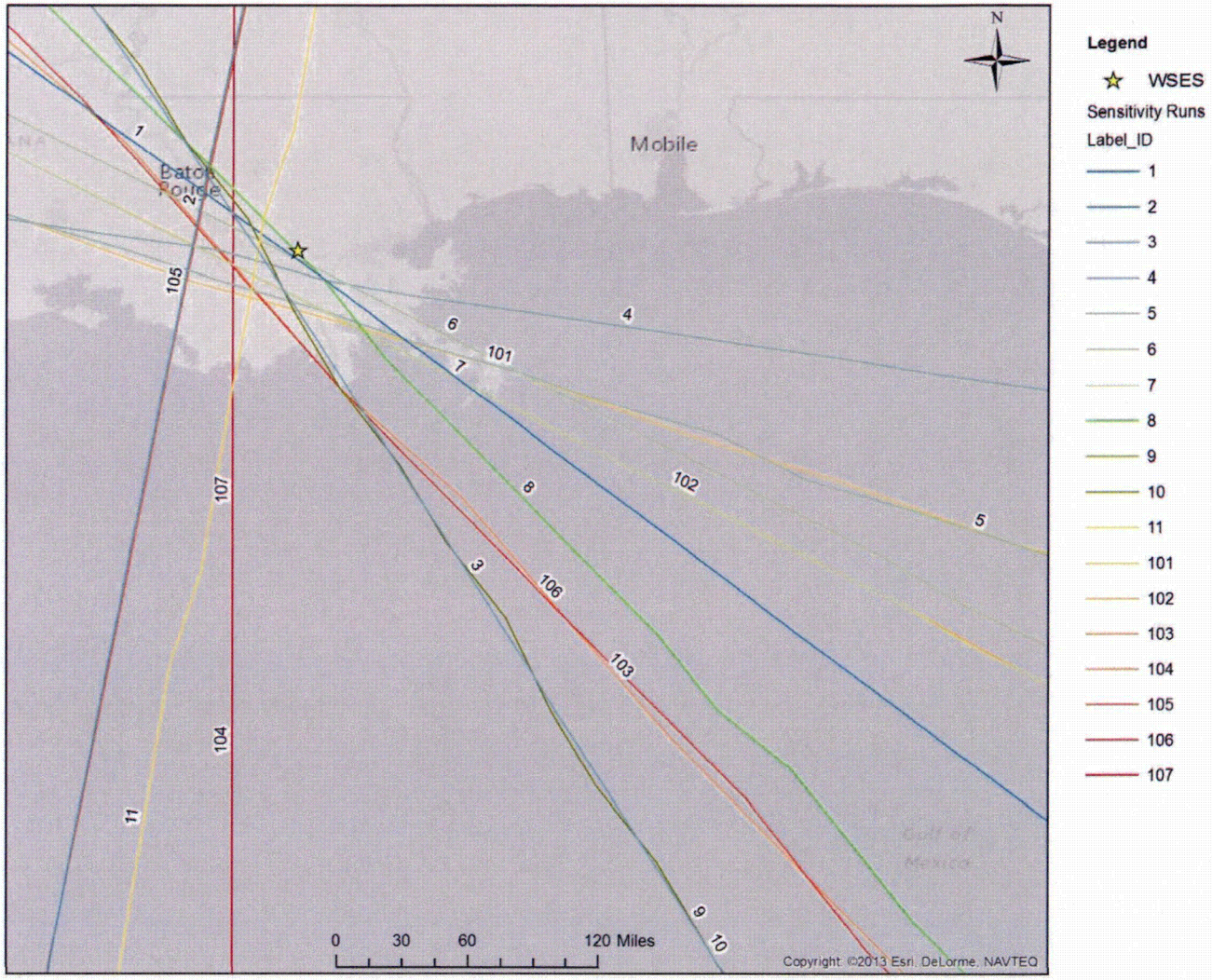

Any illegible text or features in this figure are not pertinent to the technical purposes of this document.

Figure 3-61: Water Level Time Series Plots – Storm 202 with Decay

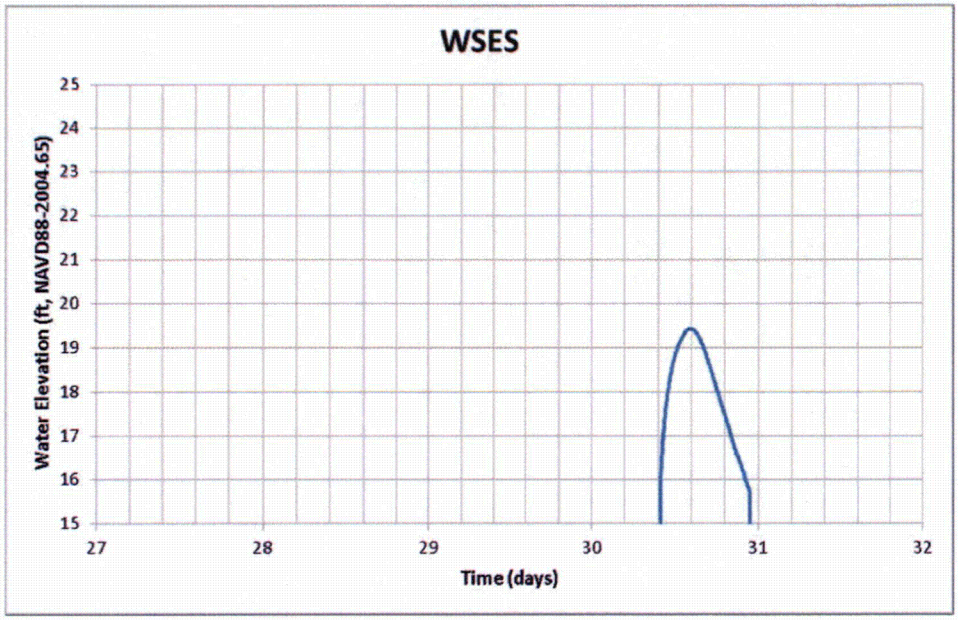

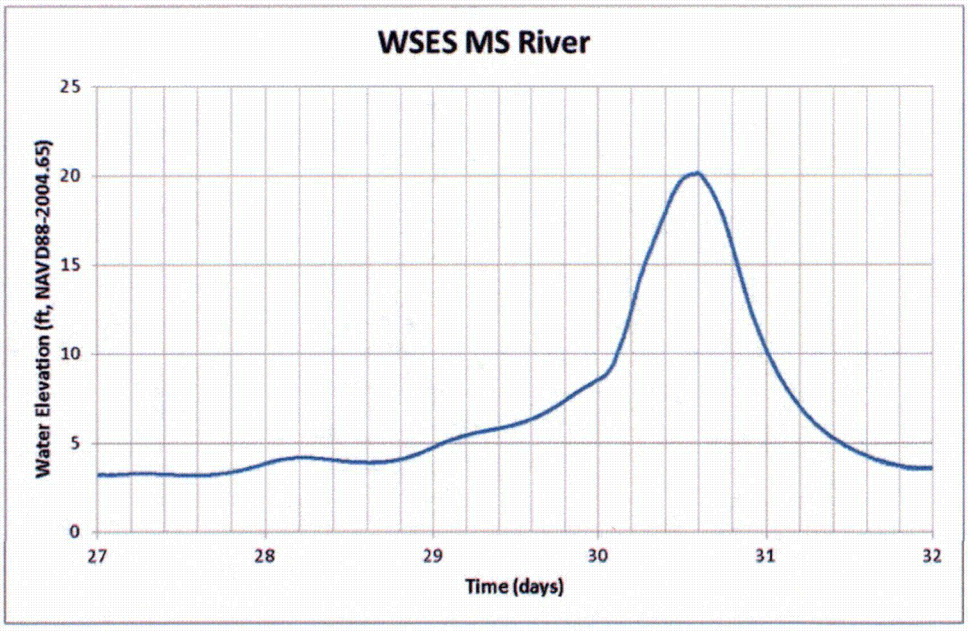

3.5 Seiche

3.5.1 Seiche Screening Discussion

A seiche is an oscillation of the water surface in an enclosed or semi-enclosed body of water initiated by an external cause. Once started, the oscillation may continue for several cycles; however, over time it gradually decays because of friction (NRC, 2011, Section 3.6).

The potential flooding hazard from a seiche at WSES is judged to be negligible because of the site's riverine setting and elevation.

The Mississippi River in the WSES area is not an enclosed or semi-enclosed water body (Figure 2-1). Instead, the river is narrow (about 0.5 miles) and meandering, which constrains and limits the geometry needed to develop a seiche and its oscillation propagation. The river geometry also limits the height of any seiche oscillations and causes rapid attenuation of any seiche oscillations.

Thus, given a seiche, there would be little, if any, effect on the WSES site. Any potential seiche development would be significantly smaller than PMF induced flooding or other flood mechanisms.

3.5.2 References

NRC, 2011. "NUREG/CR-7046: Design-Basis Flood Estimation for Site Characterization at Nuclear Power Plants in the United States of America", U.S. Nuclear Regulatory Commission, Springfield, VA, National Technical Information Service, 2011.

3.6 Tsunamis

A tsunami is a series of water waves generated by a rapid, large-scale disturbance of a water body due to seismic, landslide, or volcanic tsunamigenic sources (NRC, 2009, Section 1.1). WSES is located adjacent to the Mississippi River, approximately 35 river miles upstream of New Orleans and 130 river miles above the Head of Passes. The open Gulf of Mexico is located 60 miles to the south of WSES (see Figure 3-62). The Mississippi River is contained by man-made levees on both sides at the site location (Figure 3-63). The topography of the area south of the site is low-lying such that hydraulic connectivity of the Gulf of Mexico and WSES is possible under extreme flooding conditions (Figure 3-64).

3.6.1 Methodology

The WSES tsunami evaluation followed the HHA approach described in NUREG/CR-6966, Tsunami Hazard Assessment at Nuclear Power Plant Sites in the United States of America (NRC, 2009) and Interim Staff Guidance JLD-ISG-2012-06, Guidance for Performing a Tsunami, Surge, or Seiche Hazard Assessment (ISG) (NRC, 2013).

With respect to tsunamis, the progressive HHA is considered as a series of three tests:

1. Is the site region subject to tsunamis?
2. Is the plant site affected by tsunamis?
3. What are the hazards posed to safety of the plant by tsunamis?

At WSES, the first two tests were considered. The third test was unnecessary based on the results of the first two tests.

The first test was answered by performing a regional survey and assessment of potential tsunamigenic sources. The methodology used in the regional and site screening tests includes the following:

1. Review of the National Geophysical Data Center (NGDC) Tsunami Event Database (NGDC, 2014) and other sources relative to documented historical tsunamis at or near the site;
2. A literature search and review to identify the near-field and far-field tsunamigenic sources that are considered a risk relative to generation of tsunamis that may impact the site and;
3. Review of published Regional Assessment of Tsunami Potential in the Gulf of Mexico report by the U.S. Geological Survey, as part of the National Tsunami Hazard Mitigation Program (NTHMP), and others, for the United States.

The second test was answered by evaluating the vulnerability of the site location relative to potential tsunami sources.

3.6.2 Tsunami Results

3.6.2.1 Regional Screening Test

Tsunamis are generated by rapid, large-scale disturbance of a body of water. Therefore, only geophysical events that release a large amount of energy in a very short time into a water body generate tsunamis. The most frequent cause of tsunamis is an earthquake. Less frequently, tsunamis are generated by submarine and subaerial landslides. (NRC, 2009, Section 1.3) Meteorite impacts, volcanoes, and ice falls can also generate tsunamis, but were excluded from the regional survey because meteorite impacts and volcanoes are very rare events in comparison to earthquakes (NRC, 2009, Section 6.2) and ice falls, which are glacial ice processes (NRC, 2009, Section 1.3.2), are comparable to subaerial landslides.

The regional screening test evaluated the coastal (i.e., near the mouth of the Mississippi River) tsunami hazard from both near-field and far-field tsunamigenic sources. In addition to an oceanic tsunami generated by submarine seismic, landslide, or volcanic sources, the regional screening test also considered tsunami-like waves that can be generated in inland water bodies by subaerial landslides and seismic causes. The technical literature, reflecting the available scientific data on tsunami hazards in the Gulf of Mexico, were compiled and reviewed. The primary sources of information and scientific data used in the regional assessment include:

1. NGDC tsunami and earthquake databases: The NGDC tsunami and earthquake databases identify documented historical near-field and far-field tsunamis that have affected the coastal region near the Mississippi River. The database provides metadata, including earthquake parameters, effects, and descriptions of each event, as well as references summarizing where events were reported and analyzed (NGDC, 2014).
2. NOAA's NTHMP, performed in 2009 by the USGS: The 2009 Regional Assessment of Tsunami Potential in the Gulf of Mexico (USGS, 2009) identifies the primary tsunamigenic sources defining the tsunami hazard along the U.S. Gulf Coast. It also includes limited numerical modeling of tsunamis along the Gulf Coast.

The literature review also identified the historical occurrence of a tsunami-like wave caused by an earthquake on the Mississippi River (Lockridge et.al, 2002).

The Regional Screening Test indicates there is a regional tsunami hazard in the Gulf of Mexico as a result of the following:

Near Field Tsunami:

- Potential landslide-generated tsunamigenic sources in the Gulf of Mexico include three geologic provinces: Northwest Gulf of Mexico, Mississippi Canyon, and Florida and Campeche Margins (Figure 3-65). All provinces contain landslides of sufficient volume to potentially cause destructive tsunamis along the Gulf of Mexico Coasts.
- The northern Gulf of Mexico coast would be affected primarily by the back-going tsunami emanating from the Northwest Gulf of Mexico (East Breaks) and Mississippi Canyon landslides, and would be affected primarily by the outgoing tsunami from a landslide sourced from above the Florida and Campeche Margins.
- Results of USGS's hydrodynamic modeling in the region for the East Breaks landslide indicated that tsunami maximum bore heights near the east Texas shoreline are approximately 8 m (26 feet) (Page 41, USGS, 2009). Hydrodynamic modeling of the Campeche landslide indicated the "largest possible runup" was about 4.0 m (13.1 feet) in the vicinity of Freeport, Texas (Page 42, USGS, 2009). However, model results specific to the Louisiana coast were not available for either landslide scenario; nor was a landslide at the Mississippi Canyon studied.

Far Field Tsunami:

- It is likely that the seismic seiche waves resulting from the 1964 Gulf of Alaska earthquake are nearly the highest that can be generated owing to a predominantly continental ray path for seismic surface waves from Alaska to the Gulf Coast (Page 43, USGS, 2009). Therefore, seismically-induced seiche is not a flood causing mechanism at WSES.
- There are no far field sources likely to generate tsunamis that threaten WSES. Tsunami propagation from far field sources outside the Gulf of Mexico, such as the northern Panama

Convergence Zone, Northern South America, Cayman Trough, the Puerto Rico trench, or the Gibraltar area shows that wave amplitude is greatly attenuated by the narrow and shallow passages into the gulf, and as a result, these tsunami sources do not constitute a tsunami hazard to the Gulf of Mexico coast (USGS, 2009).

Mississippi River:

- Subaerial landslides in the Mississippi River significant enough to generate an appreciable tsunami are not likely to occur due to the low relief in the vicinity of WSES and mild river slope.
- Earthquake-induced tsunami-like waves have been recorded in the Mississippi River.
- There have been no observed historical occurrences of tsunami-induced bores traveling up the Mississippi River from the Gulf of Mexico coast.

3.6.2.2 Site Screening Test

3.6.2.2.1 Gulf of Mexico Tsunami

WSES SSCs important to safety are located within the NPIS, which is protected from external flooding to elevation 29.18 feet, MSL. The site grade around the NPIS varies from 17.5 feet, MSL on the north site to 14.5 feet, MSL on the south side (WSES, 2013, Section 2.4.1.1). WSES is about 60 miles from the coast (Figure 3-62). These are mitigating factors toward tsunami flooding at WSES directly from the Gulf of Mexico via overland flow. For example, the potential maximum runup due to tsunami of approximately 4 meters (13.1 feet, MSL) identified for the Campeche Escarpment landslide in East Texas (Page 42 of USGS, 2009), transposed directly to the Louisiana coastline without attenuation would not inundate WSES. The approximately 60 miles of land and wetlands between WSES and the Gulf of Mexico coastline is heavily vegetated and flat (Figure 3-64), which is also anticipated to attenuate potential tsunami waves.

3.6.2.2.2 Tsunami-Induced Bore in the Mississippi River

The dynamics of a bore in a channel is essentially the same as a hydraulic jump (Tsuji et al., 1991). By inspection, the supercritical flow conditions required to support the formation of bores do not exist in the Mississippi River reach from the Gulf of Mexico coast to WSES. Subcritical flow conditions are expected within this reach of the Mississippi River owing to its significant depth and mild bottom slope. The lower portion of the Mississippi River is wide and generally uniform in width (Figure 3-64). Therefore, supercritical conditions imposed by a downstream-to-upstream moving tsunami wave would be short lived.

Even in the unlikely event of a bore forming near the mouth of Mississippi River, the bore will be significantly dissipated as it propagates upstream along the approximately 130 mile long reach of the Mississippi River to WSES. Historical observations of bores indicate that they can move tens of miles inland. For example, Chanson, 2005 reports examples of bores propagating inland for 80 kilometers (50 miles). However, reports of bore propagation for 130 miles was not found in the regional or site screening literature review. Additionally, NUREG/CR-6966 states that: "*tsunami-induced bores do not travel more than a few tens of miles upstream from the mouth of a river.*" (Page 32 of NRC, 2009)

Water levels within the Mississippi River will also be contained by the man-made levees (with top elevation of approximately 30 feet, MSL) along the Mississippi River in the vicinity of WSES. Flooding of SSCs at WSES, which are flood protected to elevation 29.18 feet, MSL is highly unlikely.

3.6.2.2.3 Mississippi River Tsunami

Fault zones do exist in the vicinity of WSES. There have been ten recorded earthquakes within approximately 200 miles of WSES, the largest of which occurred in October 1930 and originated in Donaldsonville, Louisiana, about 30 miles west of the site. The epicenter intensity of the Donaldsonville earthquake was nearly VI on the Modified Mercalli scale (WSES, 2013, Page 2.5-1). The earthquake in Donaldsonville had a magnitude equivalent to about 5.0 to 5.9. There have been no historic earthquake events in the vicinity of WSES with magnitudes greater than 6.5. Tsunamis are generated by rapid, large-scale disturbance of a body of water (Page 3 of NRC, 2009). Therefore, only geophysical events such as earthquakes with magnitudes of 6.5 or greater can cause an observable tsunami (Page 4 of NRC, 2009). Based on historical events, the seismic activity level required to develop an observable tsunami in the Mississippi River near WSES (i.e. earthquake of magnitude 6.5 or greater) does not exist. The potential for a significant subaerial landslide causing a tsunami is limited because of the flat topography along the east and west river shorelines and mild Mississippi River slope. It is also noted that large waves in the river would likely overtop the Bonnet Carre spillway structure on the opposite bank of the Mississippi River before they could affect WSES.

The results of this qualitative site screening analysis indicate that significant wave amplitude attenuation will likely occur prior to tsunami waves effecting WSES, which is 60 miles (direct) from the Gulf of Mexico shoreline and 130 river miles upstream of the Mississippi River outlet. Tsunami due to local riverine sources is not anticipated to be significant. Therefore, tsunami is not expected to be a significant contributor to flooding at WSES, nor the controlling flood hazard.

3.6.3 Conclusions

The following conclusions were made:

- Review of the NGDC tsunami database (NGDC, 2014) did not identify any documented, historic tsunami events along the Gulf of Mexico that resulted in significant, historical tsunami impacts (runup heights greater than 2 to 3 feet).
- The seismic seiche waves resulting from the 1964 Gulf of Alaska earthquake are nearly the highest that can be generated because of a predominantly continental ray path for seismic surface waves from Alaska to the Gulf Coast (Page 43, USGS, 2009) and are not a significant flood causing mechanism at WSES.
- The Regional Screening indicates that tsunamis resulting in significant runup along the Gulf of Mexico coast are possible as evidenced by the occurrence of recorded historical events and the presence of near field tsunamigenic sources (USGS, 2009). However, far field tsunamigenic sources are not an appreciable flood causing mechanism for WSES.
- The results of this qualitative site screening analysis indicate that tsunami is not expected to be a significant contributor to flooding at WSES, nor the controlling flood hazard:
- The site setting of WSES provides some protection from direct flooding from the Gulf of Mexico due to tsunami. The approximately 60 miles of land and wetlands between WSES and the Gulf of Mexico coastline is heavily vegetated and flat, and would attenuate tsunami waves from the open Gulf of Mexico coast. WSES site grade is approximately 14.5 to 17.5 feet, MSL and SSCs important to safety are located in the NPIS, which is protected to 29.18 feet, MSL. Therefore, tsunami inundation due to direct flooding from the Gulf of Mexico is not anticipated.
    - Propagation of a tsunami-induced bore up the Mississippi River was considered. Propagation of tsunami-induced bores is complex and to accurately predict requires site-

specific modeling using a numerical model that is able to simulate nonlinearity, dispersion, and dissipative processes such as breaking and bottom friction. However, several site-specific mitigating factors exist that are anticipated to inhibit the formation of bores on the Mississippi River and also to attenuate bore propagation, including: (a) WSES is 130 river miles from the open coastline (Head of Passes). Documentation (Chanson, 2005; NRC, 2009) indicates bore propagation is on the order of a few tens of miles; (b) the Mississippi River has a very mild slope and is not conducive to the formation of hydraulic jumps, which is also not conducive to the propagation of a tsunami-induced bore; (c) the Mississippi River is wide and protected by levees with top elevation of approximately 30 feet, MSL. Flooding of SSCs at WSES due to a tsunami-induced bore is therefore not an appreciable flood causing mechanism.

- The potential for tsunami-like waves in the Mississippi River itself near WSES generated by an earthquake is not appreciable because an earthquake with a magnitude greater than 6.5 is absent from the historical record in the vicinity of WSES. Landslide-generated tsunami potential is not appreciable because of the flat topography along the east and west river shorelines and a mild river slope.

3.6.4 References

Chanson, 2005. Chanson, Hubert, 2005. "Physical Modelling of the Flow Field in an Undular Tidal Bore." Journal of Hydraulic Research, Volume 43, Number 3. 234-244.*

LAGIC, 2004. Lousisiana Geographic Information Center (LAGIC). Louisiana Department of Environmental Quality, and Louisiana Oil Spill Coordinator's Office, 20010423, Louisiana Digital Elevation Dataset from LDEQ source data, UTM Zone 15 NAD83, LOSCO (2004) [24KDEM_LDEQ_2004]: State coverage 1, Louisiana Oil Spill Coordinator's Office (LOSCO), Baton Rouge, LA.

Lockridge et al., 2002. Lockridge, P. A., L.S. Whiteside, and J.F. Lander. "Tsunamis and Tsunami-like Waves of the Eatsern United States". *Science of Tsunami Hazard, 20*(3), 120-157, 2002.

NGDC, 2014. National Geophysical Data Center / World Data Service (NGDC/WDS): Global Historical Tsunami Database. National Geophysical Data Center, NOAA. doi:10.7289/V5PN93H7 Accessed: 08/20/2014.

NRC, 2009. U.S. Nuclear Regulatory Commission (U.S. NRC). NUREG/CR-6966: Tsunami Hazard Assessment at Nuclear Power Plant Sites in the United States of America. Richland, WA: Pacific Northwest National Laboratory, 2009.

NRC, 2013. JLD-ISG-2012-06: Interim Staff Guidance Japan Lessons-Learned Project Directorate - Guidance for Performing a Tsunami, Surge, or Seiche Hazard Assessment, Revision 0, U.S. Nuclear Regulatory Commission, January 2013.

Tsuji et al., 1991. Tsuji, Y., T. Yanuma, I. Murata, and C. Fujiwara,1991. "Tsunami Ascending in Rivers as an Undular Bore," *Natural Hazards* 4: 257-266.*

USGS, 2009. Ten Brink, U., D. Twichell, P. Lynett, E. Geist, J. Chaytor, H. Lee, B. Buczkowski, and C. Flores, 2009. Regional Assessment of Tsunami Potential in the Gulf of Mexico: U.S. Geological Survey Administration Report.

WSES, 2013. WSES Updated Final Safety Analysis Report, 2013. See AREVA Document No. 38-9243507-000.

Figure 3-62: Location of WSES Relative to the Gulf of Mexico

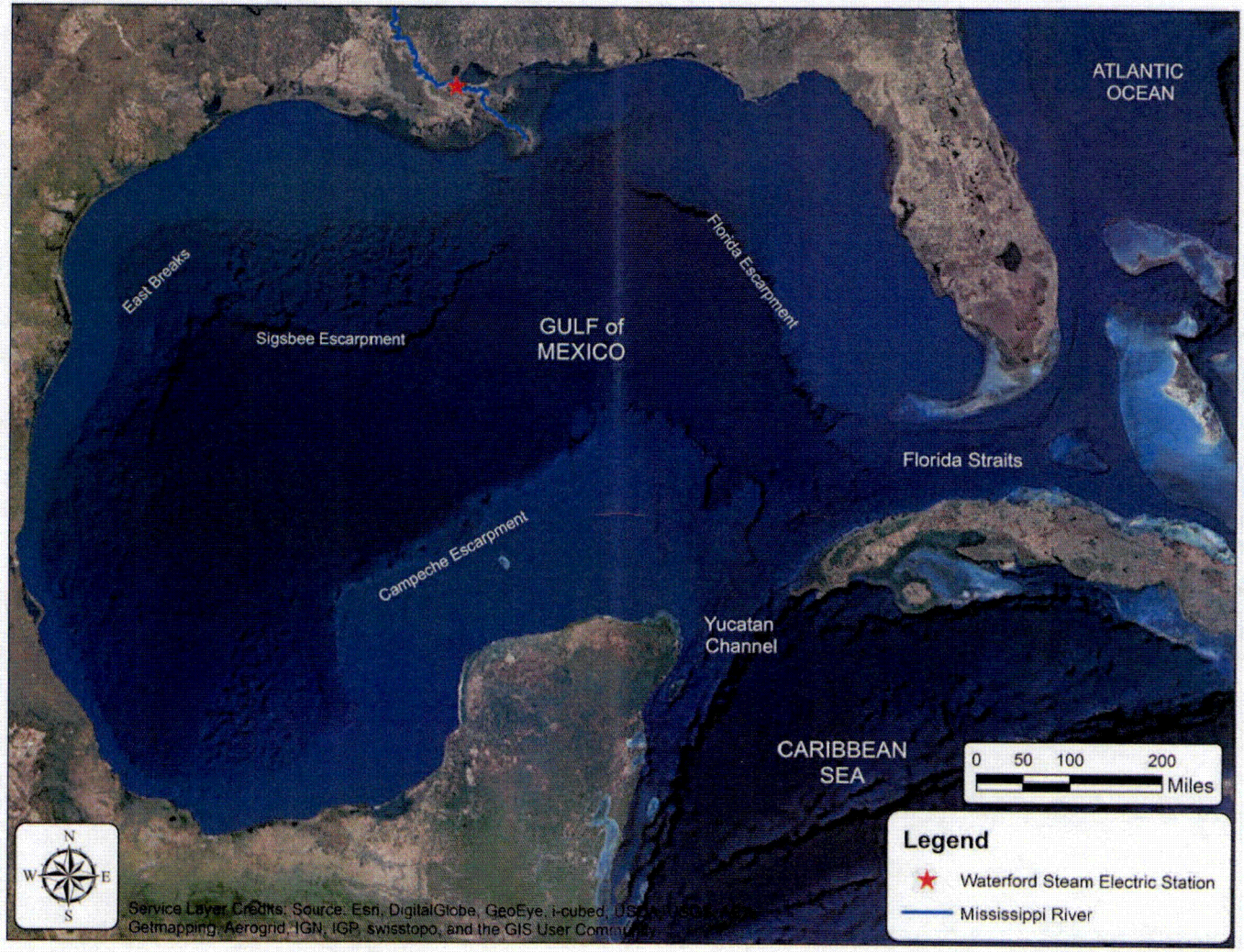

Figure 3-63: Locus Map

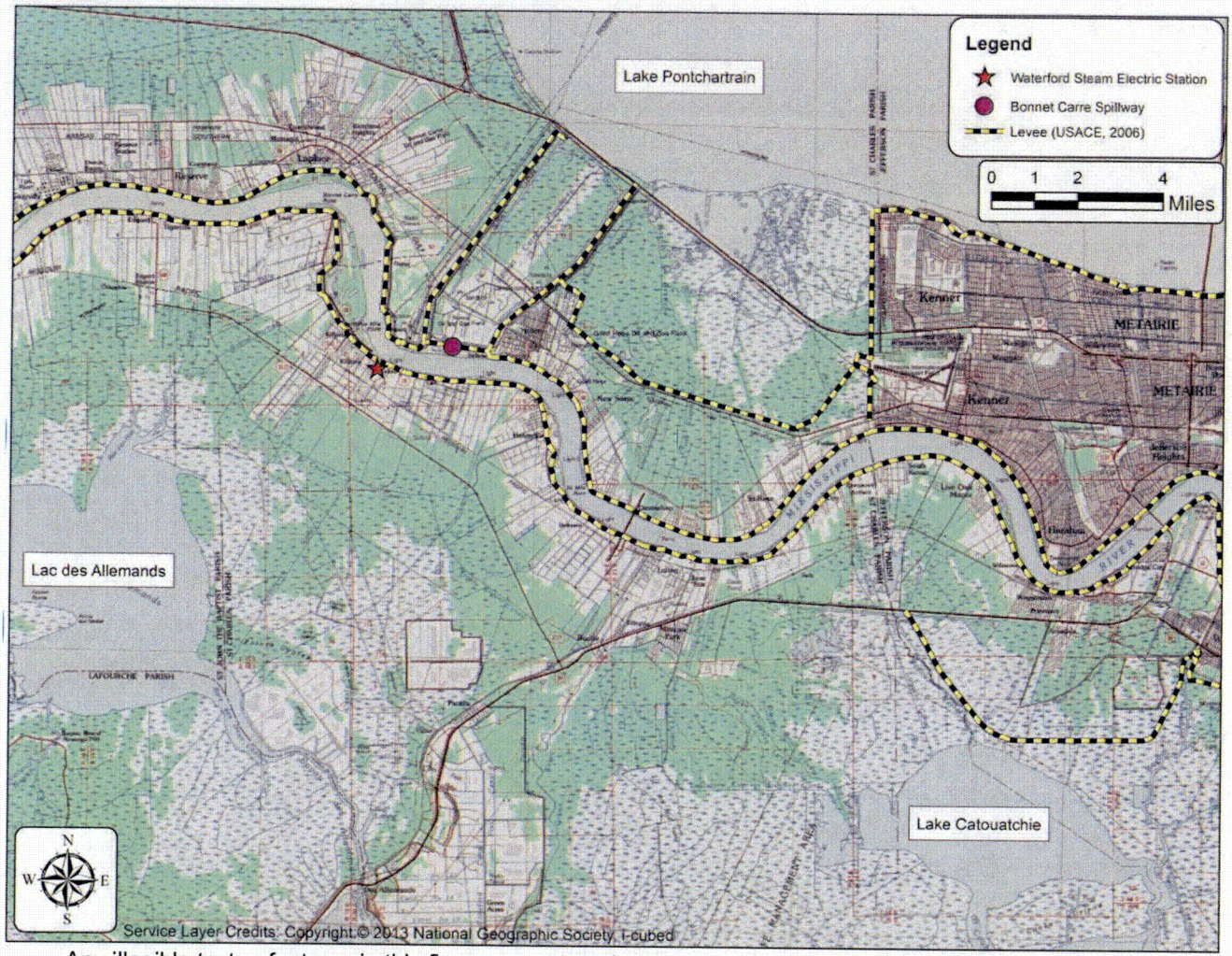

Any illegible text or features in this figure are not pertinent to the technical purposes of this document.

Figure 3-64: Locus Map with Elevation Data (LAGIC, 2004)

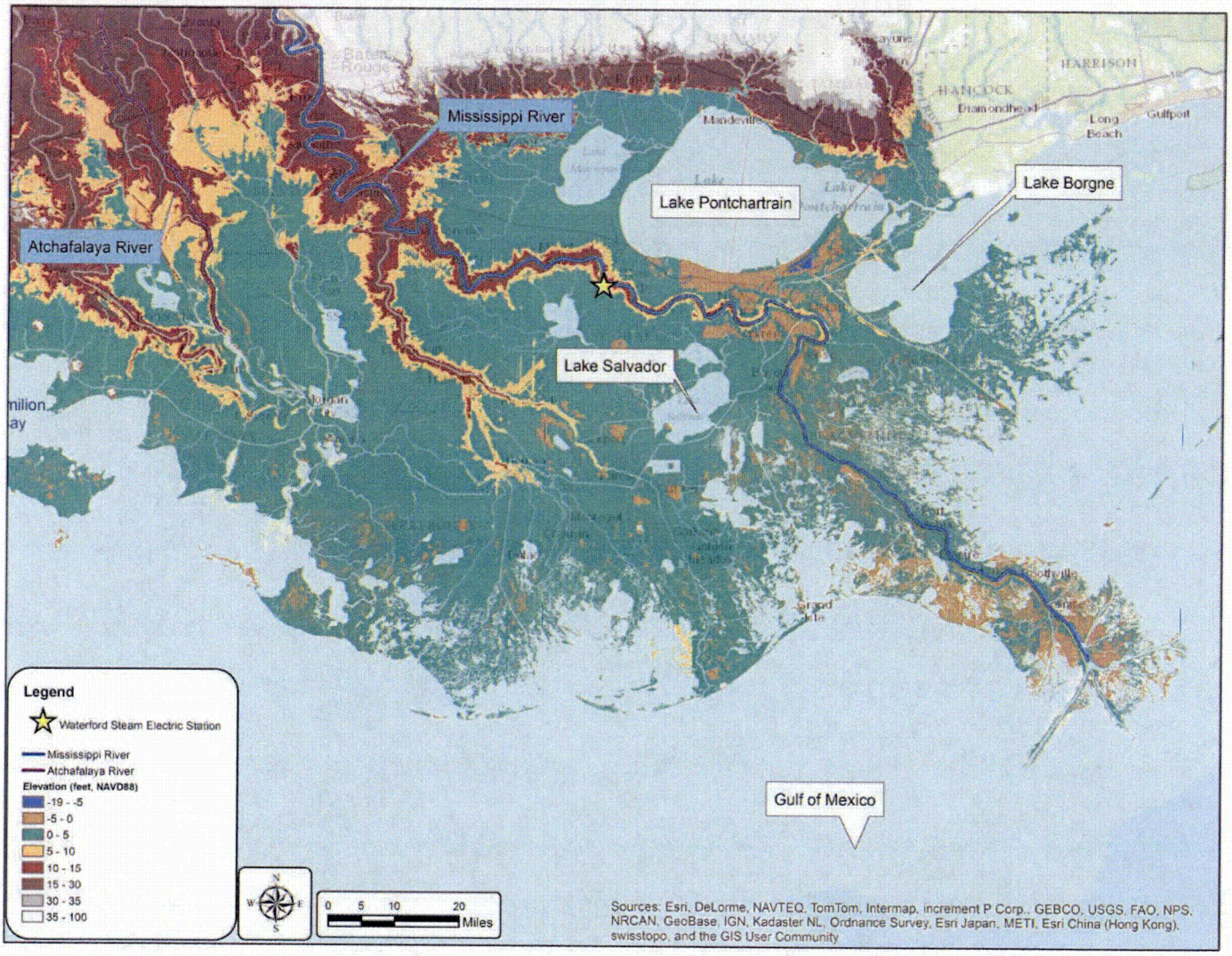

Any illegible text or features in this figure are not pertinent to the technical purposes of this document.

Figure 3-65: Shaded Relief of the Gulf of Mexico (USGS, 2009)

Landslide deposits marked in red. EB- East Breaks Landslide, MC- Mississippi Canyon, BC- Brant Canyon, EMF- East Mississippi Fan, BF- Bryant Fan, MF- Mississippi Fan.